Using MAX/MIN Transverse Regions to Study the Underlying Event in Run 2 at the Tevatron

Alberto Cruz, Rick Field, and Craig Group
Department of Physics, University of Florida
Gainesville, Florida, 32611, USA

July 20, 2005

Abstract

We study the behavior of the charged particle ($p_T > 0.5$ GeV/c, $|\eta| < 1$) and energy ($|\eta| < 1$) components of the "underlying event" in hard scattering proton-antiproton collisions at 1.96 TeV. We use the direction of the leading calorimeter jet in each event to define two "transverse" regions of η-ϕ space that are very sensitive to the "underlying event". Defining a variety of MAX and MIN "transverse" regions helps separate the "hard component" (initial and final-state radiation) from the "beam-beam remnant" and multiple parton interaction components. In addition, selecting events with at least two jets that are nearly back-to-back ($\Delta\phi_{12} > 150^o$) with P_T(jet#3) < 15 GeV/c suppress the hard initial and final-state radiation thus increasing the sensitivity of the "transverse" region to the "beam-beam remnant" and the multiple parton scattering components of the "underlying event". Unlike our previous Run 2 "underlying event" analysis which used JetClu to define "jets" and compared uncorrected data with PYTHIA Tune A and HERWIG after detector simulation (CDFSIM), in this analysis we use the MidPoint algorithm (R = 0.7, $f_{merge} = 0.75$) and correct the observables to the particle level. The corrected observables are then compared with the theory at the particle level (*i.e.* generator level). The theory includes PYTHIA Tune A, HERWIG, and a tuned version of JIMMY.

I. Introduction

Fig. 1 illustrates the way QCD Monte-Carlo models simulate a proton-antiproton collision in which a "hard" 2-to-2 parton scattering with transverse momentum, P_T(hard), has occurred. The resulting event contains particles that originate from the two outgoing partons (*plus initial and final-state radiation*) and particles that come from the breakup of the proton and antiproton (*i.e.* "beam-beam remnants"). The "underlying event" is everything except the two outgoing hard scattered "jets" and receives contributions from the "beam-beam remnants" plus initial and final-state radiation. The "hard scattering" component consists of the outgoing two jets plus initial and final-state radiation.

The "beam-beam remnants" are what is left over after a parton is knocked out of each of the initial two beam hadrons. It is the reason hadron-hadron collisions are more "messy" than electron-positron annihilations and no one really knows how it should be modeled. For the QCD Monte-Carlo models the "beam-beam remnants" are an important component of the "underlying event". Also, it is possible that multiple parton scattering contributes to the "underlying event". Fig. 2 shows the way PYTHIA [1] models the "underlying event" in proton-antiproton collision by including multiple parton interactions. In addition to the hard 2-to-2 parton-parton scattering and the "beam-beam remnants", sometimes there is a second "semi-hard" 2-to-2 parton-parton scattering that contributes particles to the "underlying event".

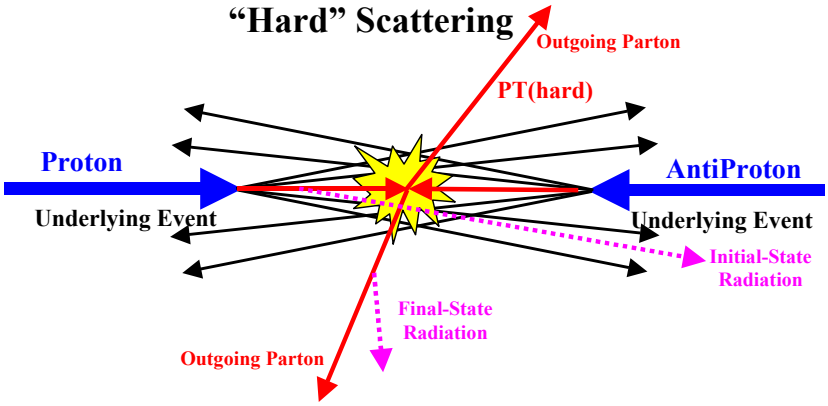

Fig. 1. Illustration of the way QCD Monte-Carlo models simulate a proton-antiproton collision in which a "hard" 2-to-2 parton scattering with transverse momentum, P_T(hard), has occurred. The resulting event contains particles that originate from the two outgoing partons (plus initial and final-state radiation) and particles that come from the breakup of the proton and antiproton (*i.e.* "beam-beam remnants"). The "underlying event" is everything except the two outgoing hard scattered "jets" and consists of the "beam-beam remnants" plus initial and final-state radiation. The "hard scattering" component consists of the outgoing two jets plus initial and final-state radiation.

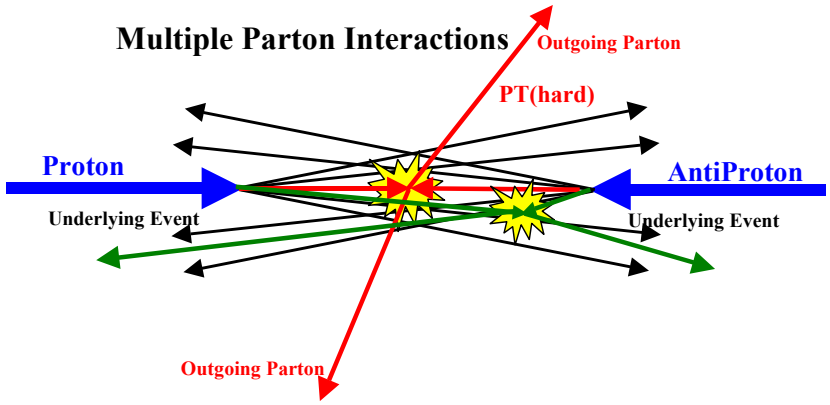

Fig. 2. Illustration of the way PYTHIA models the "underlying event" in proton-antiproton collision by including multiple parton interactions. In addition to the hard 2-to-2 parton-parton scattering with transverse momentum, P_T(hard), there is a second "semi-hard" 2-to-2 parton-parton scattering that contributes particles to the "underlying event".

Of course, from a certain point of view there is no such thing as an "underlying event" in a proton-antiproton collision. There is only an "event" and one cannot say where a given particle in the event originated. On the other hand, hard scattering collider "jet" events have a distinct topology. On the average, the outgoing hadrons "remember" the underlying the 2-to-2 hard scattering subprocess. An average hard scattering event consists of a collection (or burst) of hadrons traveling roughly in the direction of the initial beam particles and two collections of hadrons (*i.e.* "jets") with large transverse momentum. The two large transverse momentum "jets" are roughly back to back in azimuthal angle. One can use the topological structure of hadron-hadron collisions to study the "underlying event" [2-4]. We will study the "underlying event" in the Run 2 "min-bias" and jet trigger data samples using the direction of the leading calorimeter jet to isolate regions of η-ϕ space that are sensitive to the "underlying event".

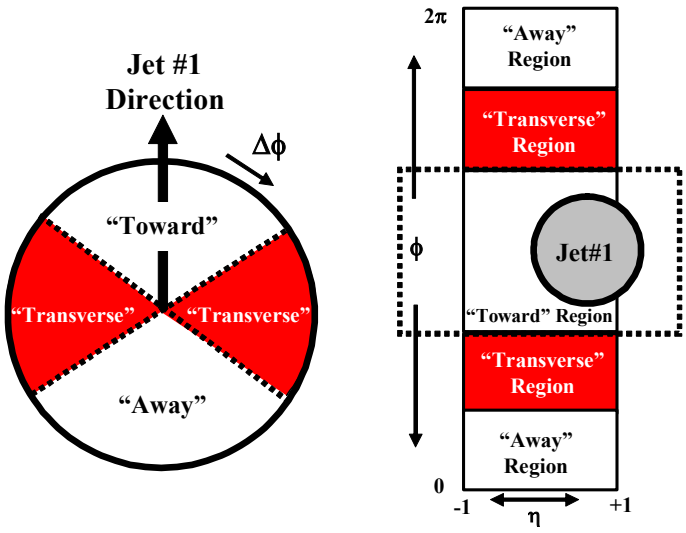

Fig. 3. Illustration of correlations in azimuthal angle $\Delta\phi$ relative to the direction of the leading jet (MidPoint, R = 0.7, f_{merge} = 0.75) in the event, jet#1. The angle $\Delta\phi = \phi - \phi_{jet\#1}$ is the relative azimuthal angle between charged particles (or calorimeter towers) and the direction of jet#1. The "toward" region is defined by $|\Delta\phi| < 60^o$ and $|\eta| < 1$, while the "away" region is $|\Delta\phi| > 120^o$ and $|\eta| < 1$. The "transverse" region is defined by $60^o < |\Delta\phi| < 120^o$ and $|\eta| < 1$. Each of the three regions "toward", "transverse", and "away" and has an overall area in η-ϕ space of $\Delta\eta\Delta\phi = 4\pi/3$. We examine charged particles in the range $p_T >$ 0.5 GeV/c and $|\eta| < 1$ and calorimeter towers with $E_T > 0.1$ GeV and $|\eta| < 1$, but allow the leading jet to be in the region $|\eta(jet\#1)| < 2$.

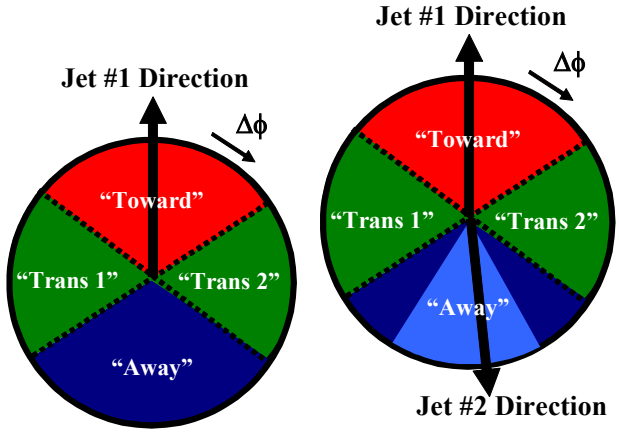

Fig. 4. Illustration of correlations in azimuthal angle $\Delta\phi$ relative to the direction of the leading jet (highest P_T jet) in the event, jet#1. The angle $\Delta\phi = \phi - \phi_{jet\#1}$ is the relative azimuthal angle between charged particles and the direction of jet#1. The "toward" region is defined by $|\Delta\phi| < 60^o$ and $|\eta| < 1$, while the "away" region is $|\Delta\phi| > 120^o$ and $|\eta| < 1$. The two "transverse" regions $60^o < \Delta\phi < 120^o$ and $60^o < -\Delta\phi < 120^o$ are referred to as "transverse 1" and "transverse 2". Each of the two "transverse" regions have an area in η-ϕ space of $\Delta\eta\Delta\phi = 4\pi/6$. The overall "transverse" region defined in Fig. 3 corresponds to combining the "transverse 1" and "transverse 2" regions. Events in which there are no restrictions placed on the on the second highest P_T jet, jet#2, are referred to as "leading jet" events (*left*). Events with at least two jets where the leading two jets are nearly "back-to-back" ($\Delta\phi_{12} > 150^o$) with $P_T(jet\#2)/P_T(jet\#1) > 0.8$ and $P_T(jet\#3) < 15$ GeV/c are referred to as "back-to-back" events (*right*).

As illustrated in Fig. 3, the direction of the leading jet, jet#1, is used to define correlations in the azimuthal angle, $\Delta\phi$. The angle $\Delta\phi = \phi - \phi_{jet\#1}$ is the relative azimuthal angle between a charged particle (or a calorimeter tower) and the direction of jet#1. The "transverse" region is perpendicular to the plane of the hard 2-to-2 scattering and is therefore very sensitive to the "underlying event". We restrict ourselves to charged particles in the range $p_T >$ 0.5 GeV/c and $|\eta| < 1$ and calorimeter towers with $E_T > 0.1$ GeV and $|\eta| < 1$, but allow the leading jet that is used to define the "transverse" region to have $|\eta(jet\#1)| < 2$. Furthermore, we consider two classes of events. As illustrated in Fig. 4, we refer to events in which there are no restrictions placed on the second and third highest E_T

jets (jet#2 and jet#3) as "leading jet" events. Events with at least two jets with $E_T > 15$ GeV where the leading two jets are nearly "back-to-back" ($|\Delta\phi_{12}| > 150^o$) with E_T(jet#2)/E_T(jet#1) > 0.8 and E_T(jet#3) < 15 GeV are referred to as "back-to-back" events (see Table 1). "Back-to-back" events are a subset of the "leading jet" events. The idea here is to suppress hard initial and final-state radiation thus increasing the sensitivity of the "transverse" region to the "beam-beam remnant" and the multiple parton scattering component of the "underlying event".

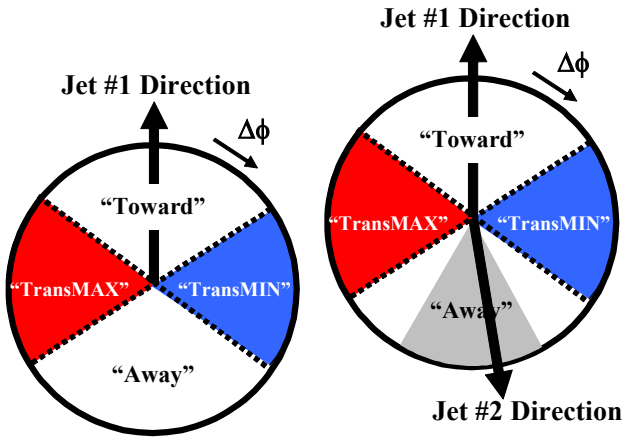

Fig. 5. Illustration of correlations in azimuthal angle $\Delta\phi$ relative to the direction of the leading jet (highest P_T jet) in the event, jet#1 for "leading jet" events (*left*) and "back-to-back" events (*right*) as defined in Fig. 4. The angle $\Delta\phi = \phi - \phi_{jet\#1}$ is the relative azimuthal angle between charged particles (or calorimeter towers) and the direction of jet#1. On an event by event basis, we define "transMAX" ("transMIN") to be the maximum (minimum) of the two "transverse" regions, $60^o < \Delta\phi < 120^o$ and $60^o < -\Delta\phi < 120^o$. "TransMAX" and "transMIN" each have an area in η-ϕ space of $\Delta\eta\Delta\phi = 4\pi/6$. The overall "transverse" region defined in Fig. 3 includes both the "transMAX" and the "transMIN" region.

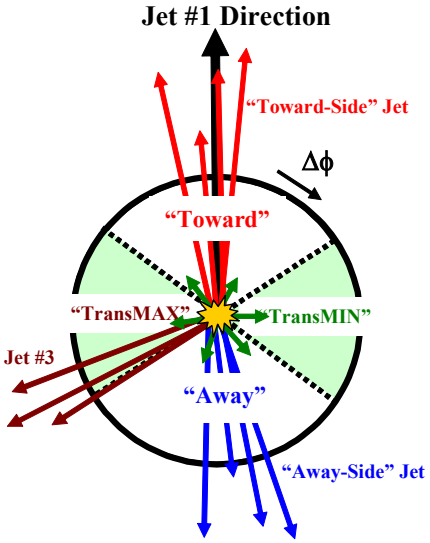

Fig. 6. Illustration of the topology of a proton-antiproton collision in which a "hard" parton-parton collision has occurred. The "toward" region as defined in Fig. 3 contains the leading "jet", while the "away" region, on the average, contains the "away-side" "jet". The "transverse" region is perpendicular to the plane of the hard 2-to-2 scattering and is very sensitive to the "underlying event". For events with large initial or final-state radiation the "transMAX" region defined in Fig.5 would contain the third jet while both the "transMAX" and "transMIN" regions receive contributions from the beam-beam remnants (see Fig. 1). Thus, the "transMIN" region is very sensitive to the beam-beam remnants, while the "transMAX" minus the "transMIN" (*i.e.* "transDIF") is very sensitive to initial and final-state radiation.

Table 1. Definition of "Leading Jet" and "Back-to-Back" events.

Name	Selection Criterion
"Leading Jet"	Require the leading MidPoint jet, jet#1, to have $\|\eta(\text{jet\#1})\| < 2$.
"Back-to-Back"	Require the leading two MidPoint jets to have $P_T(\text{jet}) > 15$ GeV and $\|\eta(\text{jet})\| < 2$. In addition require $\|\Delta\phi_{12}\| > 150^o$, $P_T(\text{jet\#2})/P_T(\text{jet\#1}) > 0.8$, and $P_T(\text{jet\#3}) < 15$ GeV/c.

The overall "transverse" region corresponds to combining the "transverse 1" and "transverse 2" regions shown in Fig. 4. As shown in Fig. 5, we define a variety of MAX and MIN "transverse" regions which helps separate the "hard component" (initial and final-state radiation) from the "beam-beam remnant" component (see Fig. 6). MAX (MIN) refer to the "transverse" region containing largest (smallest) number of charged particles or to the region containing the largest (smallest) scalar p_T sum of charged particles or the region containing the largest (smallest) scalar E_T sum of particles. Table 2 shows the observables that are considered in this paper as they are defined at the particle level and detector level. Since we will be studying regions in η-ϕ space with different areas, we will construct densities by dividing by the area. For example, the number density, $dN_{chg}/d\eta d\phi$, corresponds the number of charged particles per unit η-ϕ and the PT_{sum} density, $dPT_{sum}/d\eta d\phi$, corresponds the amount of charged scalar p_T sum per unit η-ϕ, and the ET_{sum} density, $dE_T/d\eta d\phi$, corresponds the amount of scalar E_T sum per unit η-ϕ.

Table 2. Observables examined in the "transverse" region (see Fig. 4) as they are defined at the particle level and the detector level. Charged tracks are considered "good" if they pass the selection criterion given in Table 7. The mean charged particle $<p_T>$ and the charged fraction PT_{sum}/ET_{sum} are constructed on and event-by-event basis and then averaged over the events. There is one PT_{max} per event with $PT_{max} = 0$ if there are no charged particles.

Observable	Particle Level	Detector level
$dN_{chg}/d\eta d\phi$	Number of charged particles per unit η-ϕ ($p_T > 0.5$ GeV/c, $\|\eta\| < 1$)	Number of "good" charged tracks per unit η-ϕ ($p_T > 0.5$ GeV/c, $\|\eta\| < 1$)
$dPT_{sum}/d\eta d\phi$	Scalar p_T sum of charged particles per unit η-ϕ ($p_T > 0.5$ GeV/c, $\|\eta\| < 1$)	Scalar p_T sum of "good" charged tracks per unit η-ϕ ($p_T > 0.5$ GeV/c, $\|\eta\| < 1$)
$<p_T>$	Average p_T of charged particles ($p_T > 0.5$ GeV/c, $\|\eta\| < 1$)	Average p_T of "good" charged tracks ($p_T > 0.5$ GeV/c, $\|\eta\| < 1$)
PT_{max}	Maximum p_T charged particle ($p_T > 0.5$ GeV/c, $\|\eta\| < 1$) $PT_{max} = 0$ for no charged particle	Maximum p_T "good" charged tracks ($p_T > 0.5$ GeV/c, $\|\eta\| < 1$) $PT_{max} = 0$ for no "good" charged track
$dE_T/d\eta d\phi$	Scalar E_T sum of all particles per unit η-ϕ (all p_T, $\|\eta\| < 1$)	Scalar E_T sum of all calorimeter towers per unit η-ϕ ($E_T > 0.1$ GeV, $\|\eta\| < 1$)
PT_{Sum}/ET_{sum}	Scalar p_T sum of charged particles ($p_T > 0.5$ GeV/c, $\|\eta\| < 1$) divided by the scalar E_T sum of all particles (all p_T, $\|\eta\| < 1$)	Scalar p_T sum of "good" charged tracks ($p_T > 0.5$ GeV/c, $\|\eta\| < 1$) divided by the scalar E_T sum of calorimeter towers ($E_T > 0.1$ GeV, $\|\eta\| < 1$)

Our previous Run 2 "underlying event" analysis [5] used JetClu to define "jets" and compared uncorrected data with PYTHIA Tune A and HERWIG after detector simulation (CDFSIM). In this analysis we use the MidPoint algorithm (R = 0.7, f_{merge} = 0.75) and correct the observables to the particle level. The corrected observables are then compared with PYTHIA Tune A and HERWIG at the particle level (*i.e.* generator level). In addition, for the first time we study the energy in the "transverse" region. In Section II we discuss the QCD Monte-Carlo models and the method used to correct the data to the particle level. The data selection and the systematic uncertainties are examined in Section III and the results are presented in Section IV. Section V is reserved for the summary and conclusions.

II. Monte-Carlo Generation and Correction Factors

(1) Monte-Carlo Generation

In this analysis the data are corrected to the particle level using PYTHIA Tune A. The corrected data are then compared with compared with PYTHIA Tune A [6] and HERWIG at the particle level 1.96 TeV (*i.e.* generator level). PYTHIA Tune A (5.3.3nt) was generated with the minimum P_T(hard) values shown in Table 3 and HERWIG (5.3.3nt) was generated with the minimum P_T(hard) values shown in Table 4. Stntuples (5.3.3nt dev242) were created for the QCD group by Anwar Bhatti, Ken Hatakeyama, and Craig Group.

Table 3. PYTHIA Tune A (5.3.3nt) at 1.96 TeV.

P_T(hard) minimum	Events
0 GeV/c	3,093,106
10 GeV/c	1,039,093
18 GeV/c	4,285,687
40 GeV/c	4,228,873
60 GeV/c	992,087
90 GeV/c	1,497,108
120 GeV/c	2,068,377
150 GeV/c	1,488,786
200 GeV/c	1,042,280
300 GeV/c	1,045,314
400 GeV/c	1,043,634
Total	21,824,345

Table 4. HERWIG (5.3.3nt) at 1.96 TeV.

P_T(hard) minimum	Events
3 GeV/c	1,014,070
10 GeV/c	1,018,974
18 GeV/c	5,001,261
40 GeV/c	5,071,205
60 GeV/c	1,044,202
90 GeV/c	2,057,661
120 GeV/c	2,035,473
150 GeV/c	1,922,568
200 GeV/c	968,906
300 GeV/c	885,867
400 GeV/c	858,936
Total	21,879,123

Smooth curves have been drawn through the QCD Monte-Carlo predictions to aid in comparing the theory with the data. Fig. 7 shows an example of the fits to the Monte-Carlo results.

(2) Correcting the Data to the Particle Level

We consider two methods for correcting the data from the detector level to the particle level. Method 1 is a "one-step" method. PYTHIA Tune A and HERWIG are used to calculate the observables in Table 2 at the particle level in bins of particle jet#1 P_T (GEN) and at the detector level in bins of calorimeter jet#1 P_T (uncorrected) (CDFSIM). The detector level data in bins of calorimeter jet#1 P_T (uncorrected) are corrected by multiplying by QCD Monte-Carlo correction factor, GEN/CDFSIM, as described in Table 5.

Table 5. Correction factors for Method 1. PYTHIA Tune A and HERWIG are used to calculate the observables in Table 2 at the particle level in bins of particle jet#1 P_T (GEN) and at the detector level in bins of calorimeter jet#1 P_T (uncorrected). The detector level data in bins of calorimeter jet#1 PT (uncorrected) are corrected by multiplying by QCD Monte-Carlo factor, GEN/CDFSIM.

Particle Level Observable	Detector Level Observable	Response Factor	Correction Factor
GEN = Particle Jet#1 P_T Bin	CDFSIM = Calorimeter Jet#1 P_T Bin (uncorrected)	CDFSIM/GEN	GEN/CDFSIM

Method 2 is a "two-step" method. First PYTHIA Tune A is used to correct the P_T of the leading calorimeter jet. This is done by comparing the matching leading particle jet with the leading calorimeter jet. Then PYTHIA Tune A is used to calculate the observables in Table 2 at the particle level in bins of particle jet#1 P_T (GEN) and at the detector level in bins of calorimeter jet#1 P_T (corrected) (CDFSIMcor). The detector level data in bins of calorimeter jet#1 P_T (corrected) are corrected by multiplying by the QCD Monte-Carlo correction factor, GEN/CDFSIMcor. If the QCD Monte-Carlo described the data perfectly and the detector

simulation was exact then method 1 and method 2 would yield the same result. Differences between the two methods can be used as a measure of the systematic uncertainty in correcting the data to the particle level.

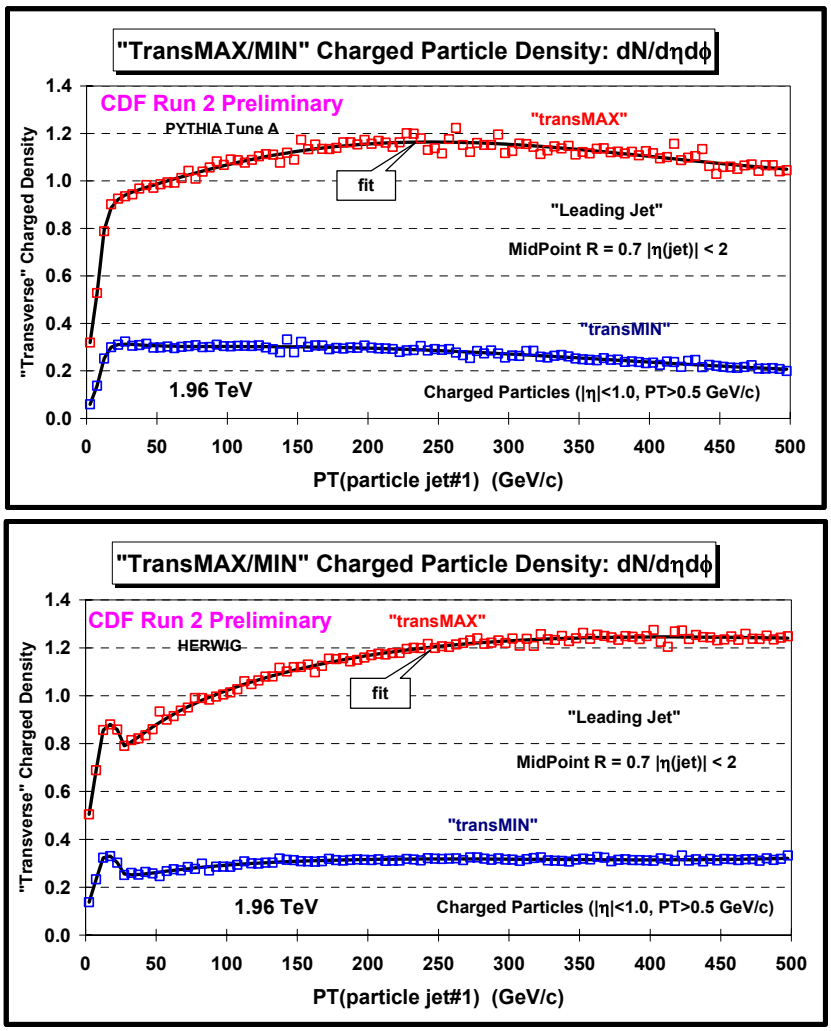

Fig. 7. Example of fits to the QCD Monte-Carlo results. Shows the particle level predictions at 1.96 TeV for the density of charged particles, $dN_{chg}/d\eta d\phi$, with $p_T > 0.5$ GeV/c and $|\eta| < 1$ in the "transMAX" and "transMIN" regions for "leading jet" events defined in Fig. 5 as a function of the leading particle jet P_T for PYTHIA Tune A (*top*) and HERWIG (*bottom*).

Fig. 8 and Fig. 9 show the particle level predictions from PYTHIA Tune A and HERWIG for average density of particles, $dN_{all}/d\eta d\phi$, for all particles with $|\eta| < 1$ in the "transverse" region as a function of the leading particle jet P_T for "leading jet" and "Back-to-back" events, respectively. It is interesting to note that HERWIG produces more particles in the "transverse" region than PYTHIA Tune A. Fig. 8 and Fig. 9 also shows the average charged particle PT_{sum} density, $dPT_{sum}/d\eta d\phi$, and the average charged particle $\langle p_T \rangle$ for particles with $|\eta| < 1$ in the "transverse" region for "leading jet" events as a function of the leading particle jet P_T. It is clear from these comparisons that HERWIG produces more "soft" particles than PYTHIA Tune A which will result in different "response" factors (see Table 5) at low leading jet P_T.

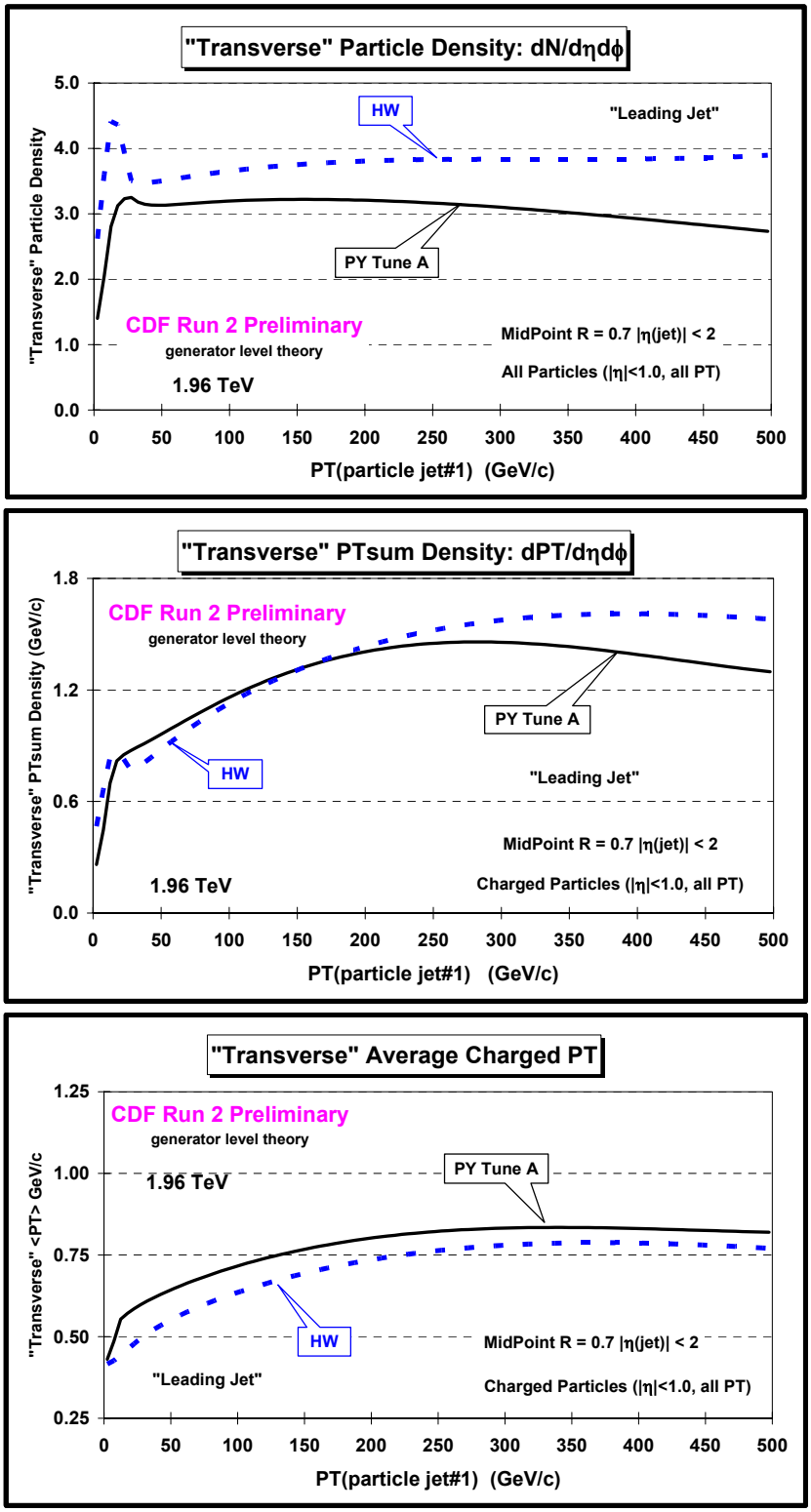

Fig. 8. Particle level predictions from PYTHIA Tune A and HERWIG for average density of particles $dN_{all}/d\eta d\phi$ (*top*), the average charged particle PT_{sum} density, $dPT_{sum}/d\eta d\phi$ (*middle*), and the average charged particle $\langle p_T \rangle$ (*bottom*) for particles with $|\eta| < 1$ in the "transverse" region for "leading jet" events defined in Fig. 5 as a function of the leading particle jet P_T.

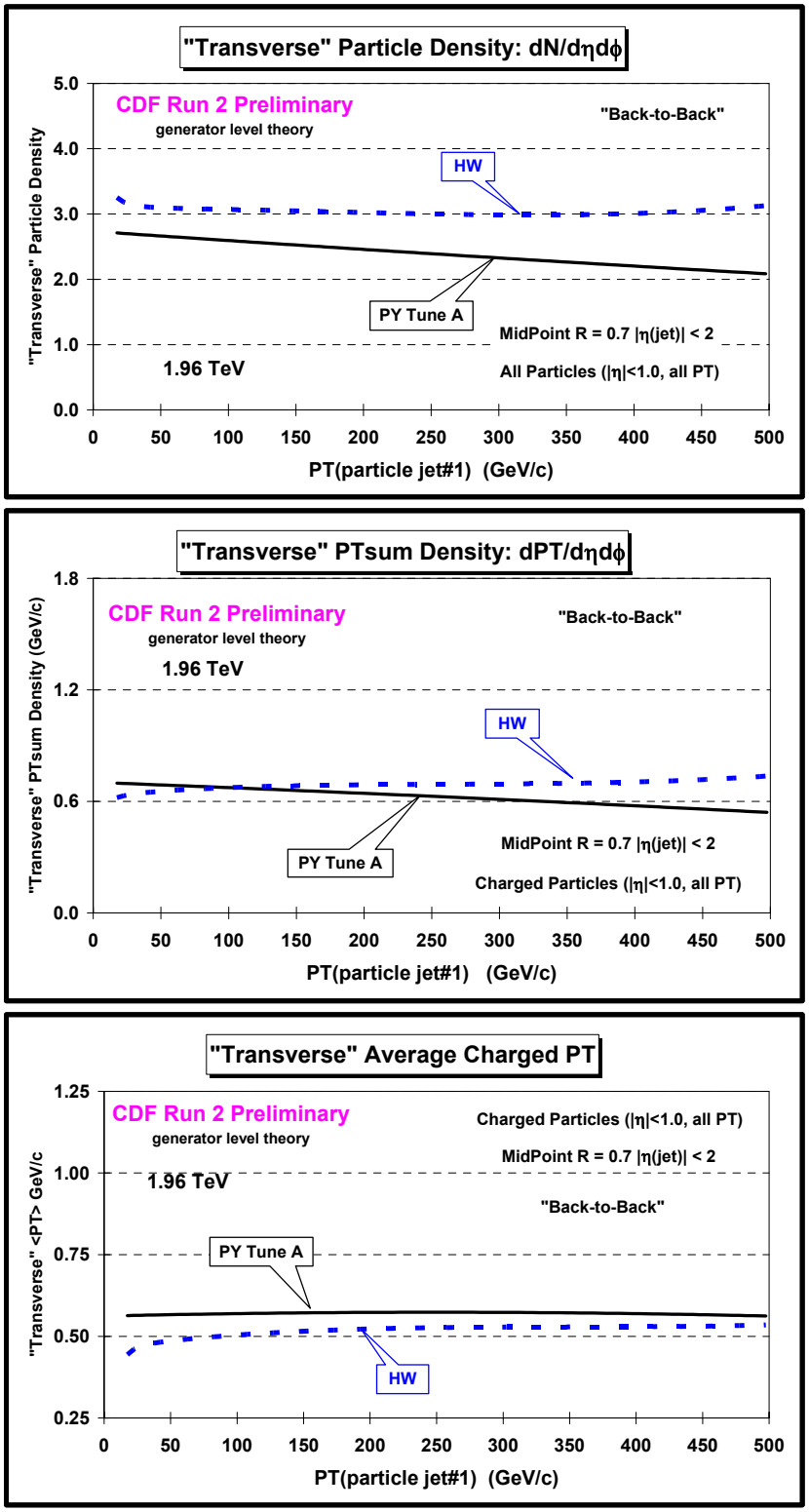

Fig. 9. Particle level predictions from PYTHIA Tune A and HERWIG for average density of particles $dN_{all}/d\eta d\phi$ (*top*), the average charged particle PT_{sum} density $dPT_{sum}/d\eta d\phi$ (*middle*), and the average charged particle $\langle p_T \rangle$ (*bottom*) for particles with $|\eta| < 1$ in the "transverse" region for "back-to-back" events defined in Fig. 5 as a function of the leading jet P_T.

Figs. 10 – 28 show the "response" factors (see Table 5) from PYTHIA Tune A and HERWIG for the observables in Table 2 for "leading jet" and "back-to-back" events as a function of the leading jet P_T. HERWIG and PYTHIA Tune A produce similar "response" factors for leading jet P_T greater than 50 GeV/c, but for lower leading jet P_T they are quite different. This will result in large systematic errors on the corrected observables in Table 2 at low leading jet P_T.

Fig. 29 shows the leading jet P_T correction used in method 2 for "leading jet" events. Figs. 30 shows the method 2 "response" factors from PYTHIA Tune A for some of the observables in Table 2 for "leading jet" events as a function of the leading jet P_T. The observable in Table 2 do not depend strongly on the leading jet P_T and hence the method 1 and method 2 correction factors are similar. This can be seen in Fig. 31 which compares the method 1 response factors versus the leading jet P_T (uncorrected) with the method 2 response factors versus the leading jet P_T (corrected) from PYTHIA Tune A. The method 2 correction factors (1/response factor) are applied data after correcting the leading jet P_T, while the method 1 correction factors are applied to the data without correcting the leading jet P_T.

Method 1 can be easily applied to both the "leading jet" and "back-to-back" events. For the "back-to-back" events method 1 corrects for calorimeter response for jet#1, jet#2 and jet#3 in one step and as can be seen from Figs. 10 – 28 the response factors for "back-to-back" events are different from the response factors for "leading jet" events. The primary source of the difference is due to requirement that P_T(jet#3) < 15 GeV/c for "back-to-back" events and the "back-to-back" correction factors are correcting for the calorimeter response for jet#3. In order to apply method 2 to the "back-to-back" events we would have to first correct the P_T of jet#1, jet#2, and jet#3. Since the observables in Table 2 do not strongly on the P_T of jet#1, jet#2, and jet#3, it is much easier to use method 1 for both "leading jet" and "back-to-back" events. We will use the differences between method 1 and method 2 in "leading jet" events as a measure of the systematic uncertainty in correcting to the particle level.

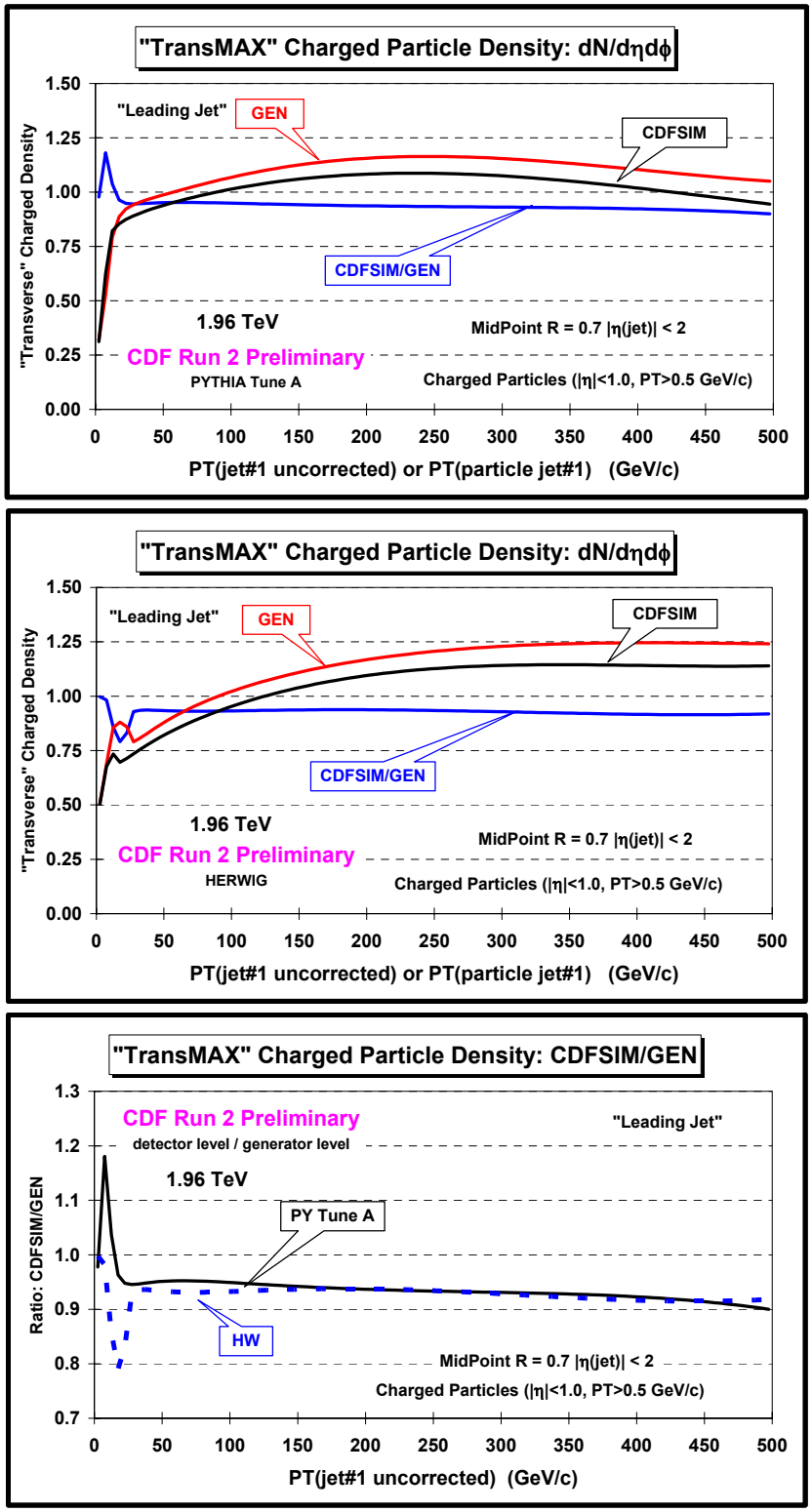

Fig. 10. Method 1 response factors for the density of charged particles, dNchg/dηdϕ, with $p_T > 0.5$ GeV/c and $|\eta| < 1$ in the "transMAX" region for "leading jet" events defined in Fig. 5 as a function of the leading jet P_T. Shows the particle level prediction (GEN) versus the leading particle jet P_T and the detector level result (CDFSIM) versus the leading calorimeter jet P_T (uncorrected) with $|\eta(\text{jet}\#1)| < 2$ for PYTHIA Tune A (*top*) and HERWIG (*middle*). Also shows the ratio of the detector level to the particle level, CDFSIM/GEN, versus the leading jet P_T (*i.e.* response factor).

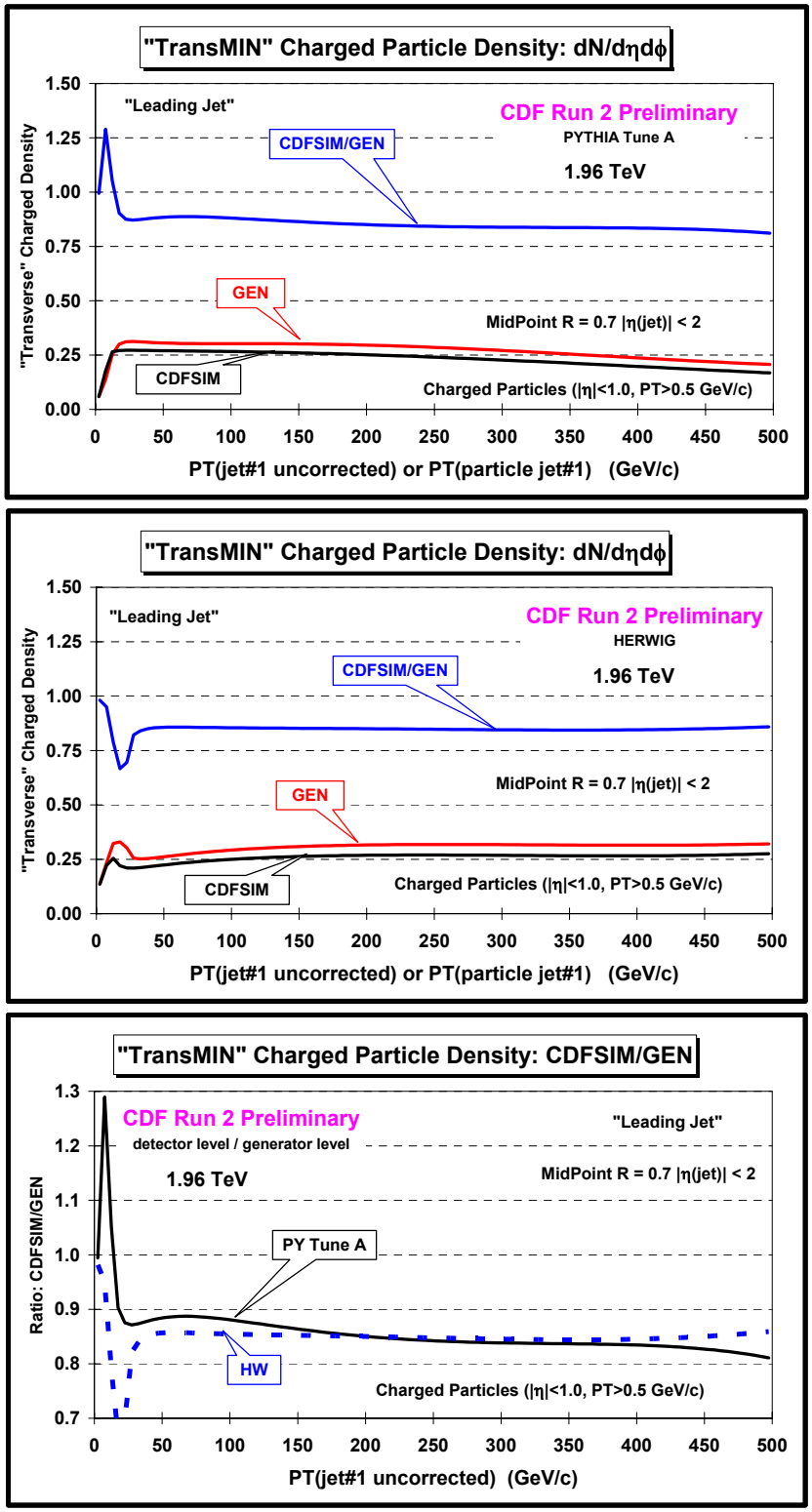

Fig. 11. Method 1 response factors for the density of charged particles, dNchg/dηdφ, with $p_T > 0.5$ GeV/c and $|\eta| < 1$ in the "transMIN" region for "leading jet" events defined in Fig. 5 as a function of the leading jet P_T. Shows the particle level prediction (GEN) versus the leading particle jet P_T and the detector level result (CDFSIM) versus the leading calorimeter jet P_T (uncorrected) with $|\eta(\text{jet}\#1)| < 2$ for PYTHIA Tune A (*top*) and HERWIG (*middle*). Also shows the ratio of the detector level to the particle level, CDFSIM/GEN, versus the leading jet P_T (*i.e.* response factor).

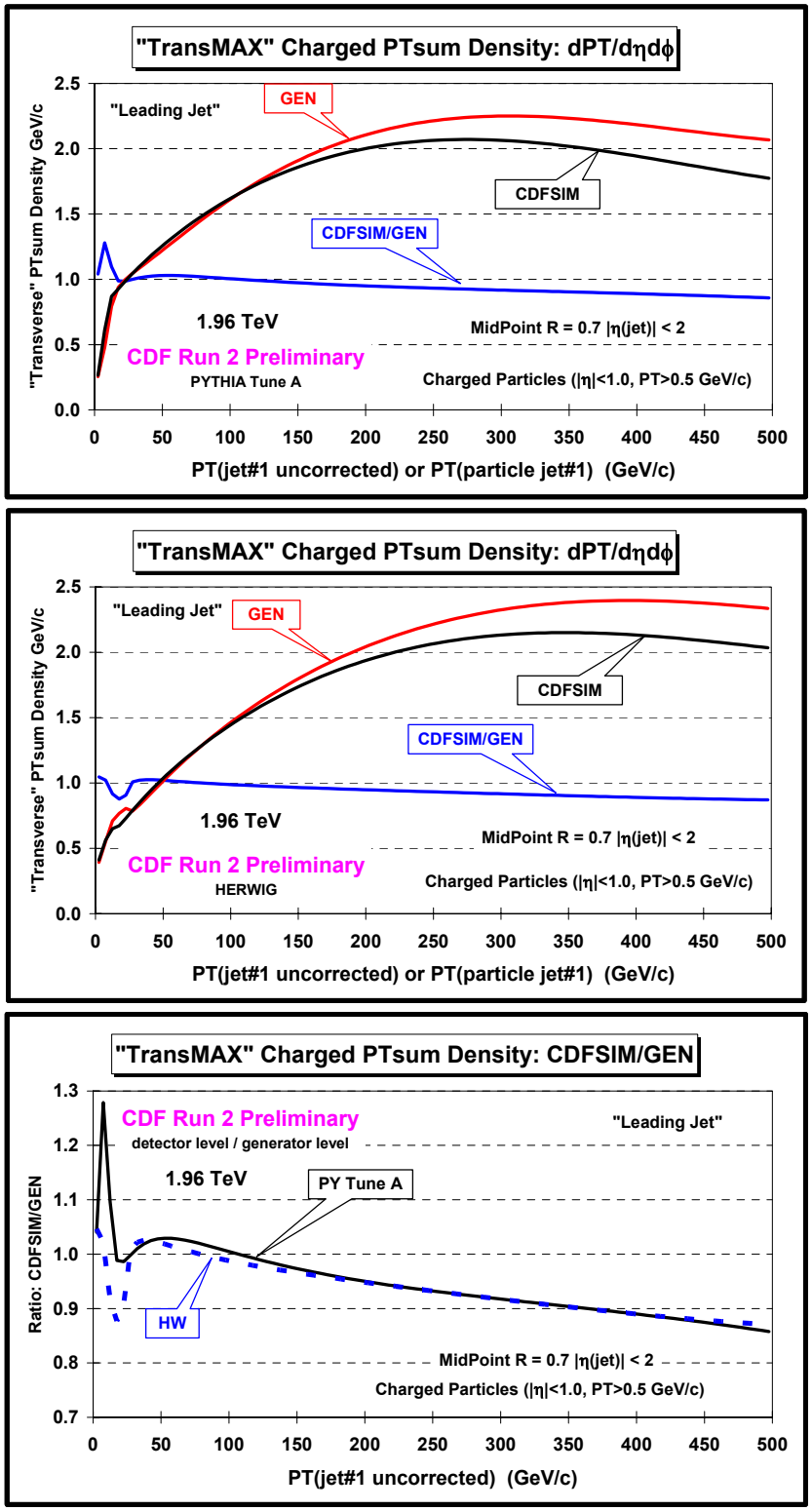

Fig. 12. Method 1 response factors for the PTsum density of charged particles, dPTsum/dηdϕ, with $p_T > 0.5$ GeV/c and $|\eta| < 1$ in the "transMAX" region for "leading jet" events defined in Fig. 5 as a function of the leading jet P_T. Shows the particle level prediction (GEN) versus the leading particle jet P_T and the detector level result (CDFSIM) versus the leading calorimeter jet P_T (uncorrected) with $|\eta(\text{jet}\#1)| < 2$ for PYTHIA Tune A (*top*) and HERWIG (*middle*). Also shows the ratio of the detector level to the particle level, CDFSIM/GEN, versus the leading jet P_T (*i.e.* response factor).

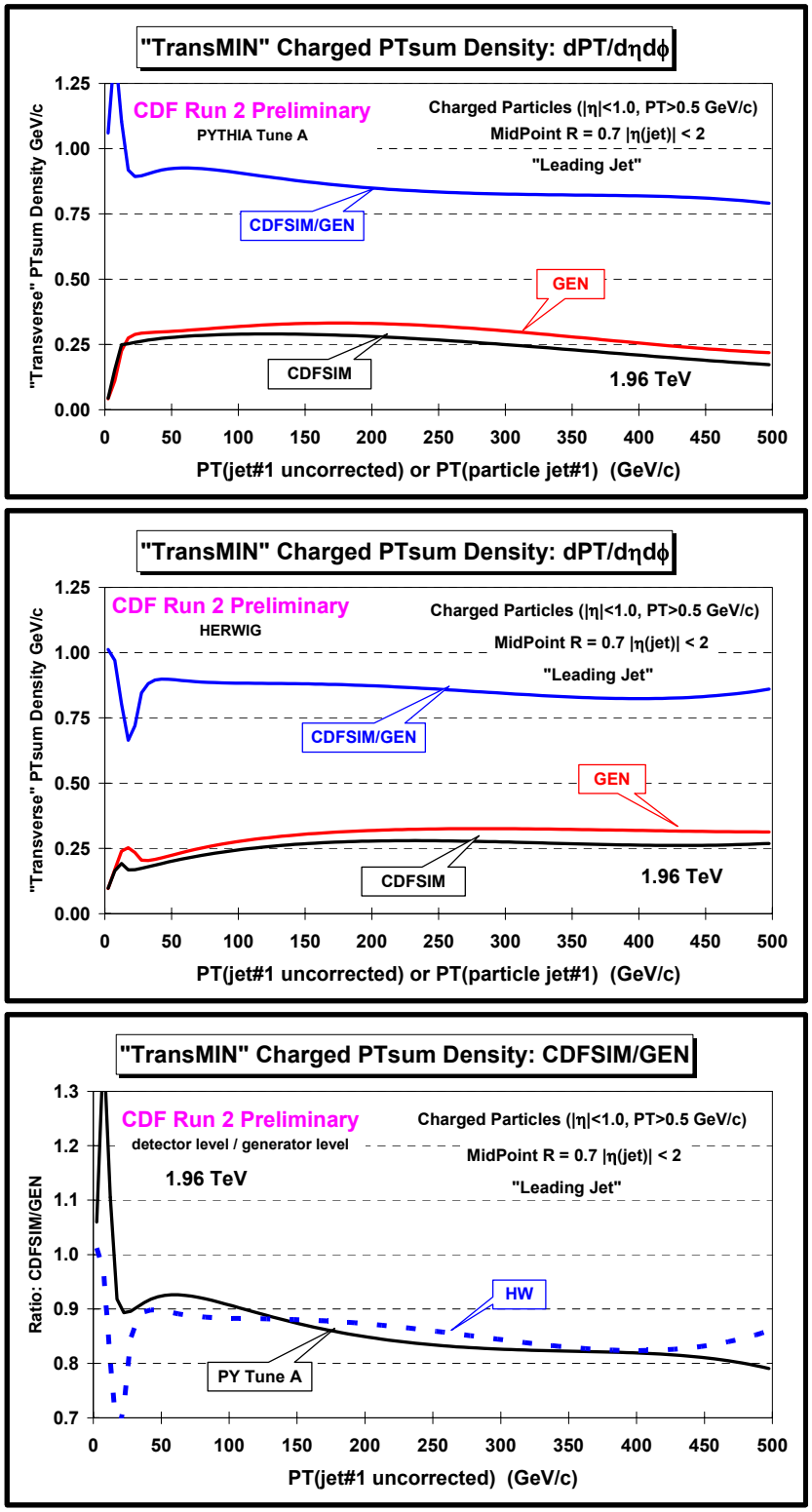

Fig. 13. Method 1 response factors for the PTsum density of charged particles, dPTsum/dηdϕ, with $p_T > 0.5$ GeV/c and $|\eta| < 1$ in the "transMIN" region for "leading jet" events defined in Fig. 5 as a function of the leading jet P_T. Shows the particle level prediction (GEN) versus the leading particle jet P_T and the detector level result (CDFSIM) versus the leading calorimeter jet P_T (uncorrected) with $|\eta(\text{jet}\#1)| < 2$ for PYTHIA Tune A (*top*) and HERWIG (*middle*). Also shows the ratio of the detector level to the particle level, CDFSIM/GEN, versus the leading jet P_T (*i.e.* response factor).

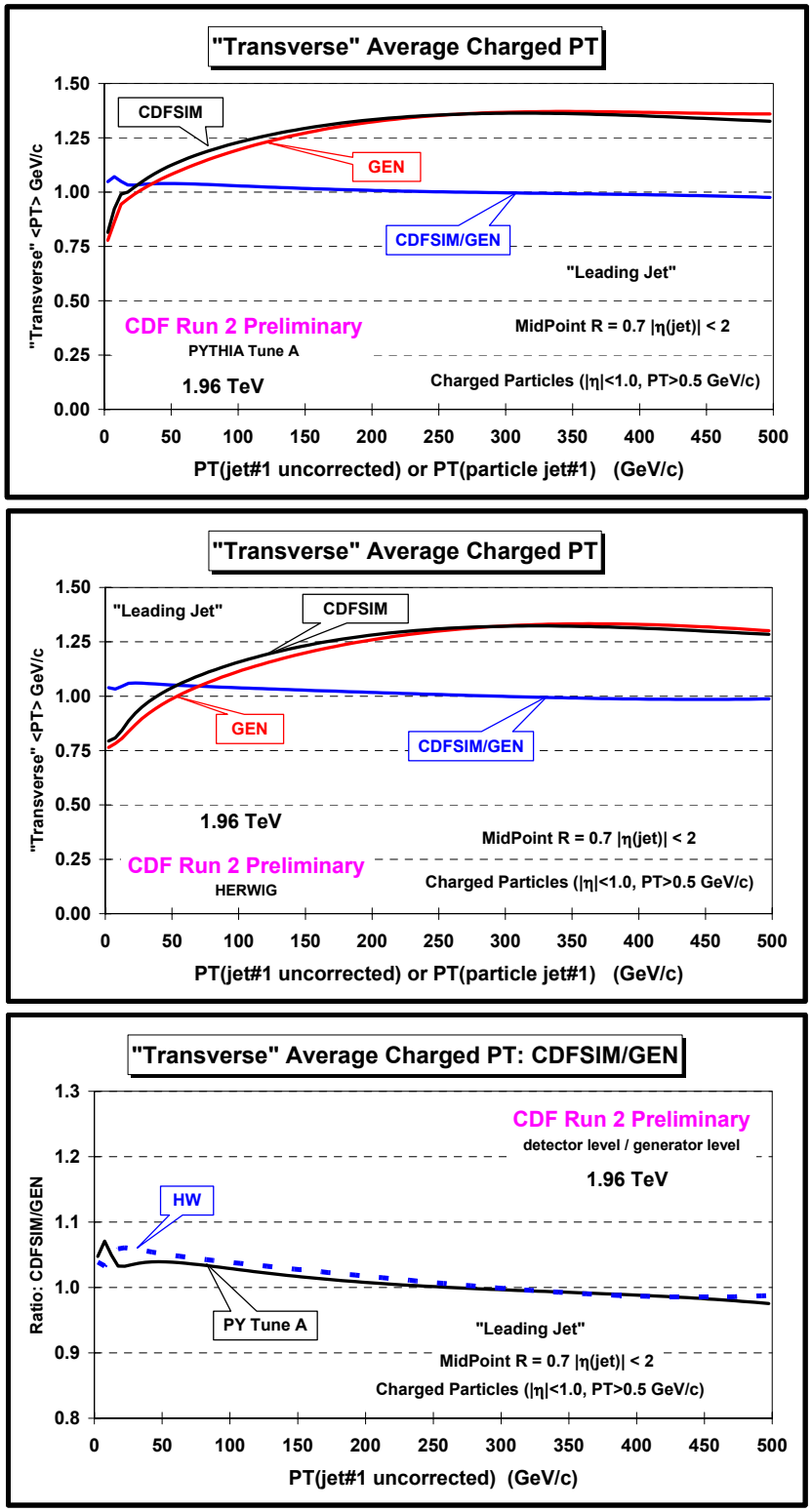

Fig. 14. Method 1 response factors for the average $\langle p_T \rangle$ of charged particles with $p_T > 0.5$ GeV/c and $|\eta| < 1$ in the "transverse" region for "leading jet" events defined in Fig. 5 as a function of the leading jet P_T. Shows the particle level prediction (GEN) versus the leading particle jet P_T and the detector level result (CDFSIM) versus the leading calorimeter jet P_T (uncorrected) with $|\eta(\text{jet}\#1)| < 2$ for PYTHIA Tune A (*top*) and HERWIG (*middle*). Also shows the ratio of the detector level to the particle level, CDFSIM/GEN, versus the leading jet P_T (*i.e.* response factor).

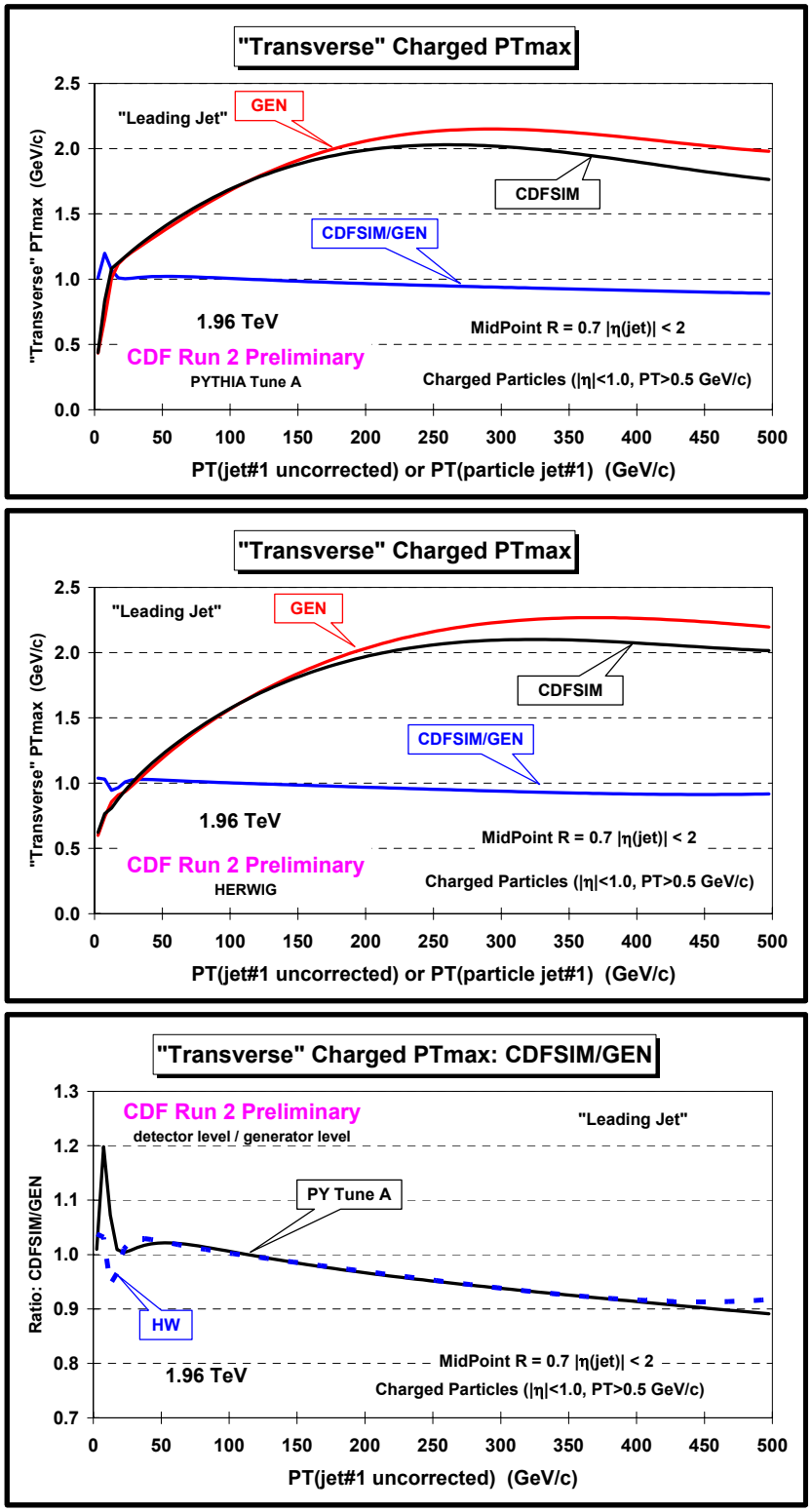

Fig. 15. Method 1 response factors for the average maximum p_T, PTmax, for charged particles with $p_T > 0.5$ GeV/c and $|\eta| < 1$ in the "transverse" region for "leading jet" events defined in Fig. 5 as a function of the leading jet P_T. Shows the particle level prediction (GEN) versus the leading particle jet P_T and the detector level result (CDFSIM) versus the leading calorimeter jet P_T (uncorrected) with $|\eta(\text{jet}\#1)| < 2$ for PYTHIA Tune A (*top*) and HERWIG (*middle*). Also shows the ratio of the detector level to the particle level, CDFSIM/GEN, versus the leading jet P_T (*i.e.* response factor).

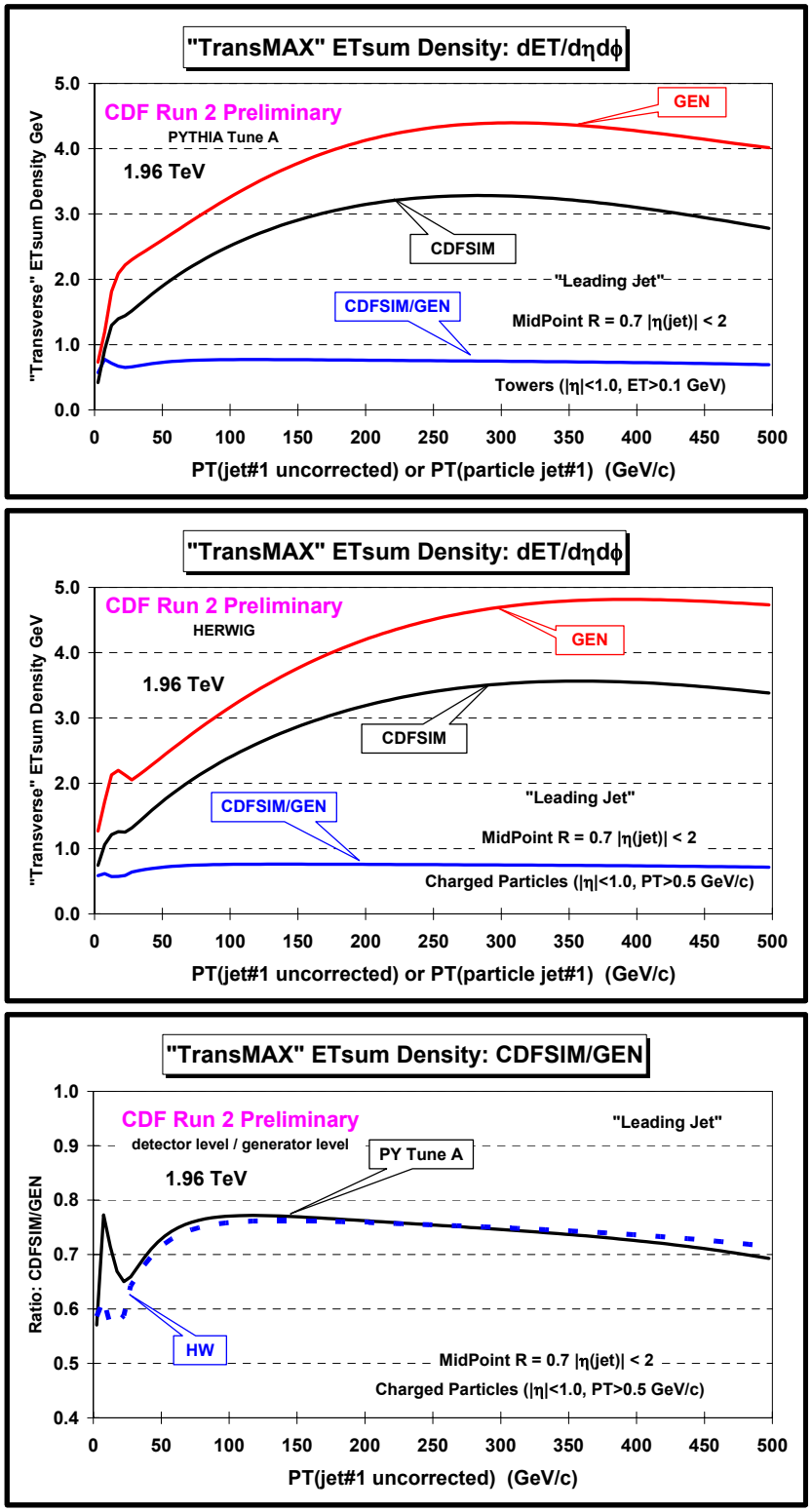

Fig. 16. Method 1 response factors for the ETsum density of all particles, $dE_T/d\eta d\phi$, with $|\eta| < 1$ in the "transMAX" regions for "leading jet" events defined in Fig. 5 as a function of the leading jet P_T. Shows the particle level prediction (GEN) versus the leading particle jet P_T and the detector level result (CDFSIM) versus the leading calorimeter jet P_T (uncorrected) with $|\eta(\text{jet}\#1)| < 2$ for PYTHIA Tune A (*top*) and HERWIG (*middle*). Also shows the ratio of the detector level to the particle level, CDFSIM/GEN, versus the leading jet P_T (*i.e.* response factor).

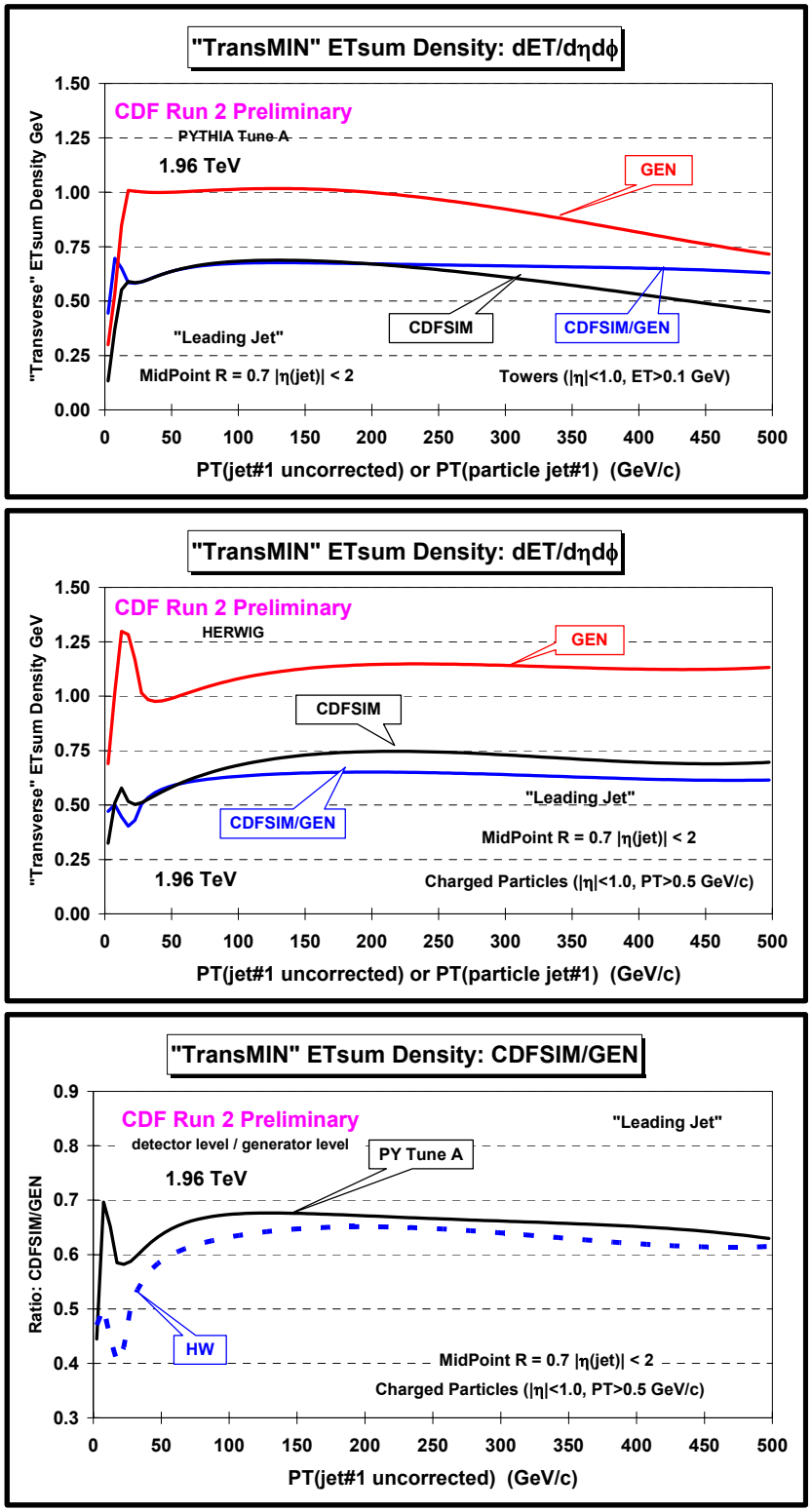

Fig. 17. Method 1 response factors for the ETsum density of all particles, $dE_T/d\eta d\phi$, with $|\eta| < 1$ in the "transMIN" regions for "leading jet" events defined in Fig. 5 as a function of the leading jet P_T. Shows the particle level prediction (GEN) versus the leading particle jet P_T and the detector level result (CDFSIM) versus the leading calorimeter jet P_T (uncorrected) with $|\eta(\text{jet}\#1)| < 2$ for PYTHIA Tune A (*top*) and HERWIG (*middle*). Also shows the ratio of the detector level to the particle level, CDFSIM/GEN, versus the leading jet P_T (*i.e.* response factor).

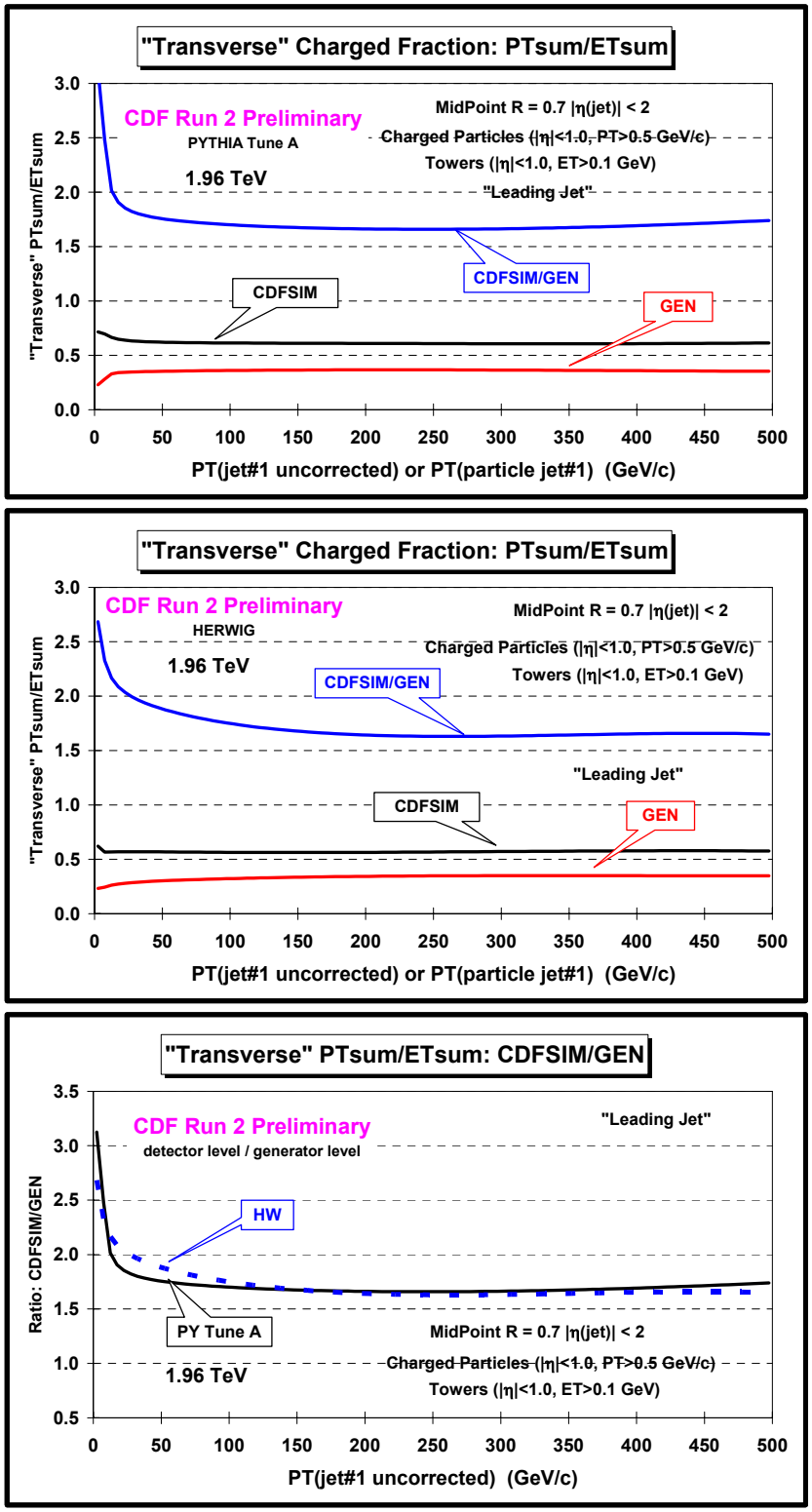

Fig. 18. Method 1 response factors for the charged fraction, PTsum/ETsum, in the "transverse" region for "leading jet" events defined in Fig. 5 as a function of the leading jet P_T, where PTsum includes charged particles with $p_T > 0.5$ GeV/c and $|\eta| < 1$ and the ETsum includes all particles with $|\eta| < 1$. Shows the particle level prediction (GEN) versus the leading particle jet P_T and the detector level result (CDFSIM) versus the leading calorimeter jet P_T (uncorrected) with $|\eta(\text{jet}\#1)| < 2$ for PYTHIA Tune A (*top*) and HERWIG (*middle*). Also shows the ratio of the detector level to the particle level, CDFSIM/GEN, versus the leading jet P_T (*i.e.* response factor).

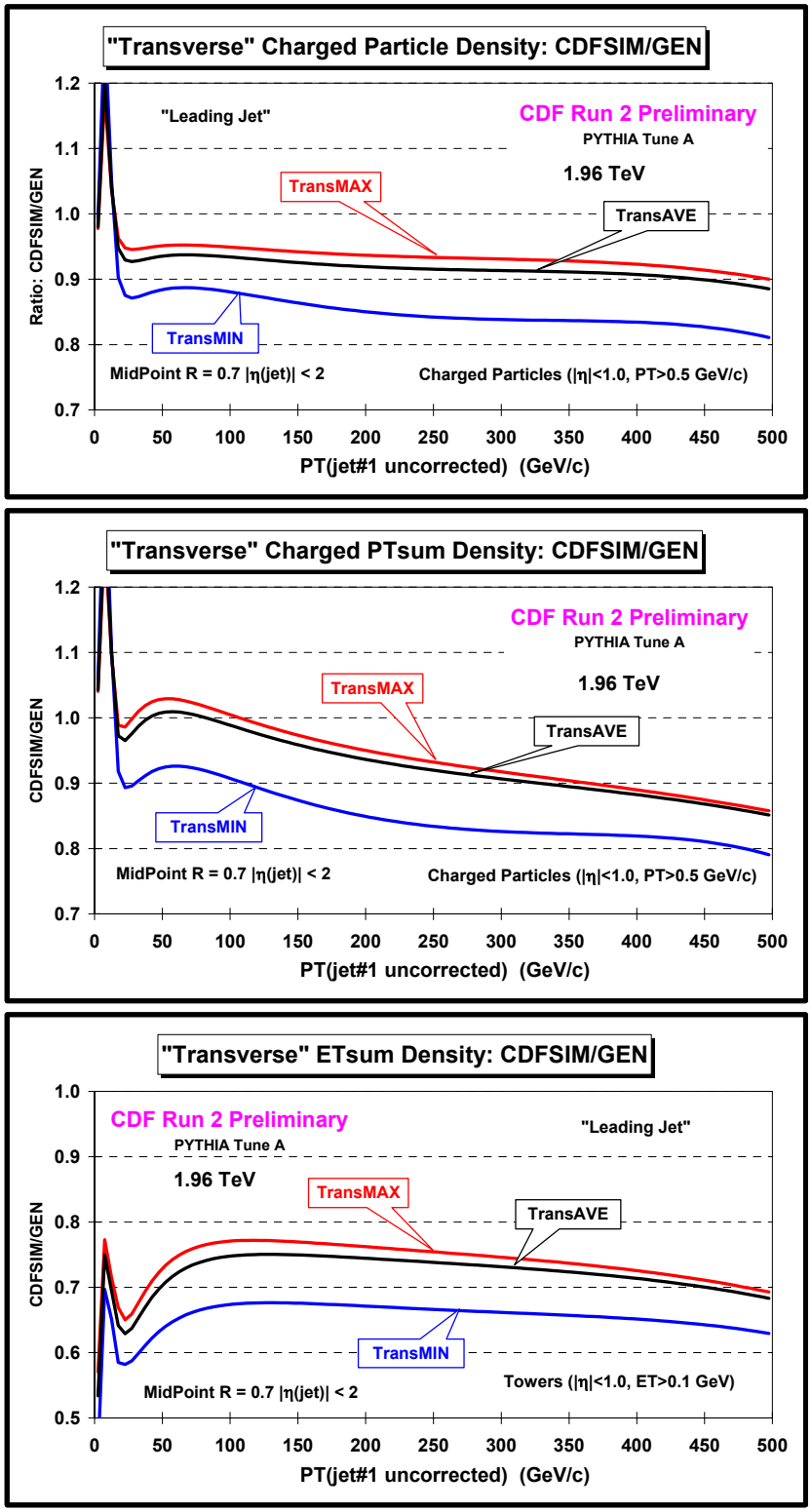

Fig. 19. Shows the ratio of the detector level to the particle level, CDFSIM/GEN, versus the leading jet P_T (method 1 response factors) for PYTHIA Tune A for the "transMAX", "transMIN", and "transverse" regions for "leading jet" events defined in Fig. 5 as a function of the leading jet P_T. Shows the density of charged particles $dN_{chg}/d\eta d\phi$ with $p_T > 0.5$ GeV/c and $|\eta| < 1$ (*top*), the PTsum density of charged particles $dPT_{sum}/d\eta d\phi$ with $p_T > 0.5$ GeV/c and $|\eta| < 1$ (*middle*), and ETsum density of all particles $dE_T/d\eta d\phi$ with $|\eta| < 1$ (*bottom*).

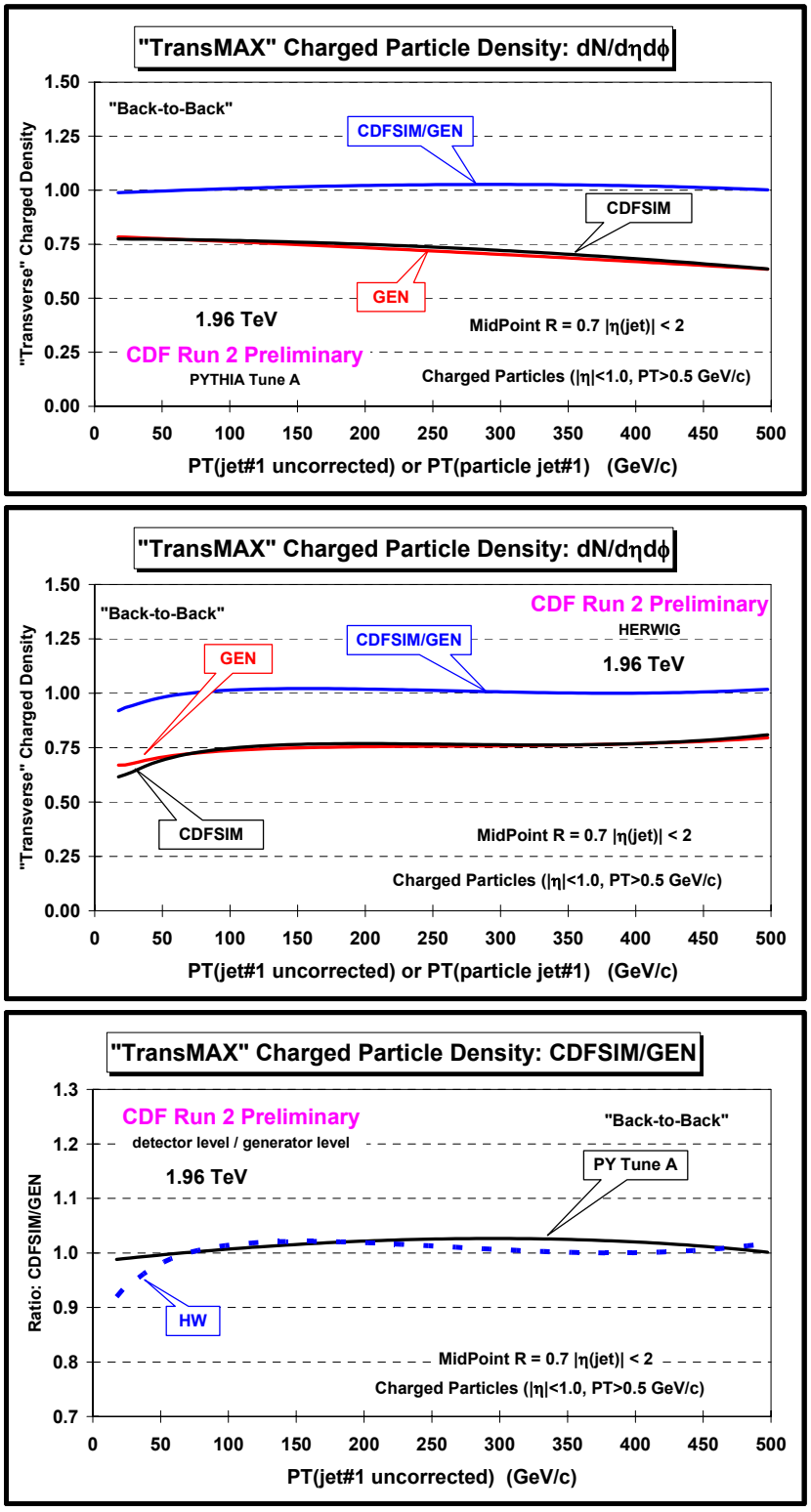

Fig. 20. Method 1 response factors for the density of charged particles, dNchg/dηdϕ, with $p_T > 0.5$ GeV/c and $|\eta| < 1$ in the "transMAX" region for "back-to-back" events defined in Fig. 5 as a function of the leading jet P_T. Shows the particle level prediction (GEN) versus the leading particle jet P_T and the detector level result (CDFSIM) versus the leading calorimeter jet P_T (uncorrected) with $|\eta(\text{jet}\#1)| < 2$ for PYTHIA Tune A (*top*) and HERWIG (*middle*). Also shows the ratio of the detector level to the particle level, CDFSIM/GEN, versus the leading jet P_T (*i.e.* response factor).

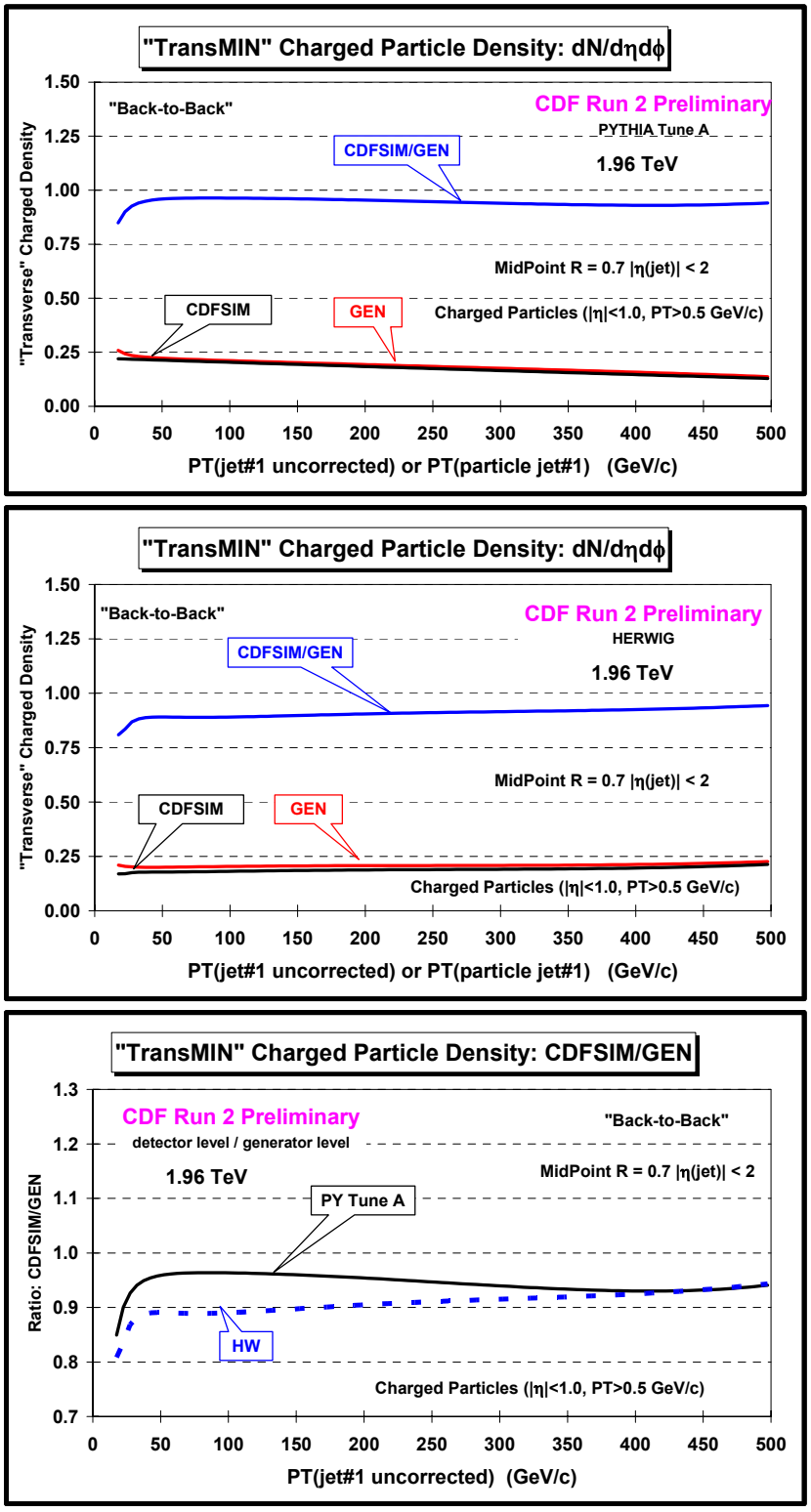

Fig. 21. Method 1 response factors for the density of charged particles, dNchg/dηdϕ, with $p_T > 0.5$ GeV/c and $|\eta| < 1$ in the "transMIN" region for "back-to-back" events defined in Fig. 5 as a function of the leading jet P_T. Shows the particle level prediction (GEN) versus the leading particle jet P_T and the detector level result (CDFSIM) versus the leading calorimeter jet P_T (uncorrected) with $|\eta(\text{jet}\#1)| < 2$ for PYTHIA Tune A (*top*) and HERWIG (*middle*). Also shows the ratio of the detector level to the particle level, CDFSIM/GEN, versus the leading jet P_T (*i.e.* response factor).

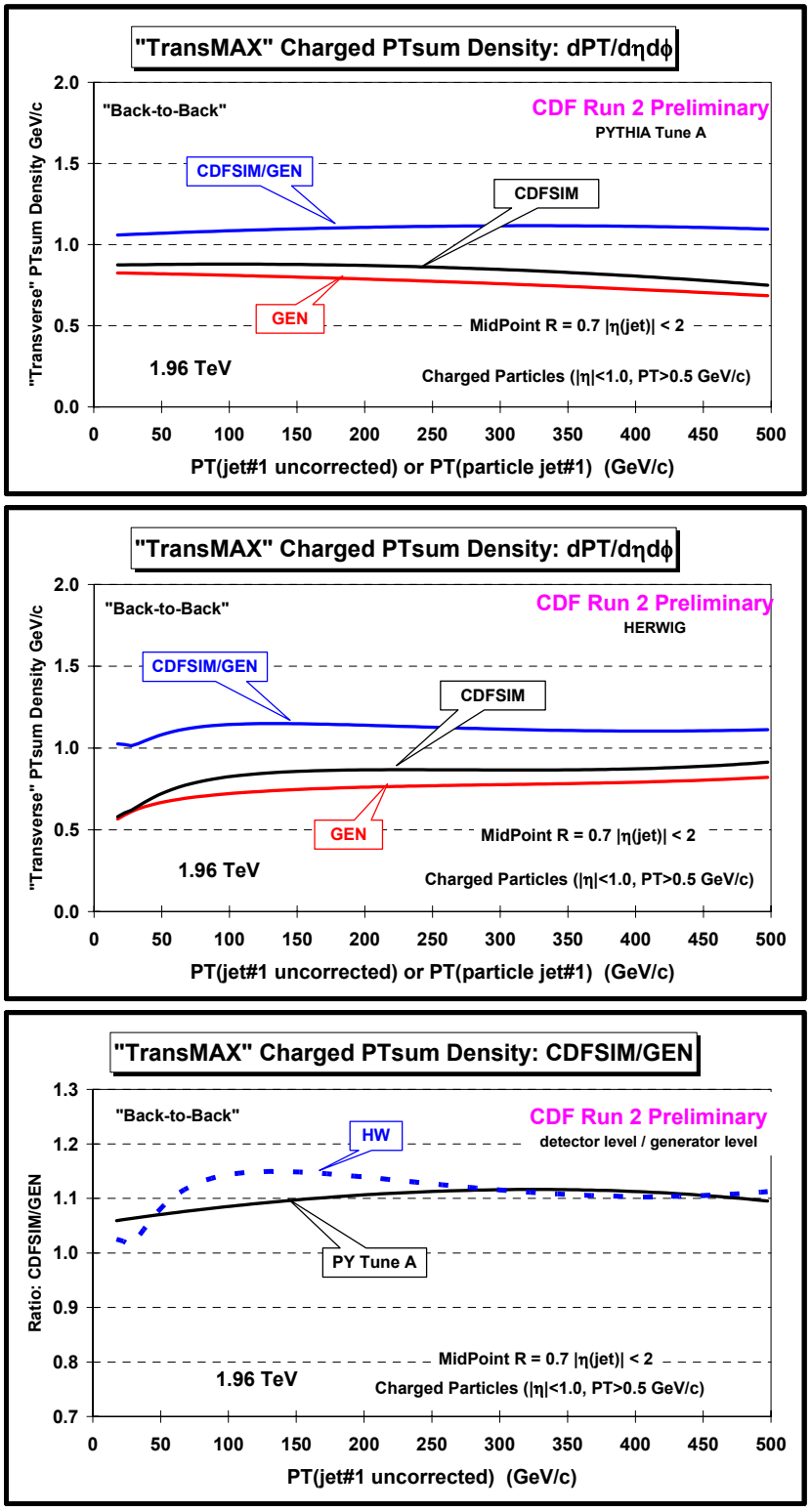

Fig. 22. Method 1 response factors for the PTsum density of charged particles, dPTsum/dηdϕ, with $p_T > 0.5$ GeV/c and $|\eta| < 1$ in the "transMAX" region for "back-to-back" events defined in Fig. 5 as a function of the leading jet P_T. Shows the particle level prediction (GEN) versus the leading particle jet P_T and the detector level result (CDFSIM) versus the leading calorimeter jet P_T (uncorrected) with $|\eta(\text{jet}\#1)| < 2$ for PYTHIA Tune A (*top*) and HERWIG (*middle*). Also shows the ratio of the detector level to the particle level, CDFSIM/GEN, versus the leading jet P_T (*i.e.* response factor).

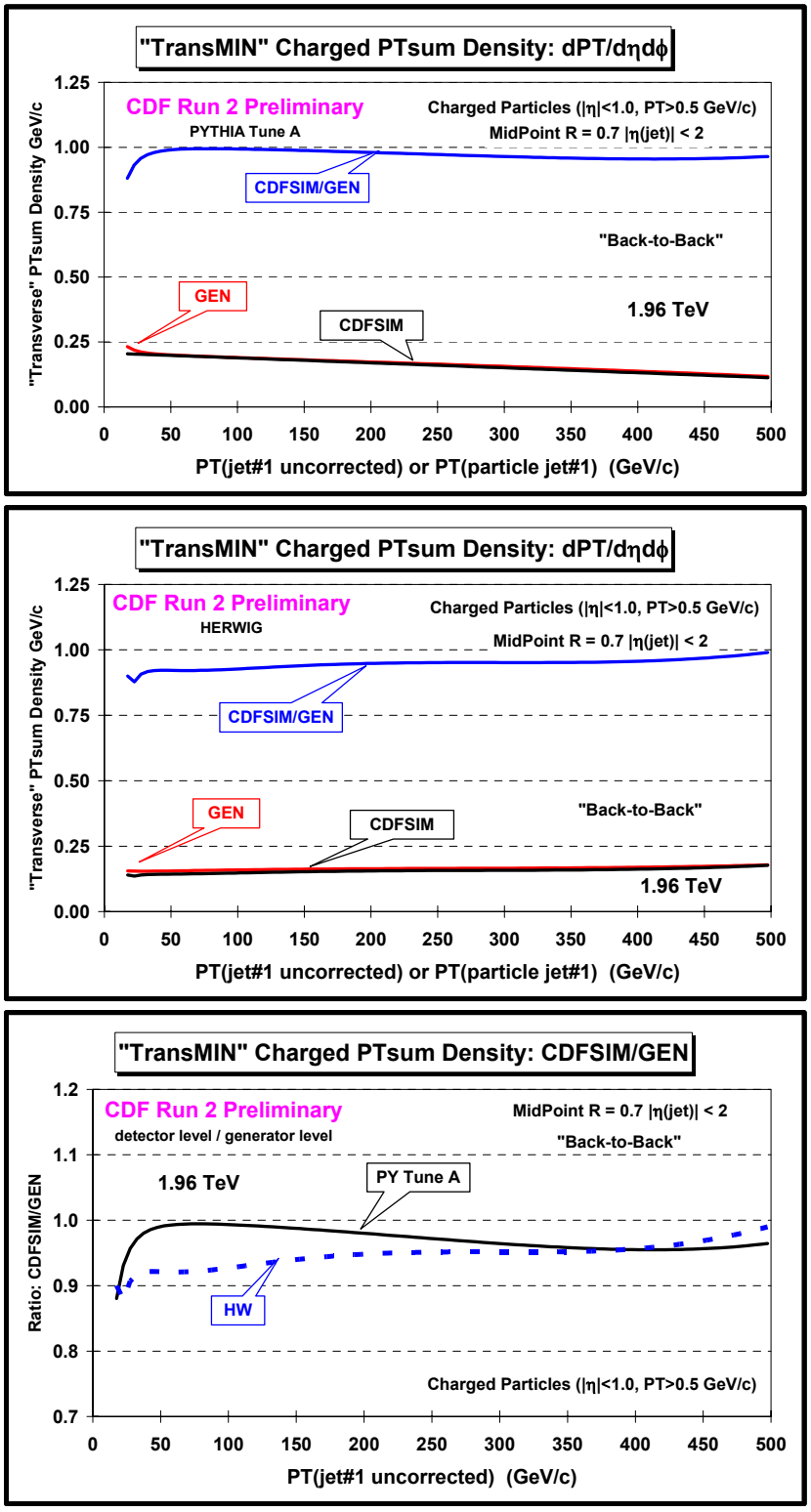

Fig. 23. Method 1 response factors for the PTsum density of charged particles, dPTsum/dηdϕ, with $p_T > 0.5$ GeV/c and $|\eta| < 1$ in the "transMIN" region for "back-to-back" events defined in Fig. 5 as a function of the leading jet P_T. Shows the particle level prediction (GEN) versus the leading particle jet P_T and the detector level result (CDFSIM) versus the leading calorimeter jet P_T (uncorrected) with $|\eta(\text{jet}\#1)| < 2$ for PYTHIA Tune A (*top*) and HERWIG (*middle*). Also shows the ratio of the detector level to the particle level, CDFSIM/GEN, versus the leading jet P_T (*i.e.* response factor).

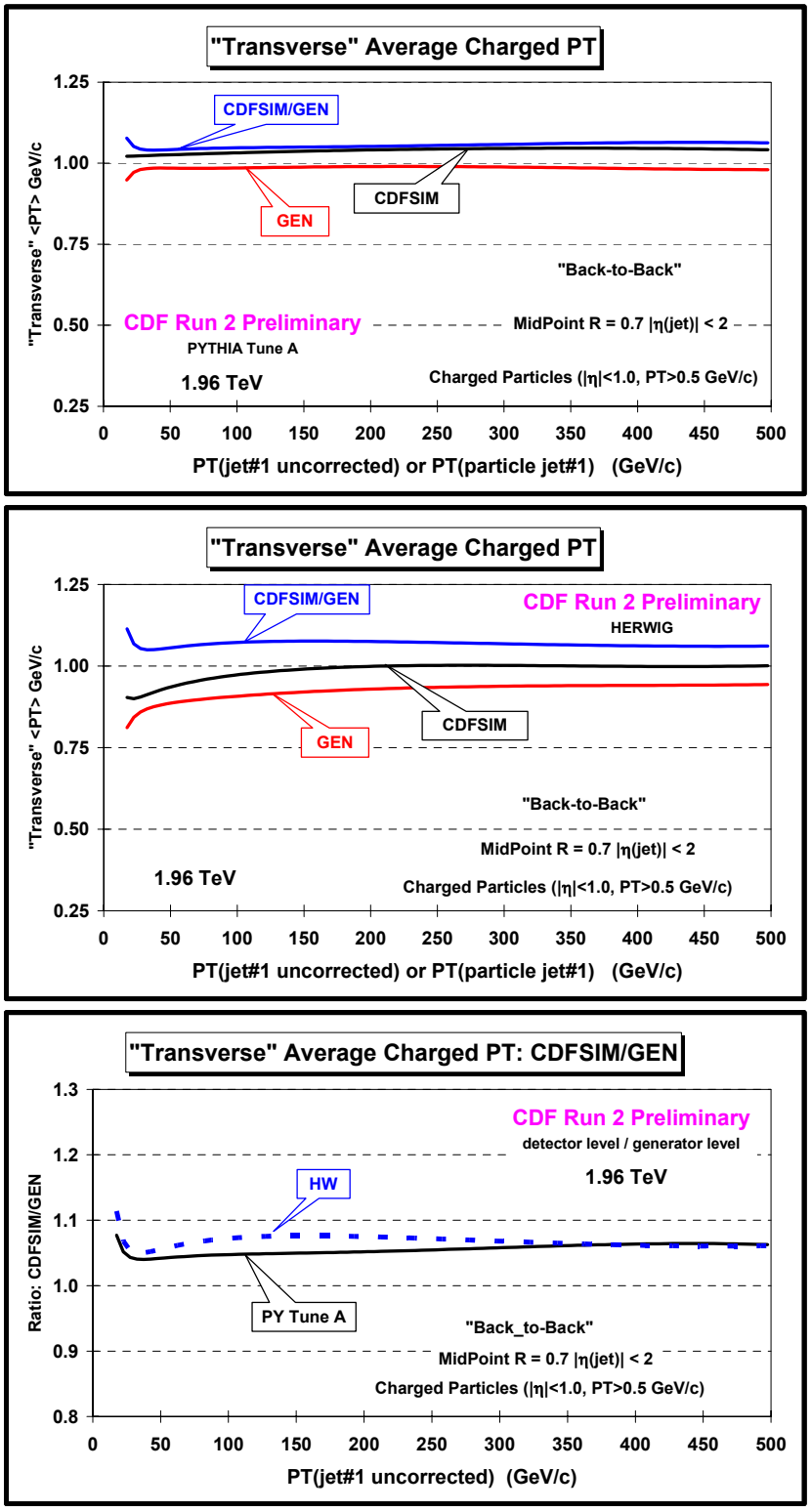

Fig. 24. Method 1 response factors for the average $\langle p_T \rangle$ of charged particles with $p_T > 0.5$ GeV/c and $|\eta| < 1$ in the "transverse" region for "back-to-back" events defined in Fig. 5 as a function of the leading jet P_T. Shows the particle level prediction (GEN) versus the leading particle jet P_T and the detector level result (CDFSIM) versus the leading calorimeter jet P_T (uncorrected) with $|\eta(\text{jet}\#1)| < 2$ for PYTHIA Tune A (*top*) and HERWIG (*middle*). Also shows the ratio of the detector level to the particle level, CDFSIM/GEN, versus the leading jet P_T (*i.e.* response factor).

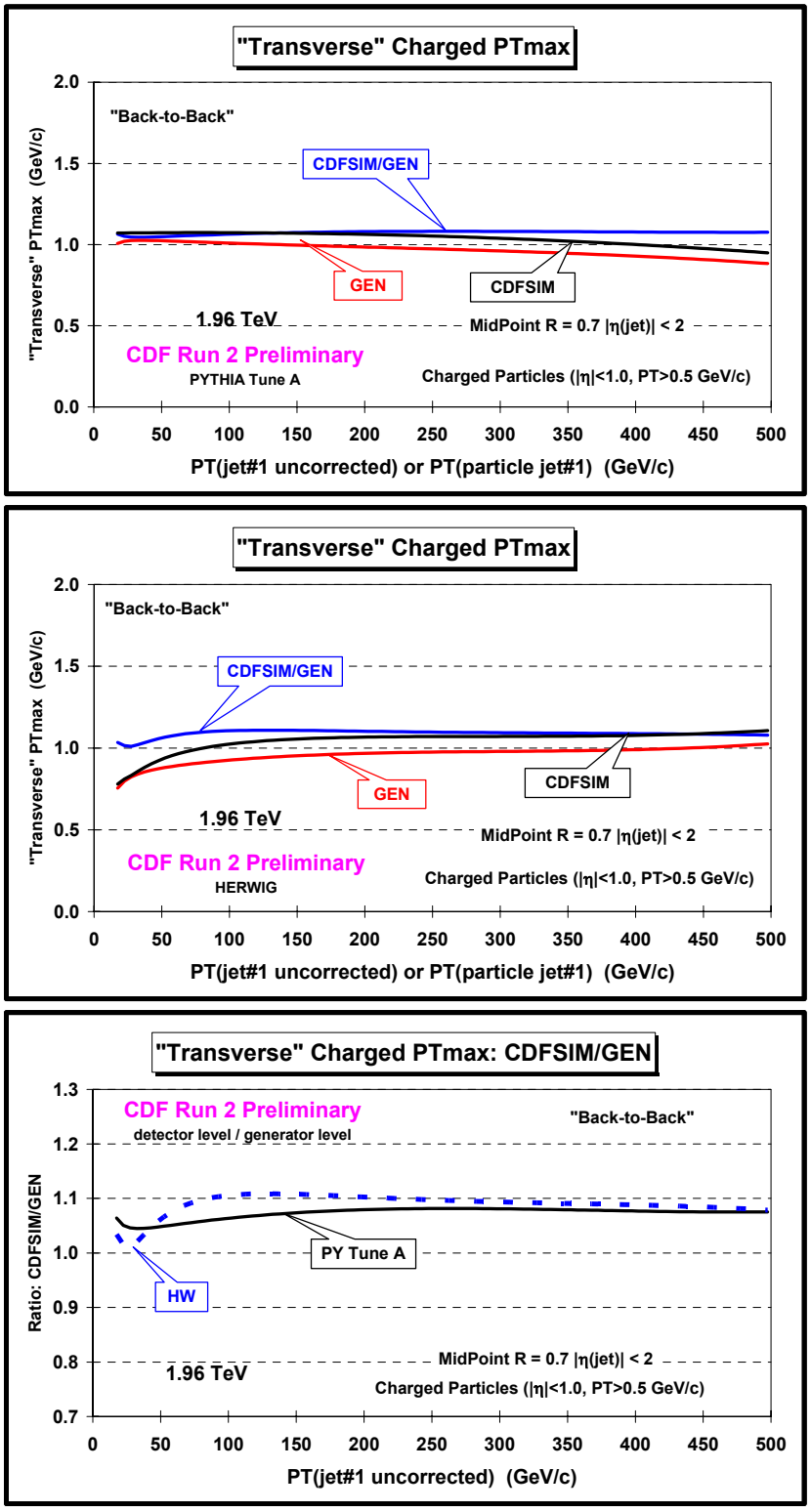

Fig. 25. Method 1 response factors for the average maximum p_T, PTmax, for charged particles with $p_T > 0.5$ GeV/c and $|\eta| < 1$ in the "transverse" region for "back-to-back" events defined in Fig. 5 as a function of the leading jet P_T. Shows the particle level prediction (GEN) versus the leading particle jet P_T and the detector level result (CDFSIM) versus the leading calorimeter jet P_T (uncorrected) with $|\eta(\text{jet}\#1)| < 2$ for PYTHIA Tune A (*top*) and HERWIG (*middle*). Also shows the ratio of the detector level to the particle level, CDFSIM/GEN, versus the leading jet P_T (*i.e.* response factor).

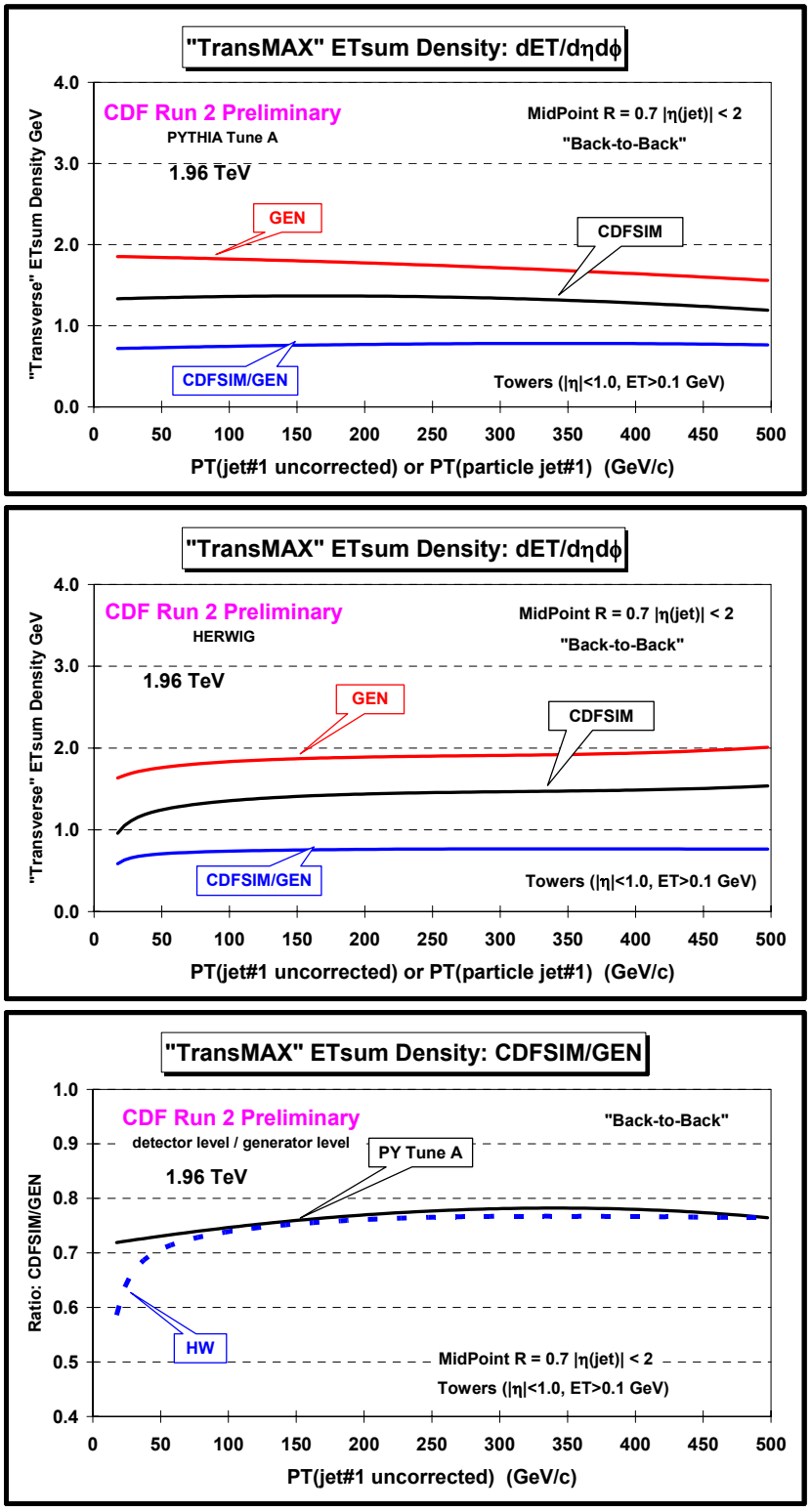

Fig. 26. Method 1 response factors for the ETsum density of all particles, $dE_T/d\eta d\phi$, with $|\eta| < 1$ in the "transMAX" regions for "back-to-back" events defined in Fig. 5 as a function of the leading jet P_T. Shows the particle level prediction (GEN) versus the leading particle jet P_T and the detector level result (CDFSIM) versus the leading calorimeter jet P_T (uncorrected) with $|\eta(\text{jet}\#1)| < 2$ for PYTHIA Tune A (*top*) and HERWIG (*middle*). Also shows the ratio of the detector level to the particle level, CDFSIM/GEN, versus the leading jet P_T (*i.e.* response factor).

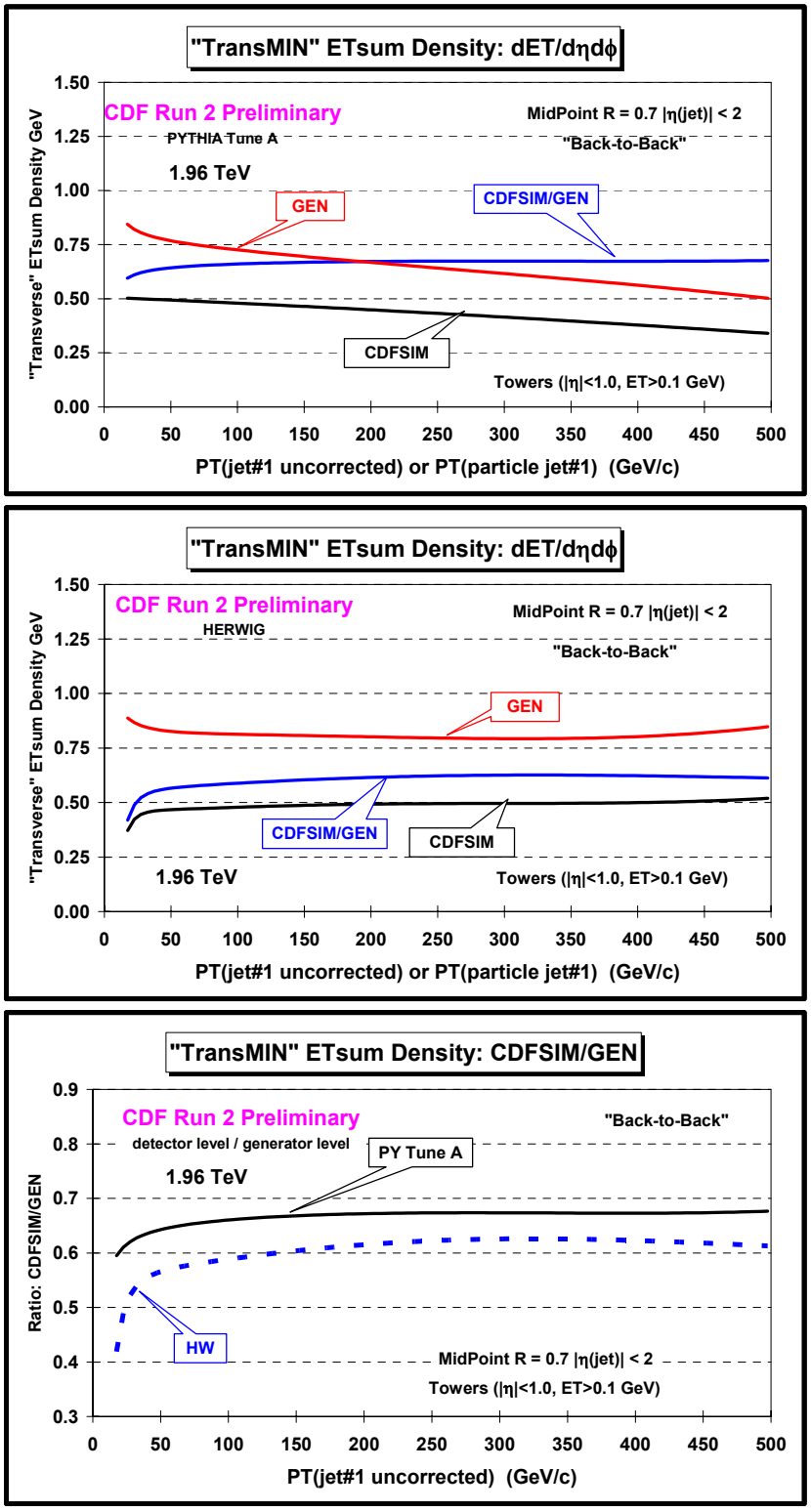

Fig. 27. Method 1 response factors for the ETsum density of all particles, $dE_T/d\eta d\phi$, with $|\eta| < 1$ in the "transMIN" regions for "back-to-back" events defined in Fig. 5 as a function of the leading jet P_T. Shows the particle level prediction (GEN) versus the leading particle jet P_T and the detector level result (CDFSIM) versus the leading calorimeter jet P_T (uncorrected) with $|\eta(\text{jet}\#1)| < 2$ for PYTHIA Tune A (*top*) and HERWIG (*middle*). Also shows the ratio of the detector level to the particle level, CDFSIM/GEN, versus the leading jet P_T (*i.e.* response factor).

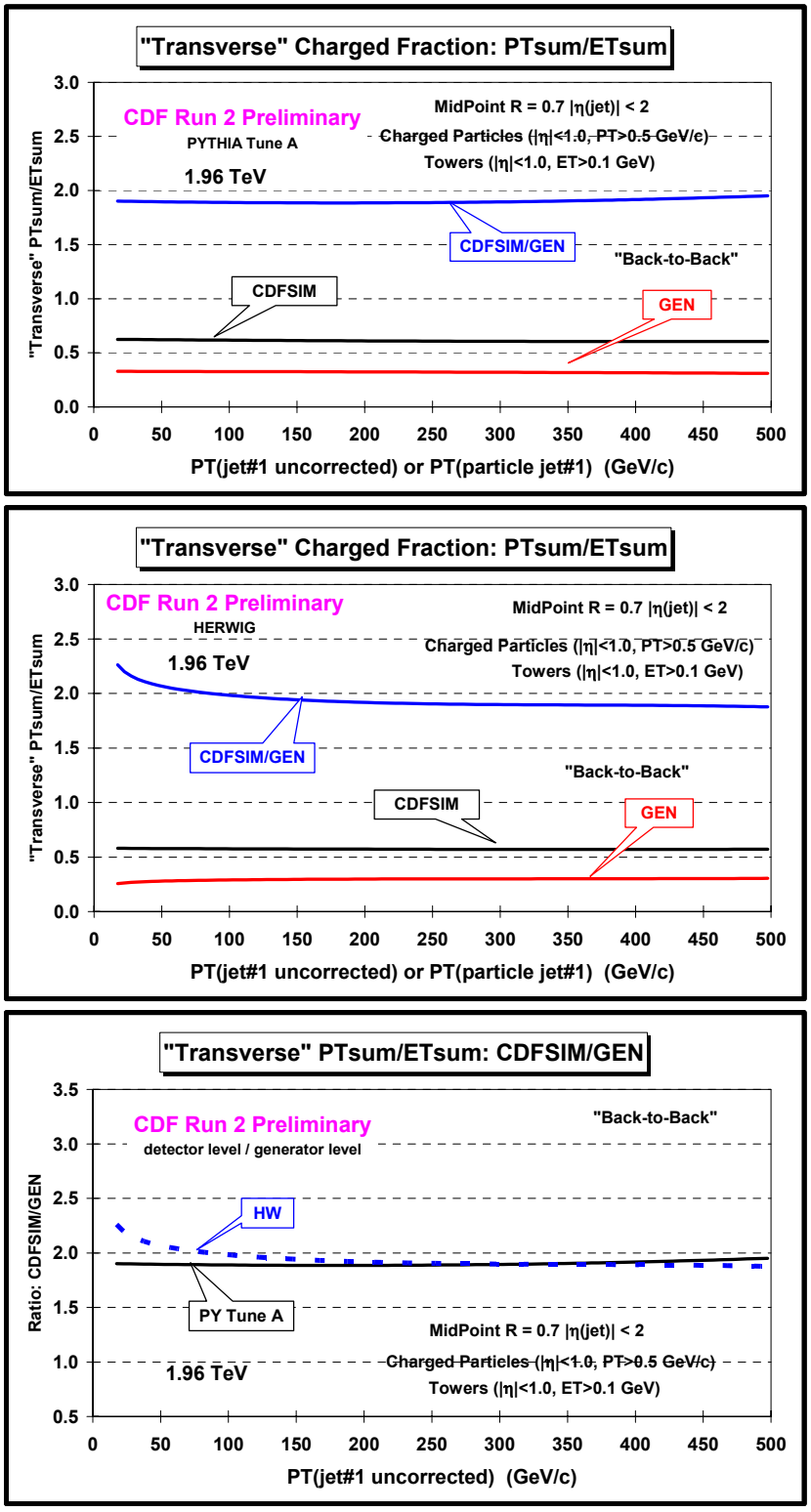

Fig. 28. Method 1 response factors for the charged fraction, PTsum/ETsum, in the "transverse" region for "back-to-back" events defined in Fig. 5 as a function of the leading jet P_T, where PTsum includes charged particles with $p_T > 0.5$ GeV/c and $|\eta| < 1$ and the ETsum includes all particles with $|\eta| < 1$. Shows the particle level prediction (GEN) versus the leading particle jet P_T and the detector level result (CDFSIM) versus the leading calorimeter jet P_T (uncorrected) with $|\eta(\text{jet}\#1)| < 2$ for PYTHIA Tune A (*top*) and HERWIG (*middle*). Also shows the ratio of the detector level to the particle level, CDFSIM/GEN, versus the leading jet P_T (*i.e.* response factor).

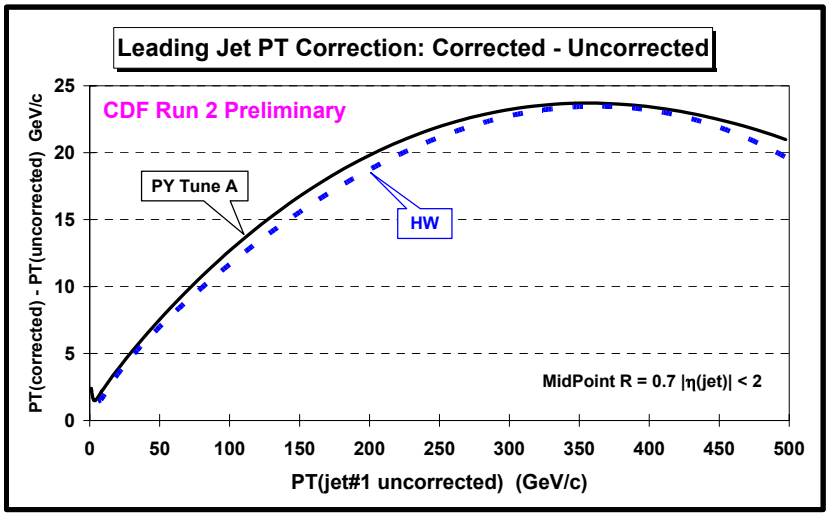

Fig. 29. Leading jet P_T correction used in method 2 for "leading jet" events. Shows the difference in the observed leading jet P_T at the detector level (*i.e.* in the calorimeter) compared with the true P_T (*i.e.* corrected) of matched leading particle jets using PYTHIA Tune A and HERWIG.

III. Data Selection and Systematic Errors

(1) Data Selection

The data used in this analysis arise from the set of Stntuples created for the QCD group by Anwar Bhatti, Ken Hatakeyama, and Craig Group (see Table 6). Events are required to be on the "goodrun" list (version 7). They are also required to have a missing E_T significance less than 5 $GeV^{1/2}$ and to have a sumET < 1.5 TeV. Except for the Min-Bias data we require events to have one and only one quality 12 vertex with |z| < 60 cm. For the Min-Bias data we allow zero or one quality 12 vertices. This only affects the observables in Table 2 for leading jet P_T below 10 GeV/c. Above P_T(jet#1) = 10 GeV/c the fraction of events with no quality 12 vertex is negligible.

Table 6. Data sets (5.3.3nt) and event selection criterion used in this analysis ($L \sim 380$ pb^{-1}).

Event Selection	Min-Bias	JET20	JET50	JET70	JET100
Total Events	20,586,733	30,470,383	9,908,366	4,641,247	5,366,515
"Good" Events (version 7)	18,180,015	19,835,681	6,868,114	3,432,992	4,031,324
MetSig < 5 $GeV^{1/2}$, sumET < 1.5 TeV	18,179,280	19,818,879	6,785,357	3,316,514	3,602,989
1 Q12 ZVtx, |z| < 60 cm	15,416,180	10,851,963	3,745,616	1,794,739	1,939,382
"Leading Jet" |η(jet#1) < 2|	3,712,407	7,679,594	3,200,065	1,648,764	1,884,353
"Back-to-Back" P_T(jet#3) < 15 GeV/c	2,474	1,462,547	878,014	491,930	602,256
"Back-to-Back"/"Leading Jet"	0.07%	19.04%	27.44%	29.84%	31.96%

As in our Run 1 analysis [2] we consider charged particles in the region $p_T > 0.5$ GeV/c and |η| < 1 where the COT efficiency is high. Our track selection criterion shown in Table 7 is the same as our Run 1 analysis.

Table 7. Track Selection criterion.

Track Selection
COT measured tracks
$\|z\text{-}z_0\| < 2$ cm
$\|d_0\| < 1$ cm
$p_T > 0.5$ GeV/c, $\|\eta\| < 1$

In forming the observables in Table 2 the five trigger sets shown in Table 6 are pieced together as shown in Table 8. The "looser" trigger set is used until it overlaps the next trigger set and then that trigger set is used until it overlaps the next trigger set etc..

Table 8. Range of P_T(jet#1) used for each data set.

Trigger Set	Calorimeter Jets
Min-Bias	P_T(jet#1) < 30 GeV
JET20	30 < P_T(jet#1) < 70 GeV
JET50	70 < P_T(jet#1) < 95 GeV
JET70	95 < P_T(jet#1) < 130 GeV
JET100	P_T(jet#1) > 130 GeV

(2) Systematic Uncertainty

The systematic uncertainty in correcting to the particle level is estimated by combining the two factors shown in Table 9. The first factor, σ_1, comes from correcting the observables in Table 2 to the particle level using method 1 and examining the bin-by-bin difference between PYTHIA Tune A and HERWIG for each observable. The second factor, σ_2, is set large enough to include the differences between method 1 and method 2 and pile-up (only affects the transverse energy).

Table 9. The errors on the corrected observables in Table 3 include both the statistical error and the systematic uncertainty (added in quadrature). The systematic uncertainty consists of σ_1 and σ_2 (added in quadrature).

Uncertainty	Origin
σ_1	Bin by bin difference between the data corrected by PYTHIA Tune A and HERWIG using method 1.
σ_2	Difference between method 1 and method 2 and pile-up and miscellaneous (3% for charged particle, 5% for energy)

Fig. 32 shows the data at 1.96 TeV corrected to the particle level using method 1 and method 2. The open red squares are the data corrected to the particle level using method 1 with errors that include both the statistical error and the systematic uncertainty (see Table 9). The black dots are the data corrected to the particle level using method 2 (with no errors). The method 2 points lie within the errors of the method 1 data points.

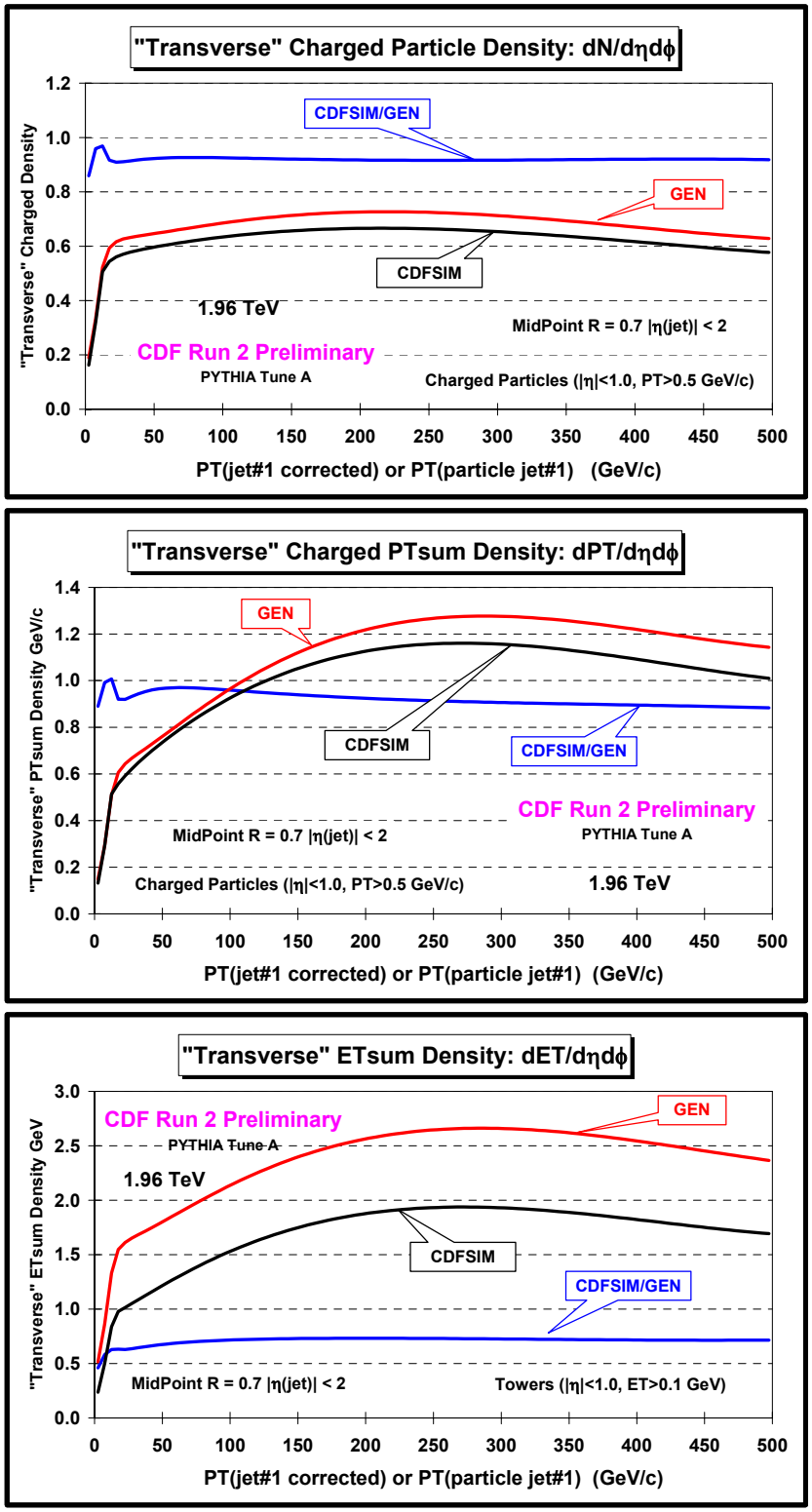

Fig. 30. Method 2 response factors from PYTHIA Tune A for "leading jet" events defined in Fig. 5 as a function of the leading jet P_T. Shows the particle level prediction (GEN) versus the leading particle jet P_T and the detector level result (CDFSIMcor) versus the leading calorimeter jet P_T (corrected) with $|\eta(\text{jet}\#1)| < 2$. Also shows the ratio of the detector level to the particle level, CDFSIMcor/GEN, versus the leading jet P_T (*i.e.* response factor).

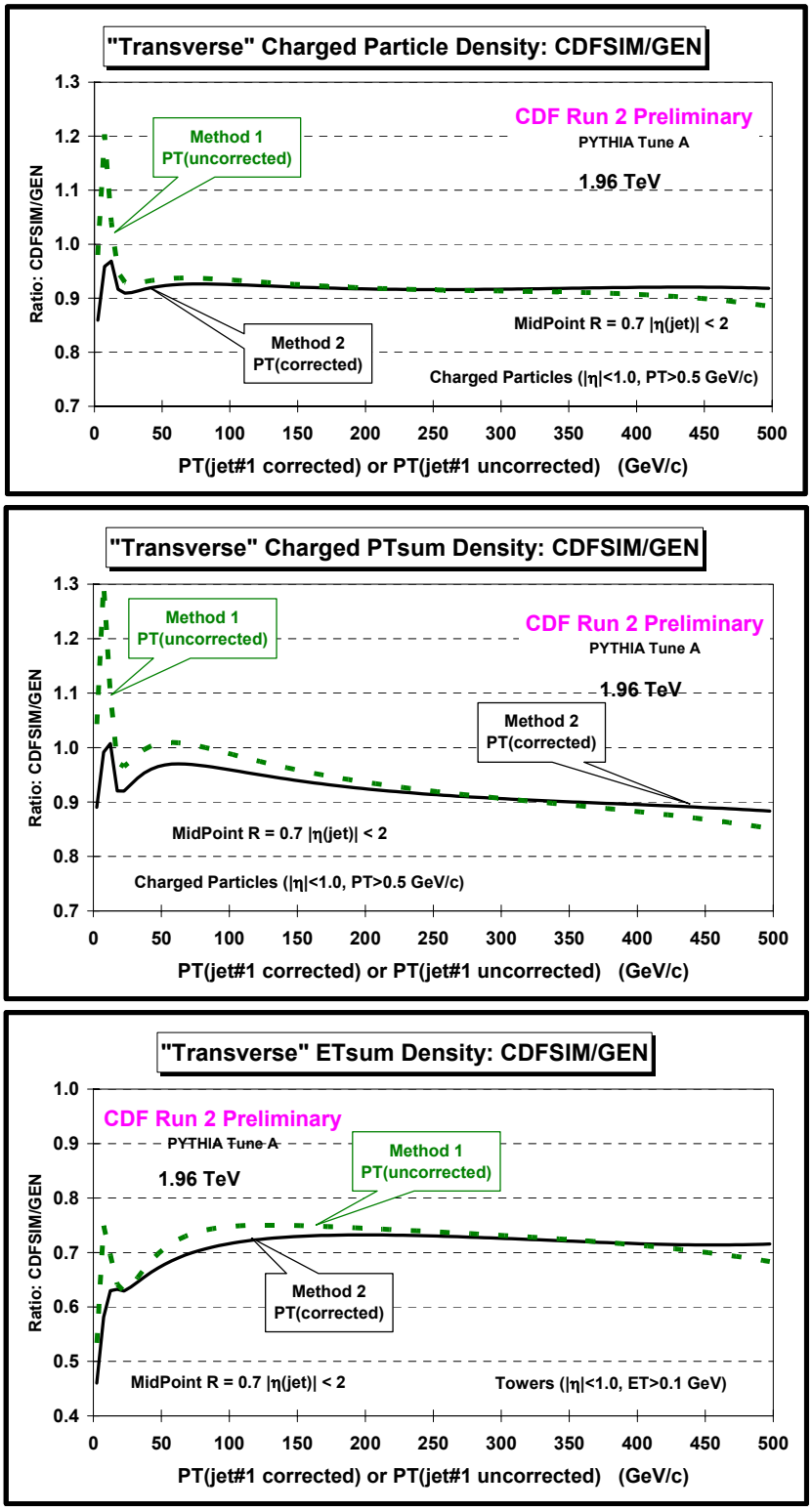

Fig. 31. Compares the method 1 response factors versus the leading jet P_T (uncorrected) with the method 2 response factors versus the leading jet P_T (corrected) from PYTHIA Tune A.

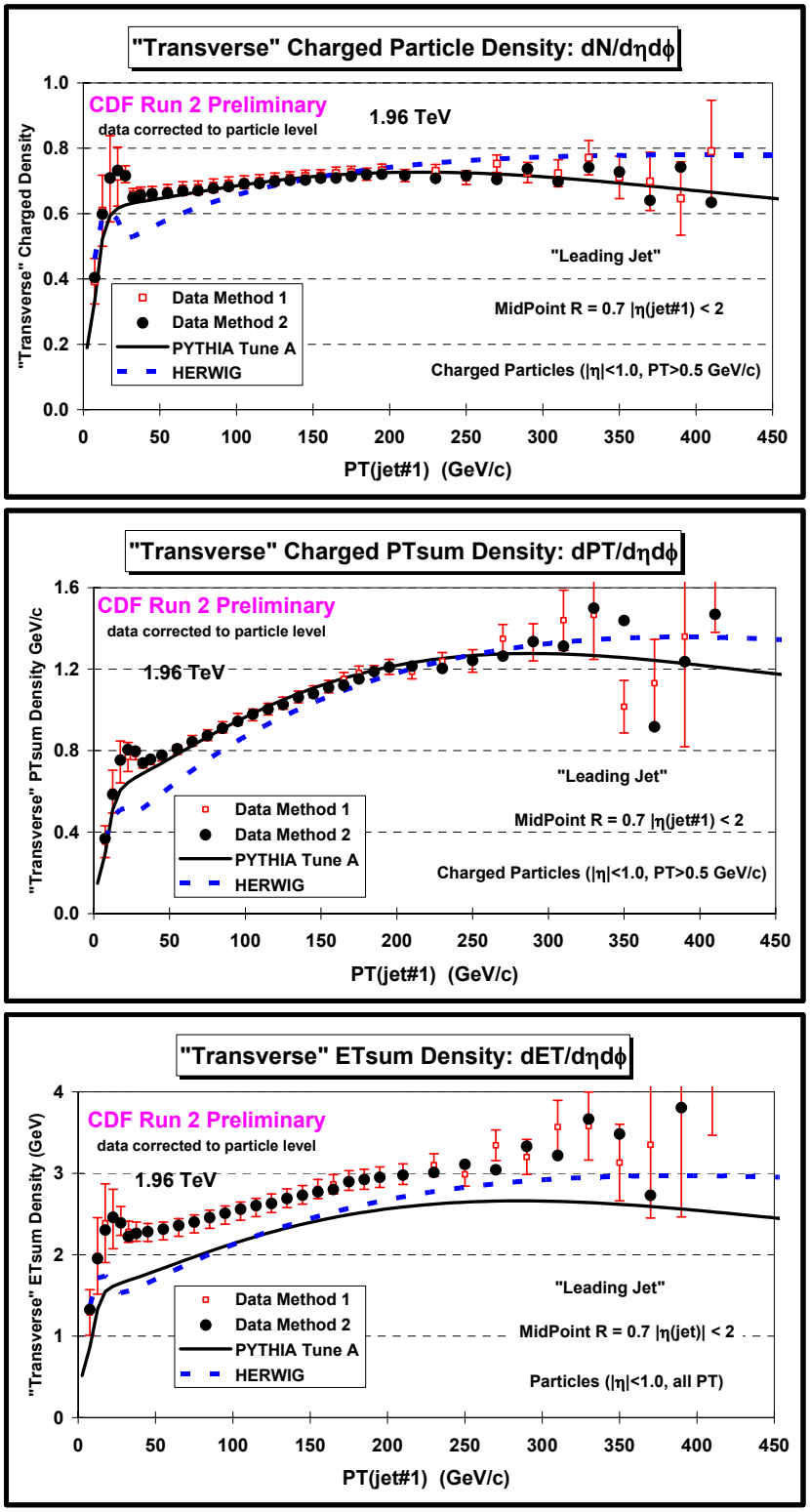

Fig. 32. Data at 1.96 TeV corrected to the particle level using method 1 and method 2 compared with PYTHIA Tune A and HERWIG at the particle level. Shows the density of charged particles, $dN_{chg}/d\eta d\phi$ (*top*), the PTsum density of charged particles, $dPT_{sum}/d\eta d\phi$ (*middle*), ($p_T > 0.5$ GeV/c and $|\eta| < 1$), and the ETsum density, $dE_T/d\eta d\phi$ (*bottom*), for particles with $|\eta| < 1$ in the "transverse" region (average of "transMAX" and "transMIN") for "leading jet" events defined in Fig. 5 as a function of the leading jet P_T.

IV. The "Transverse" Region

(1) MAX/MIN Transverse Regions

As shown in Fig. 5 we use the direction of the highest P_T jet in the region $|\eta| < 2$, jet#1, to define the two "transverse" regions, $60^o < |\Delta\phi| < 120^o$ and $60^o < -|\Delta\phi| < 120^o$. On an event-by-event basis, we define "transMAX" and "transMIN" to be the maximum and minimum of these two regions. "TransMAX" and "transMIN" each have an area in η-ϕ space of $\Delta\eta\Delta\phi = 4\pi/6$. When looking at multiplicities MAX and MIN refer to the number of charged particles. When we consider PTsum, then MAX and MIN refer to the scalar p_T sum of charged particles and when we consider ETsum, then MAX and MIN refer to the scalar E_T sum of particles (or calorimeter towers). The overall "transverse" region which correspond to the average of the "transMAX" and "transMIN" densities.

As illustrated in Fig. 6, one expects that "transMAX" will pick up the hardest initial or final-state radiation while both "transMAX" and "transMIN" should receive "beam-beam remnant" contributions. Hence one expects "transMIN" to be more sensitive to the "beam-beam remnant" component of the "underlying event". This idea, was first suggested by Bryan Webber, and implemented by in a paper by Jon Pumplin [8]. Also, Valaria Tano [9] studied this in her Run 1 analysis of maximum and minimum transverse cones (R = 0.7).

(2) "Leading Jet" Events

Fig. 33 - 41 show the data on the observables in Table 2 at 1.96 TeV for "leading jet" events defined in Fig. 5 as a function of the leading jet P_T compared with PYTHIA Tune A and HERWIG. The plots shows the uncorrected data (with statistical errors only) compared with the theory after detector simulation (CDFSIM). The plots also shows the data corrected to the particle level (with errors that include both the statistical error and the systematic uncertainty as described in Table 9) compared with the theory at the particle level (*i.e.* generator level).

(3) "Back-to-Back" Events

Fig. 42 - 50 show the data on the observables in Table 2 at 1.96 TeV for "back-to-back" events defined in Fig. 5 as a function of the leading jet P_T compared with PYTHIA Tune A and HERWIG. The plots shows the uncorrected data (with statistical errors only) compared with the theory after detector simulation (CDFSIM). The plots also shows the data corrected to the particle level (with errors that include both the statistical error and the systematic uncertainty as described in Table 9) compared with the theory at the particle level (*i.e.* generator level).

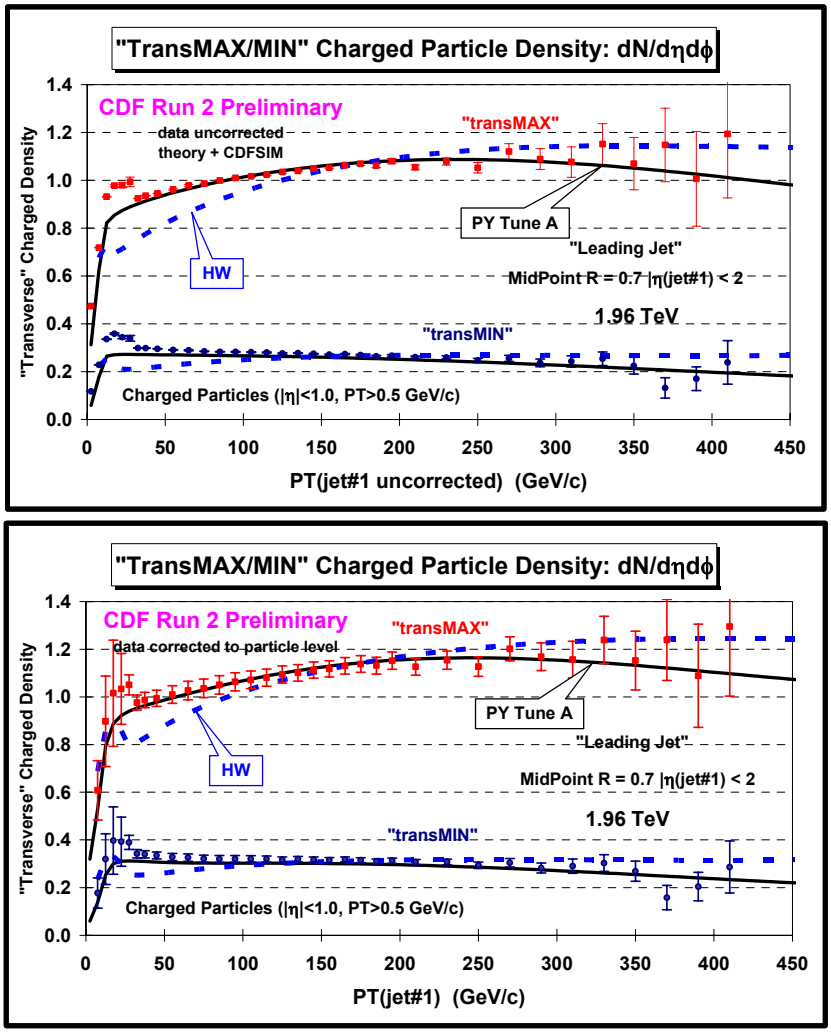

Fig. 33. Data at 1.96 TeV on the density of charged particles, $dN_{chg}/d\eta d\phi$, with $p_T > 0.5$ GeV/c and $|\eta| < 1$ in the "transMAX" and "transMIN" regions for "leading jet" events defined in Fig. 5 as a function of the leading jet P_T compared with PYTHIA Tune A and HERWIG. (*top*) Shows the uncorrected data (with statistical errors only) compared with the theory after detector simulation (CDFSIM). (*bottom*) Shows the data corrected to the particle level (with errors that include both the statistical error and the systematic uncertainty) compared with the theory at the particle level (*i.e.* generator level).

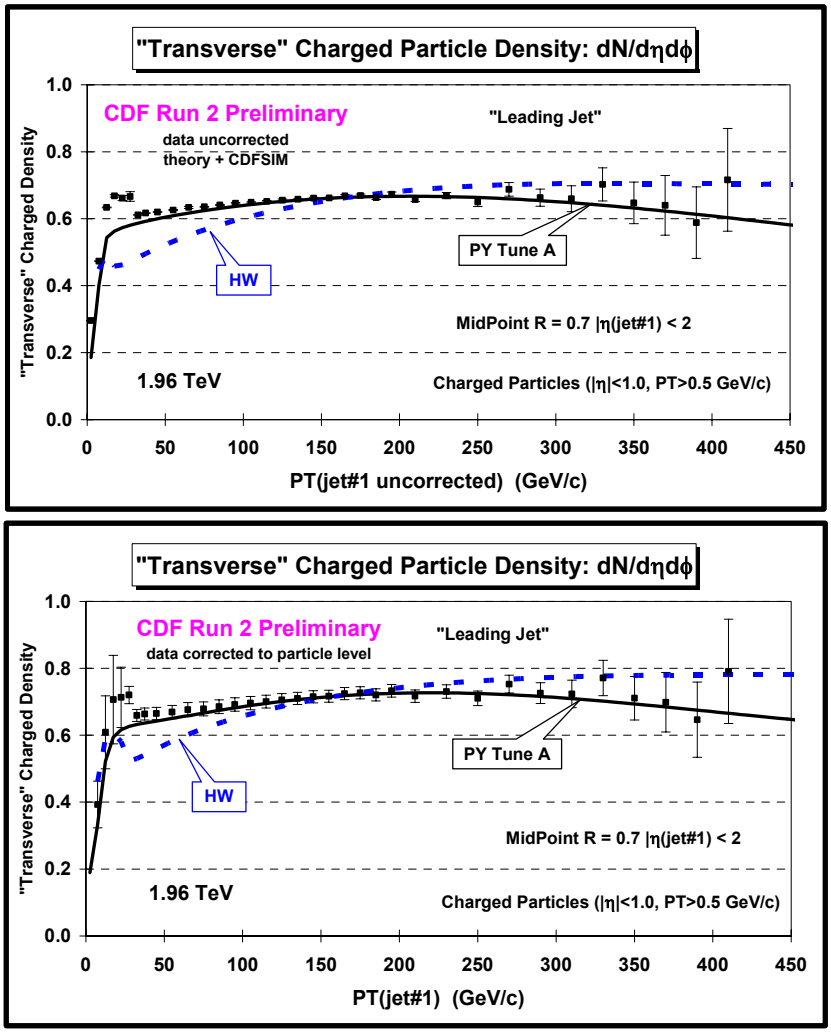

Fig. 34. Data at 1.96 TeV on the density of charged particles, $dN_{chg}/d\eta d\phi$, with $p_T > 0.5$ GeV/c and $|\eta| < 1$ in the "transverse" region (average of "transMAX" and "transMIN") for "leading jet" events defined in Fig. 5 as a function of the leading jet P_T compared with PYTHIA Tune A and HERWIG. (*top*) Shows the uncorrected data (with statistical errors only) compared with the theory after detector simulation (CDFSIM). (*bottom*) Shows the data corrected to the particle level (with errors that include both the statistical error and the systematic uncertainty) compared with the theory at the particle level (*i.e.* generator level).

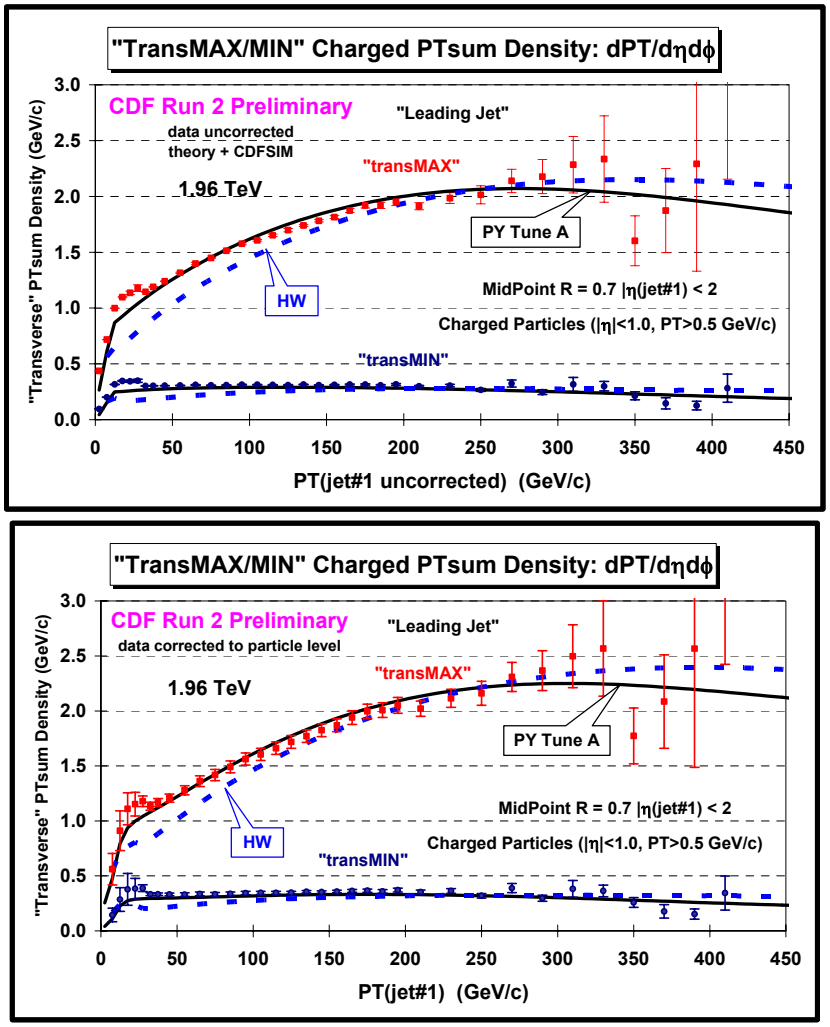

Fig. 35. Data at 1.96 TeV on the PTsum density of charged particles, $dPT_{sum}/d\eta d\phi$, with $p_T > 0.5$ GeV/c and $|\eta| < 1$ in the "transMAX" and "transMIN" regions for "leading jet" events defined in Fig. 5 as a function of the leading jet P_T compared with PYTHIA Tune A and HERWIG. (*top*) Shows the uncorrected data (with statistical errors only) compared with the theory after detector simulation (CDFSIM). (*bottom*) Shows the data corrected to the particle level (with errors that include both the statistical error and the systematic uncertainty) compared with the theory at the particle level (*i.e.* generator level).

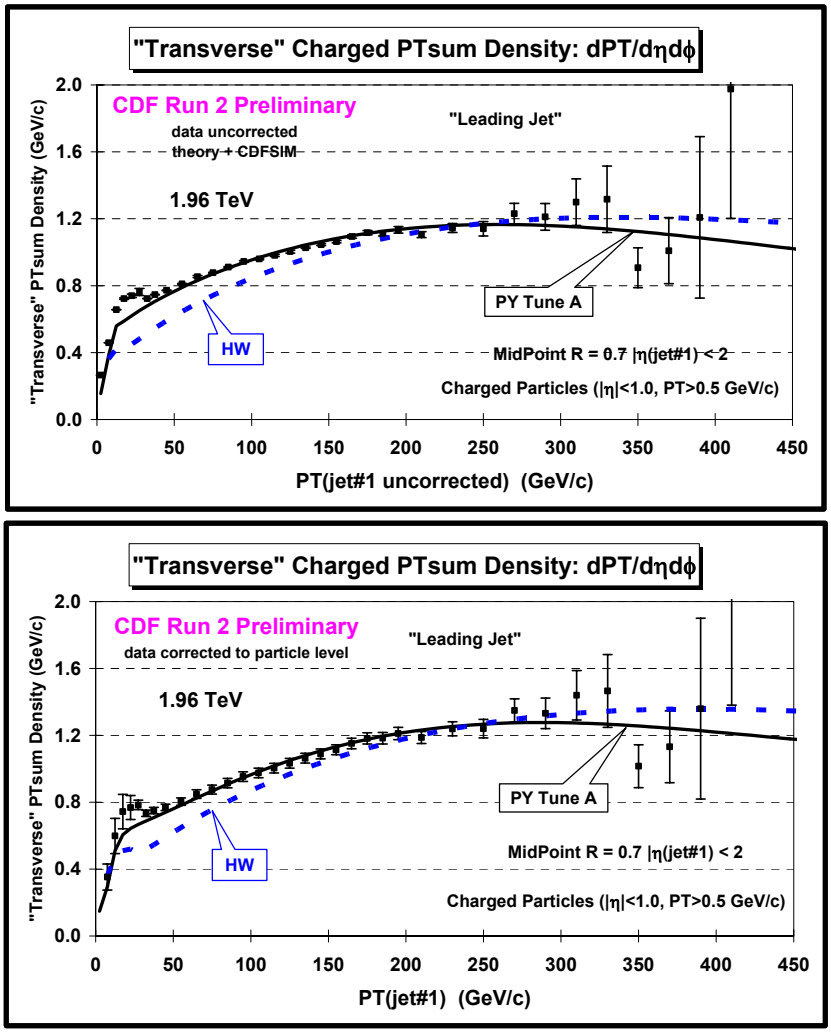

Fig. 36. Data at 1.96 TeV on the charged PTsum density, $dPT_{sum}/d\eta d\phi$, with $p_T > 0.5$ GeV/c and $|\eta| < 1$ in the "transverse" region (average of "transMAX" and "transMIN") for "leading jet" events defined in Fig. 5 as a function of the leading jet P_T compared with PYTHIA Tune A and HERWIG. (*top*) Shows the uncorrected data (with statistical errors only) compared with the theory after detector simulation (CDFSIM). (*bottom*) Shows the data corrected to the particle level (with errors that include both the statistical error and the systematic uncertainty) compared with the theory at the particle level (*i.e.* generator level).

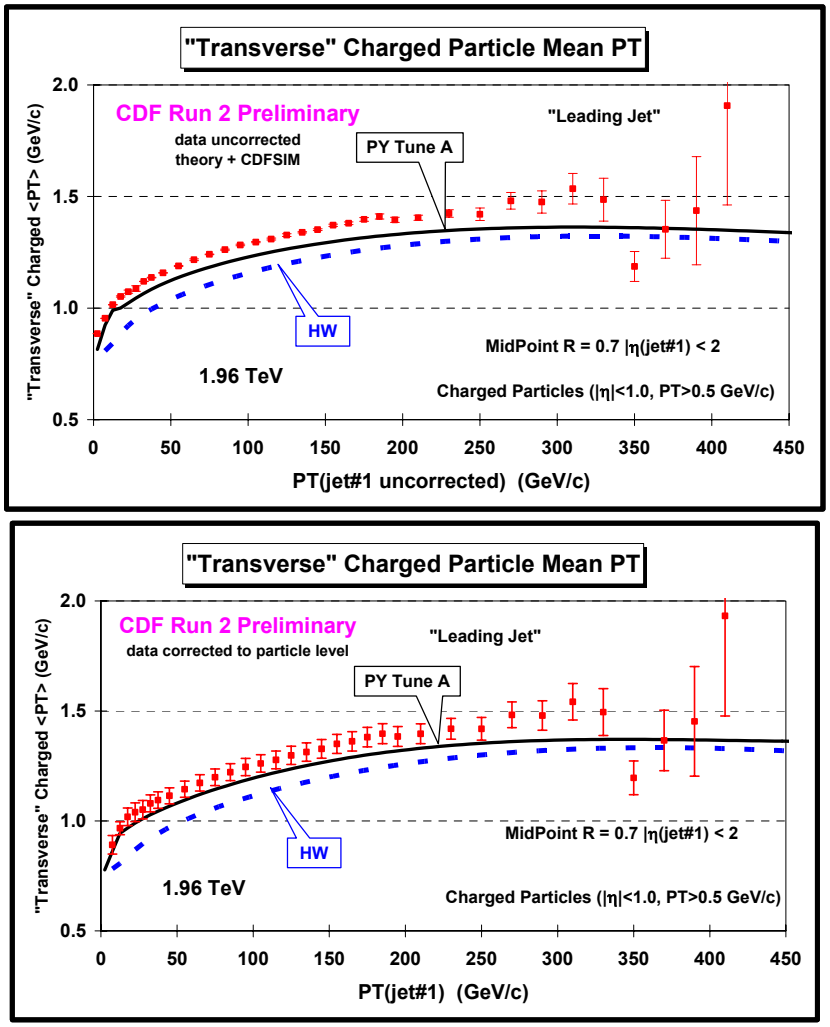

Fig. 37. Data at 1.96 TeV on the average $\langle p_T \rangle$ of charged particles with $p_T > 0.5$ GeV/c and $|\eta| < 1$ in the "transverse" region for "leading jet" events defined in Fig. 5 as a function of the leading jet P_T compared with PYTHIA Tune A and HERWIG. (*top*) Shows the uncorrected data (with statistical errors only) compared with the theory after detector simulation (CDFSIM). (*bottom*) Shows the data corrected to the particle level (with errors that include both the statistical error and the systematic uncertainty) compared with the theory at the particle level (*i.e.* generator level).

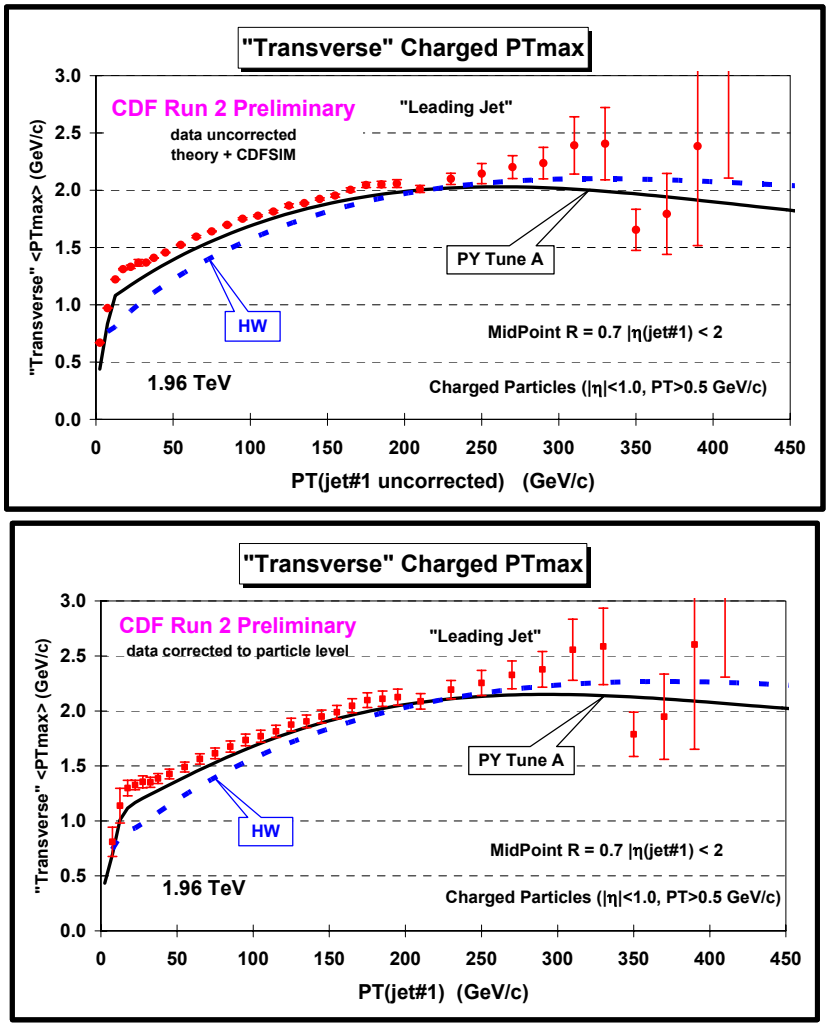

Fig. 38. Data at 1.96 TeV on the average maximum p_T, PTmax, for charged particles with $p_T > 0.5$ GeV/c and $|\eta| < 1$ in the "transverse" region for "leading jet" events defined in Fig. 5 as a function of the leading jet P_T compared with PYTHIA Tune A and HERWIG. (*top*) Shows the uncorrected data (with statistical errors only) compared with the theory after detector simulation (CDFSIM). (*bottom*) Shows the data corrected to the particle level (with errors that include both the statistical error and the systematic uncertainty) compared with the theory at the particle level (*i.e.* generator level).

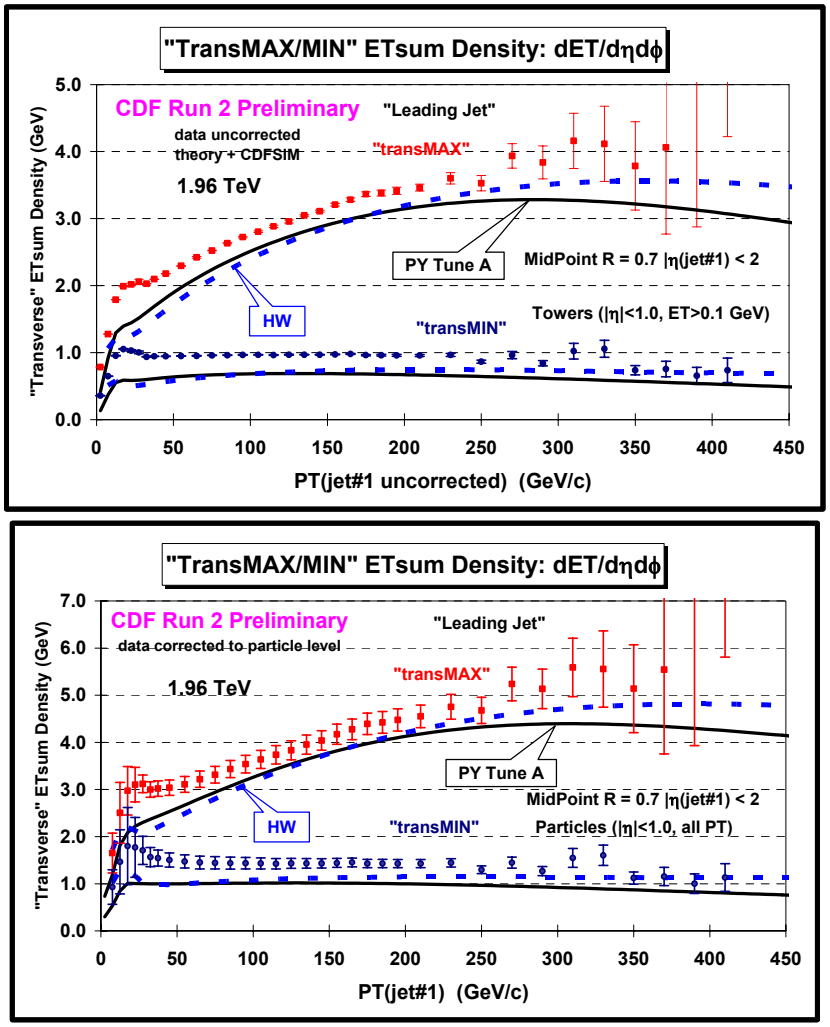

Fig. 39. Data at 1.96 TeV on the ETsum density, $dE_T/d\eta d\phi$, for particles with $|\eta| < 1$ in the "transMAX" and "transMIN" regions for "leading jet" events defined in Fig. 5 as a function of the leading jet P_T compared with PYTHIA Tune A and HERWIG. (*top*) Shows the uncorrected data (with statistical errors only) compared with the theory after detector simulation (CDFSIM). (*bottom*) Shows the data corrected to the particle level (with errors that include both the statistical error and the systematic uncertainty) compared with the theory at the particle level (*i.e.* generator level).

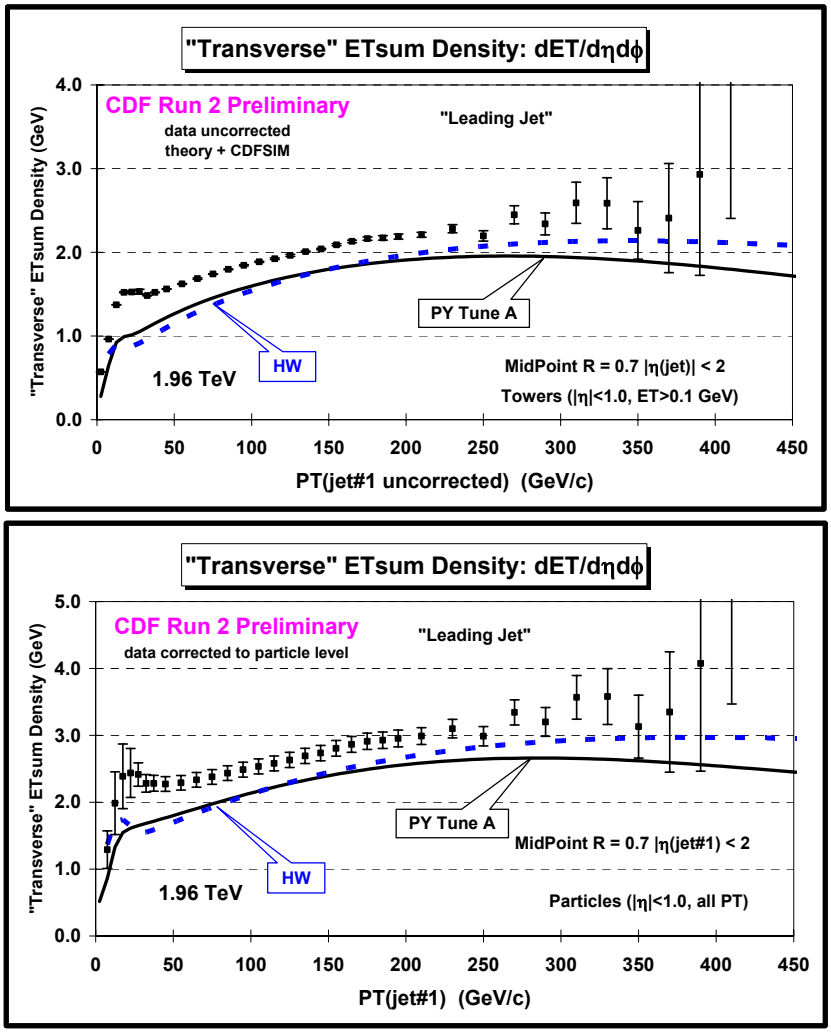

Fig. 40. Data at 1.96 TeV on the ETsum density, $dE_T/d\eta d\phi$, for particles with $|\eta| < 1$ in the "transverse" region (average of "transMAX" and "transMIN") for "leading jet" events defined in Fig. 5 as a function of the leading jet P_T compared with PYTHIA Tune A and HERWIG. (*top*) Shows the uncorrected data (with statistical errors only) compared with the theory after detector simulation (CDFSIM). (*bottom*) Shows the data corrected to the particle level (with errors that include both the statistical error and the systematic uncertainty) compared with the theory at the particle level (*i.e.* generator level).

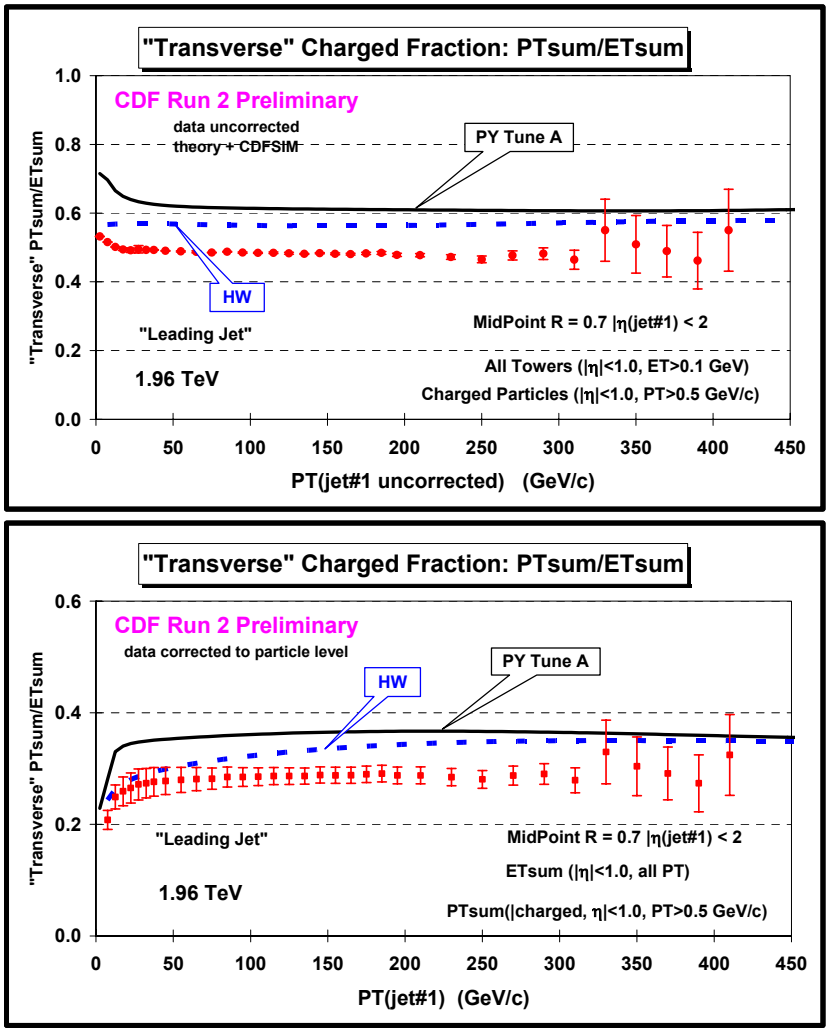

Fig. 41. Data at 1.96 TeV on the charged fraction, PTsum/ETsum, in the "transverse" region for "leading jet" events defined in Fig. 5 as a function of the leading jet P_T, where PTsum includes charged particles with $p_T > 0.5$ GeV/c and $|\eta| < 1$ and the ETsum includes all particles with $|\eta| < 1$. The data are compared with PYTHIA Tune A and HERWIG. (*top*) Shows the uncorrected data (with statistical errors only) compared with the theory after detector simulation (CDFSIM). (*bottom*) Shows the data corrected to the particle level (with errors that include both the statistical error and the systematic uncertainty) compared with the theory at the particle level (*i.e.* generator level).

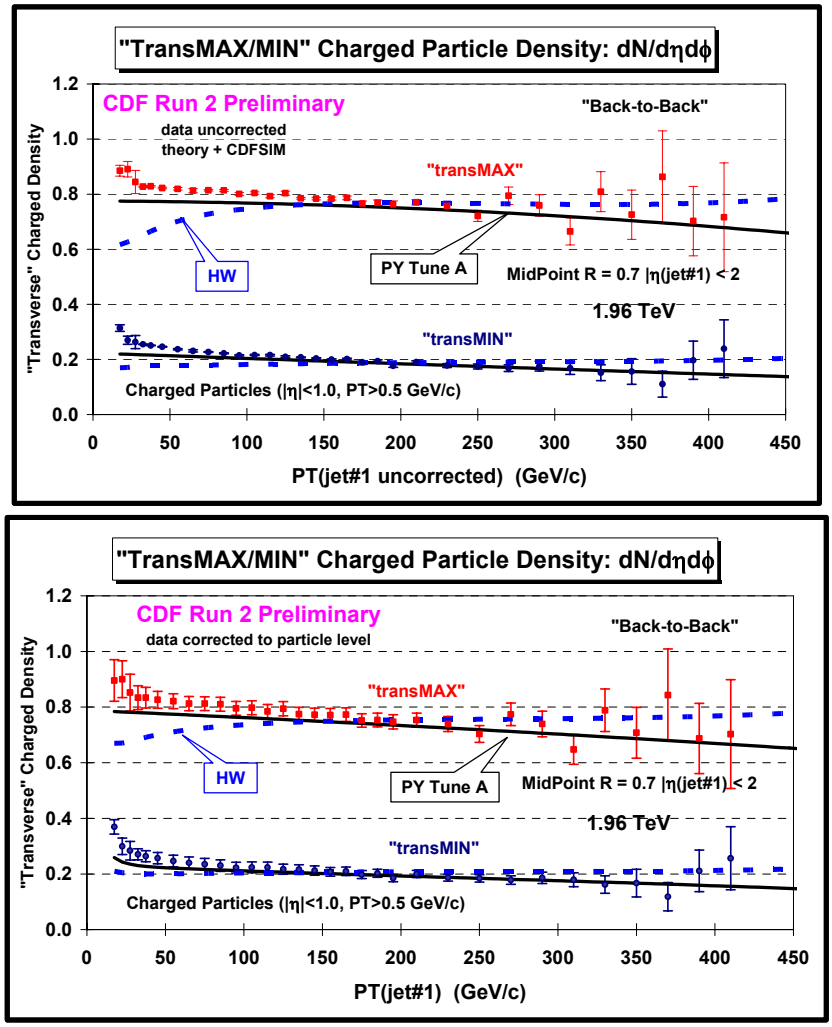

Fig. 42. Data at 1.96 TeV on the density of charged particles, $dN_{chg}/d\eta d\phi$, with $p_T > 0.5$ GeV/c and $|\eta| < 1$ in the "transMAX" and "transMIN" regions for "back-to-back" events defined in Fig. 5 as a function of the leading jet P_T compared with PYTHIA Tune A and HERWIG. (*top*) Shows the uncorrected data (with statistical errors only) compared with the theory after detector simulation (CDFSIM). (*bottom*) Shows the data corrected to the particle level (with errors that include both the statistical error and the systematic uncertainty) compared with the theory at the particle level (*i.e.* generator level).

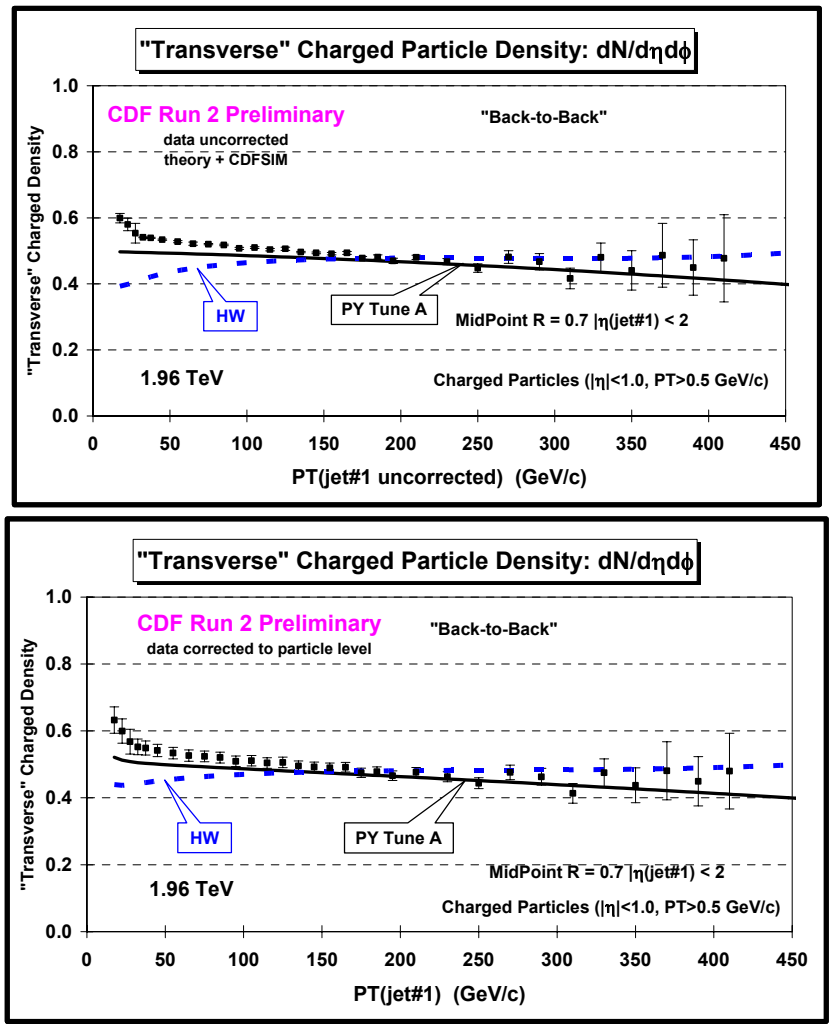

Fig. 43. Data at 1.96 TeV on the density of charged particles, $dN_{chg}/d\eta d\phi$, with $p_T > 0.5$ GeV/c and $|\eta| < 1$ in the "transverse" region (average of "transMAX" and "transMIN") for "back-to-back" events defined in Fig. 5 as a function of the leading jet P_T compared with PYTHIA Tune A and HERWIG. (*top*) Shows the uncorrected data (with statistical errors only) compared with the theory after detector simulation (CDFSIM). (*bottom*) Shows the data corrected to the particle level (with errors that include both the statistical error and the systematic uncertainty) compared with the theory at the particle level (*i.e.* generator level).

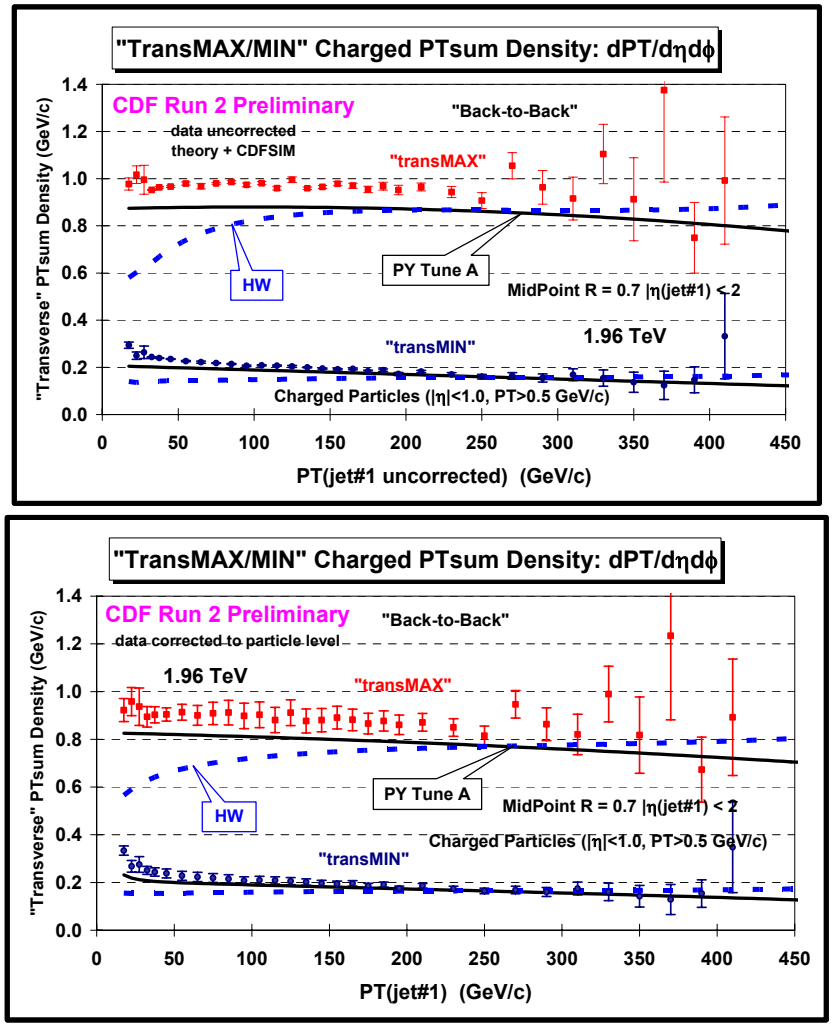

Fig. 44. Data at 1.96 TeV on the PTsum density of charged particles, $dPT_{sum}/d\eta d\phi$, with $p_T > 0.5$ GeV/c and $|\eta| < 1$ in the "transMAX" and "transMIN" regions for "back-to-back" events defined in Fig. 5 as a function of the leading jet P_T compared with PYTHIA Tune A and HERWIG. (*top*) Shows the uncorrected data (with statistical errors only) compared with the theory after detector simulation (CDFSIM). (*bottom*) Shows the data corrected to the particle level (with errors that include both the statistical error and the systematic uncertainty) compared with the theory at the particle level (*i.e.* generator level).

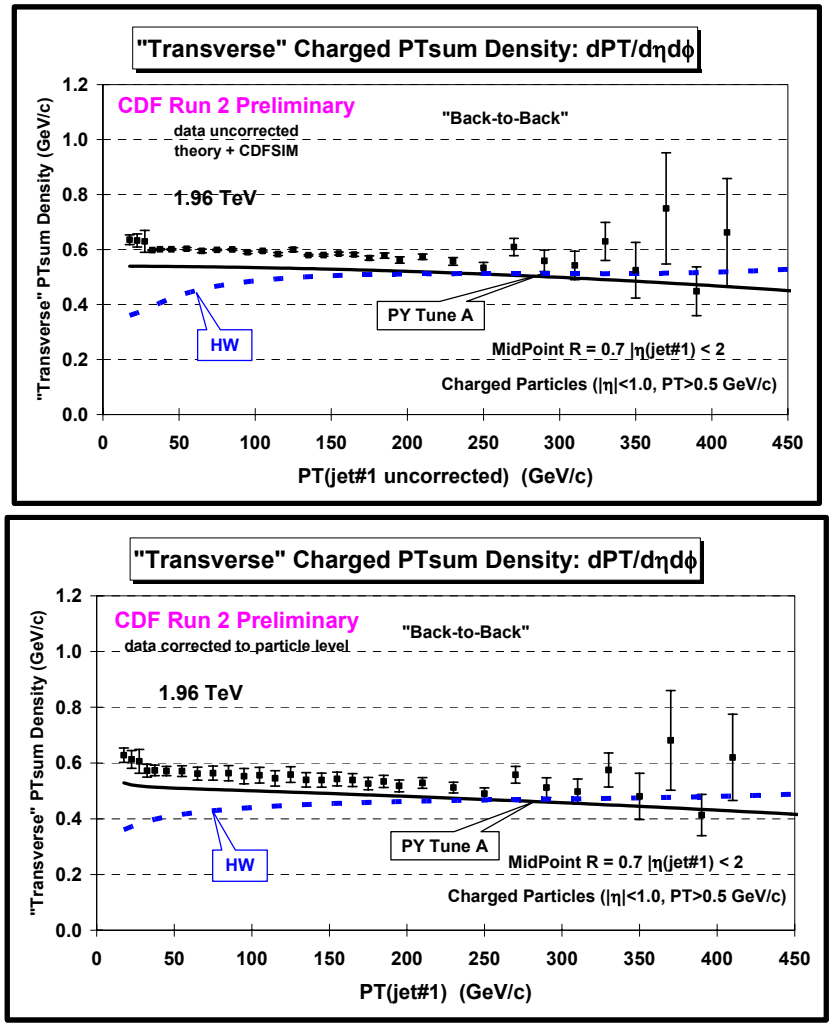

Fig. 45. Data at 1.96 TeV on the PTsum density, dPTsum/dηdϕ, with $p_T > 0.5$ GeV/c and $|\eta| < 1$ in the "transverse" region (average of "transMAX" and "transMIN") for "back-to-back" events defined in Fig. 5 as a function of the leading jet P_T compared with PYTHIA Tune A and HERWIG. (*top*) Shows the uncorrected data (with statistical errors only) compared with the theory after detector simulation (CDFSIM). (*bottom*) Shows the data corrected to the particle level (with errors that include both the statistical error and the systematic uncertainty) compared with the theory at the particle level (*i.e.* generator level).

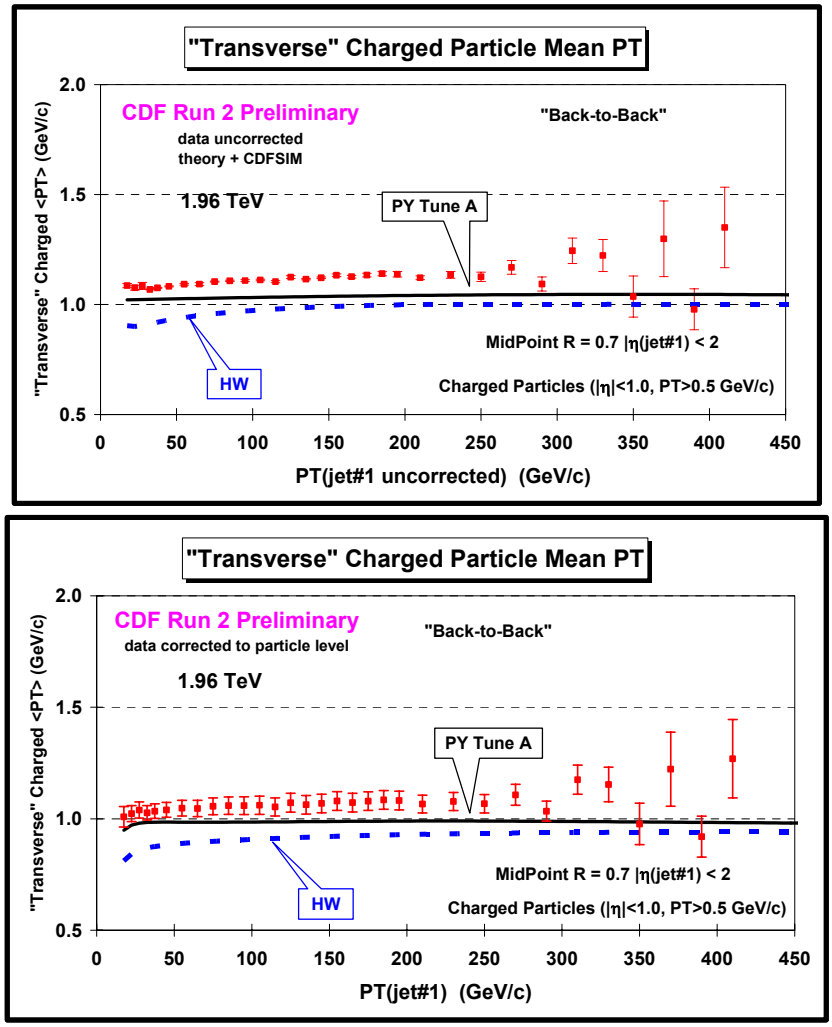

Fig. 46. Data at 1.96 TeV on the average $\langle p_T \rangle$ of charged particles with $p_T > 0.5$ GeV/c and $|\eta| < 1$ in the "transverse" region for "back-to-back" events defined in Fig. 5 as a function of the leading jet P_T compared with PYTHIA Tune A and HERWIG. (*top*) Shows the uncorrected data (with statistical errors only) compared with the theory after detector simulation (CDFSIM). (*bottom*) Shows the data corrected to the particle level (with errors that include both the statistical error and the systematic uncertainty) compared with the theory at the particle level (*i.e.* generator level).

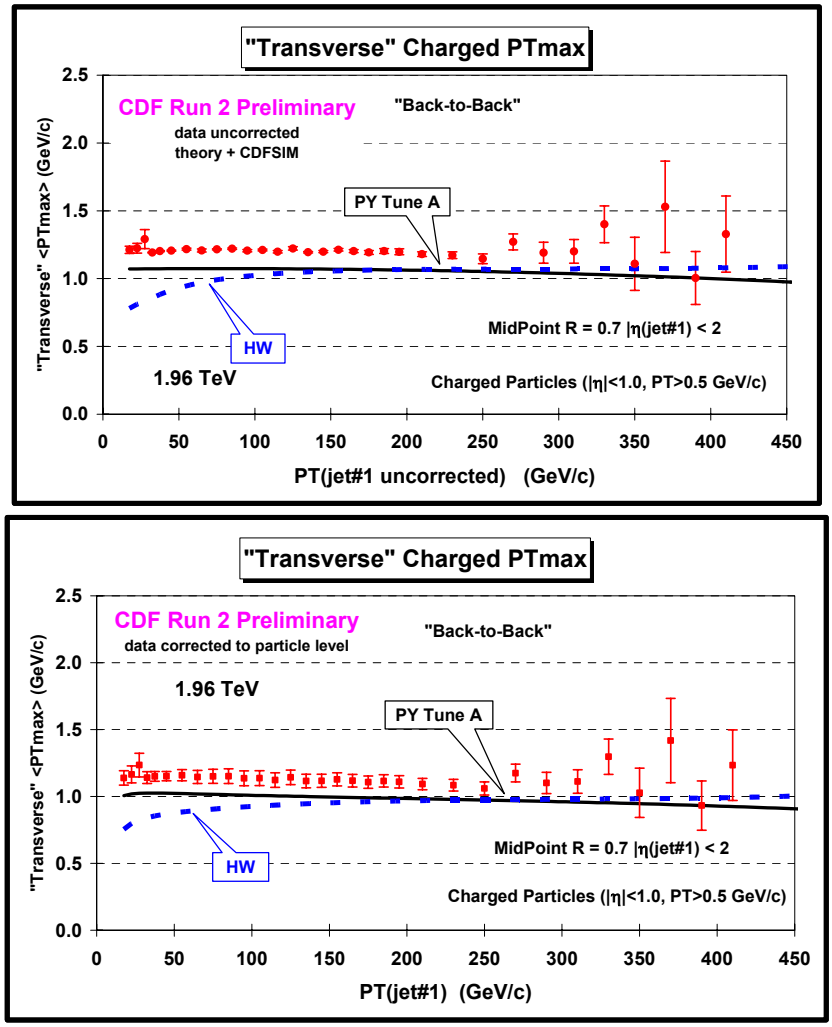

Fig. 47. Data at 1.96 TeV on the average maximum p_T, PTmax, for charged particles with $p_T > 0.5$ GeV/c and $|\eta| < 1$ in the "transverse" region for "back-to-back" events defined in Fig. 5 as a function of the leading jet P_T compared with PYTHIA Tune A and HERWIG. (*top*) Shows the uncorrected data (with statistical errors only) compared with the theory after detector simulation (CDFSIM). (*bottom*) Shows the data corrected to the particle level (with errors that include both the statistical error and the systematic uncertainty) compared with the theory at the particle level (*i.e.* generator level).

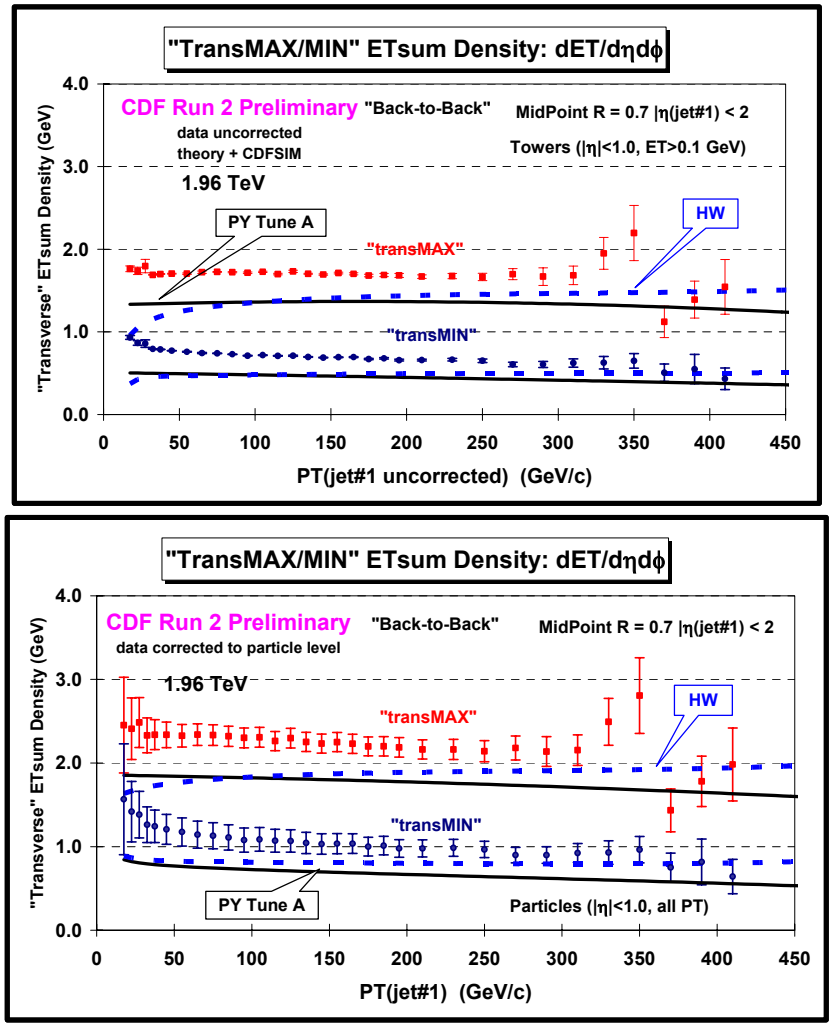

Fig. 48. Data at 1.96 TeV on the ETsum density, $dE_T/d\eta d\phi$, for particles with $|\eta| < 1$ in the "transMAX" and "transMIN" regions for "back-to-back" events defined in Fig. 5 as a function of the leading jet P_T compared with PYTHIA Tune A and HERWIG. (*top*) Shows the uncorrected data (with statistical errors only) compared with the theory after detector simulation (CDFSIM). (*bottom*) Shows the data corrected to the particle level (with errors that include both the statistical error and the systematic uncertainty) compared with the theory at the particle level (*i.e.* generator level).

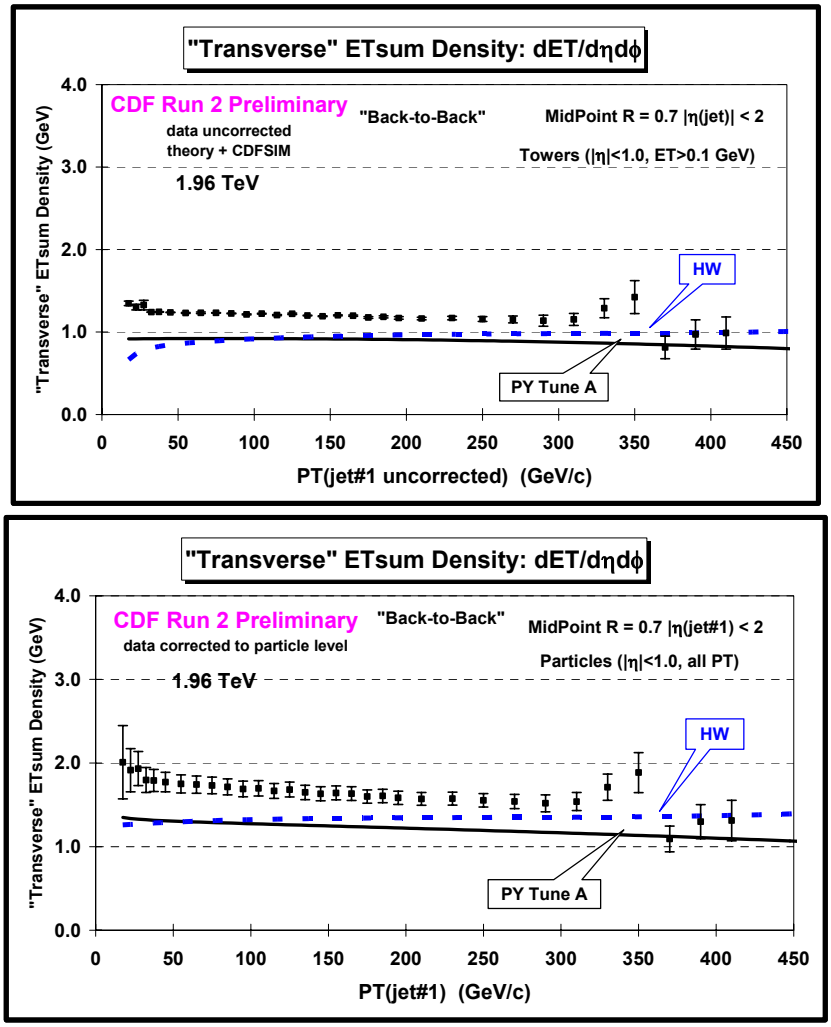

Fig. 49. Data at 1.96 TeV on the ETsum density, $dE_T/d\eta d\phi$, for particles with $|\eta| < 1$ in the "transverse" region (average of "transMAX" and "transMIN") for "back-to-back" events defined in Fig. 5 as a function of the leading jet P_T compared with PYTHIA Tune A and HERWIG. (*top*) Shows the uncorrected data (with statistical errors only) compared with the theory after detector simulation (CDFSIM). (*bottom*) Shows the data corrected to the particle level (with errors that include both the statistical error and the systematic uncertainty) compared with the theory at the particle level (*i.e.* generator level).

(4) "Leading Jet" versus "Back-to-Back" Events

Fig. 51 and Fig 52 compare the data on the density of charged particles and the charged PTsum density in the "transverse" region corrected to the particle level for "leading jet" and "back-to-back" events with PYTHIA Tune A and HERWIG at the particle level. As expected, the "leading jet" and "back-to-back" events behave quite differently. For the "leading jet" case the "transMAX" densities rise with increasing P_T(jet#1), while for the "back-to-back" case they fall with increasing P_T(jet#1). The rise in the "leading jet" case is, of course, due to hard initial and final-state radiation, which has been suppressed in the "back-to-back" events. The "back-to-back" events allow for a more close look at the "beam-beam remnant" and multiple parton scattering component of the "underlying event" and PYTHIA Tune A (with multiple parton interactions) does a better job describing the data than HERWIG (without multiple parton interactions).

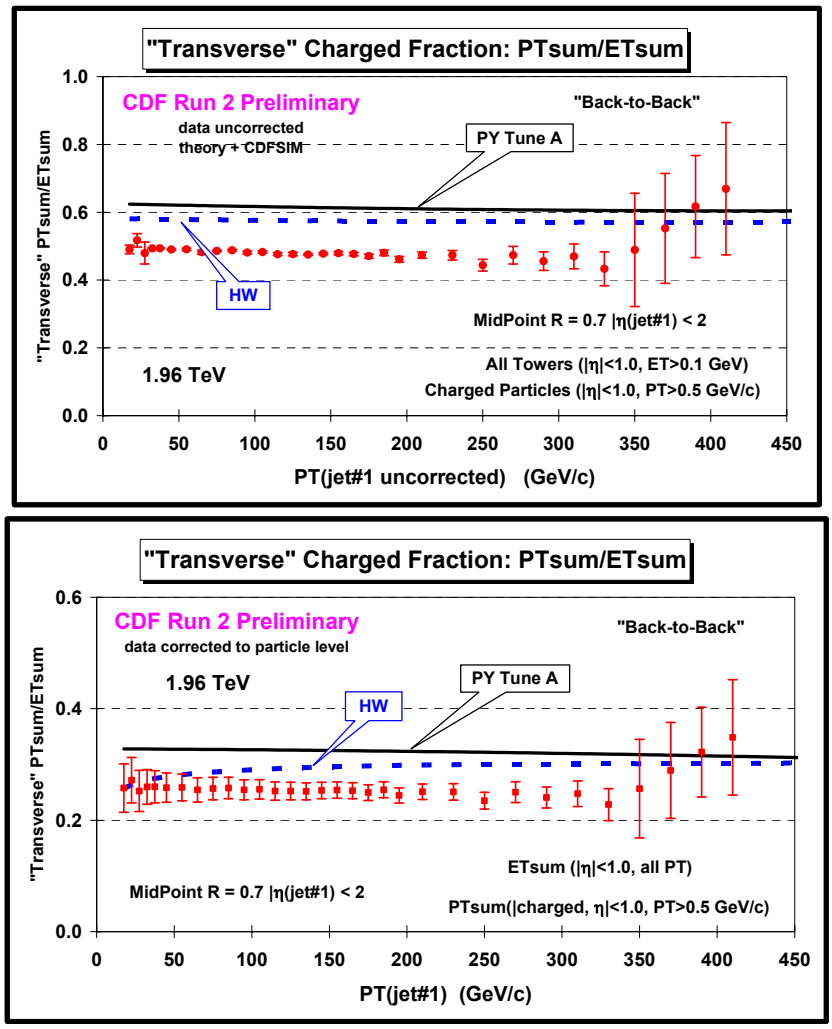

Fig. 50. Data at 1.96 TeV on the charged fraction, PTsum/ETsum, in the "transverse" region for "back-to-back" events defined in Fig. 5 as a function of the leading jet P_T, where PTsum includes charged particles with $p_T > 0.5$ GeV/c and $|\eta| < 1$ and the ETsum includes all particles with $|\eta| < 1$. The data are compared with PYTHIA Tune A and HERWIG. (*top*) Shows the uncorrected data (with statistical errors only) compared with the theory after detector simulation (CDFSIM). (*bottom*) Shows the data corrected to the particle level (with errors that include both the statistical error and the systematic uncertainty) compared with the theory at the particle level (*i.e.* generator level).

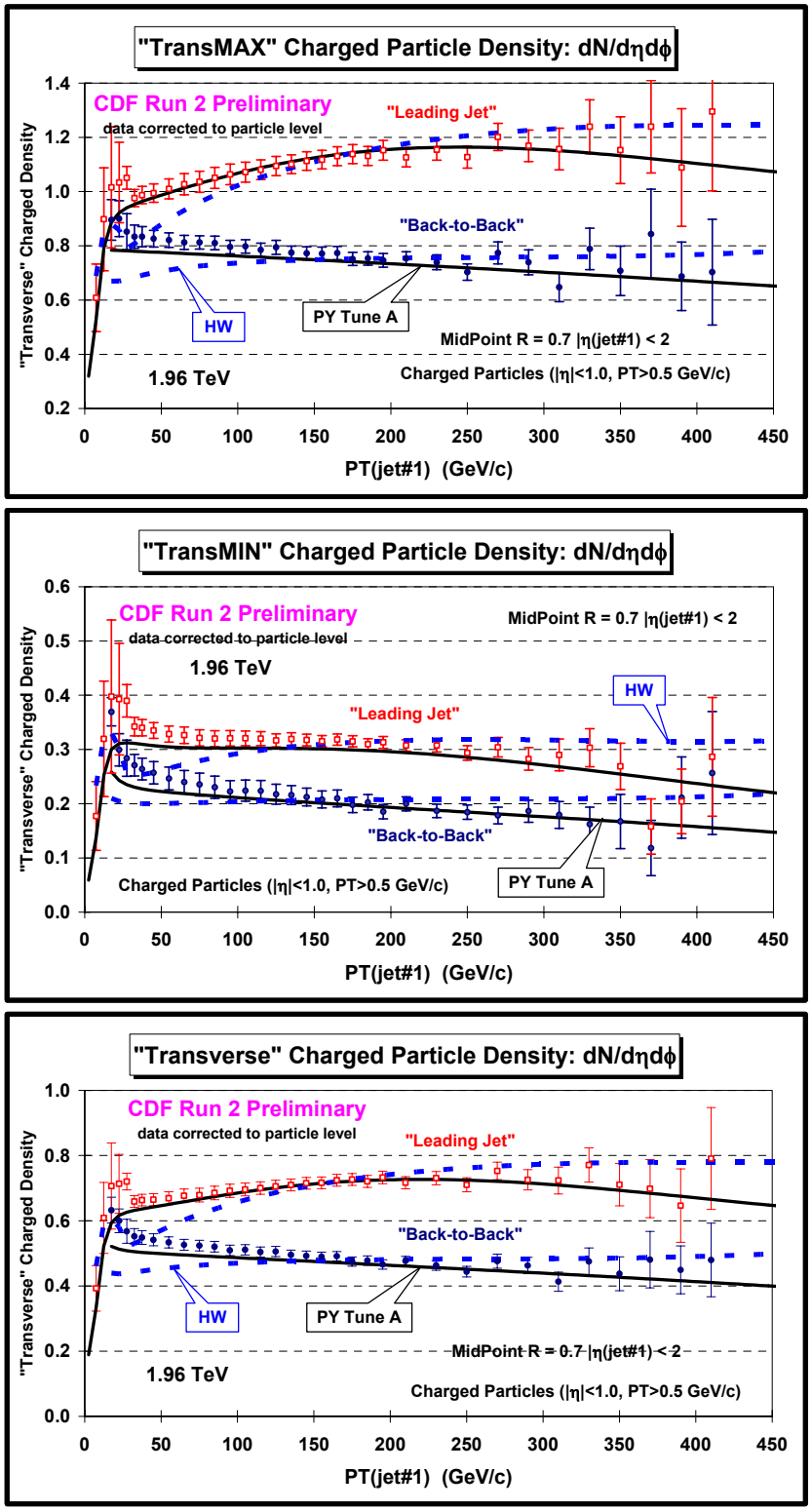

Fig. 51. Data at 1.96 TeV on the density of charged particles, dNchg/dηdϕ, with $p_T > 0.5$ GeV/c and $|\eta| < 1$ in the "transMAX" region (*top*), "transMIN" region (*middle*), and "transverse" region (average of "transMAX" and "transMIN") (*bottom*) for "leading jet" and "back-to-back" events defined in Fig. 5 as a function of the leading jet P_T compared with PYTHIA Tune A and HERWIG. The data are corrected to the particle level (with errors that include both the statistical error and the systematic uncertainty) and compared with the theory at the particle level (*i.e.* generator level).

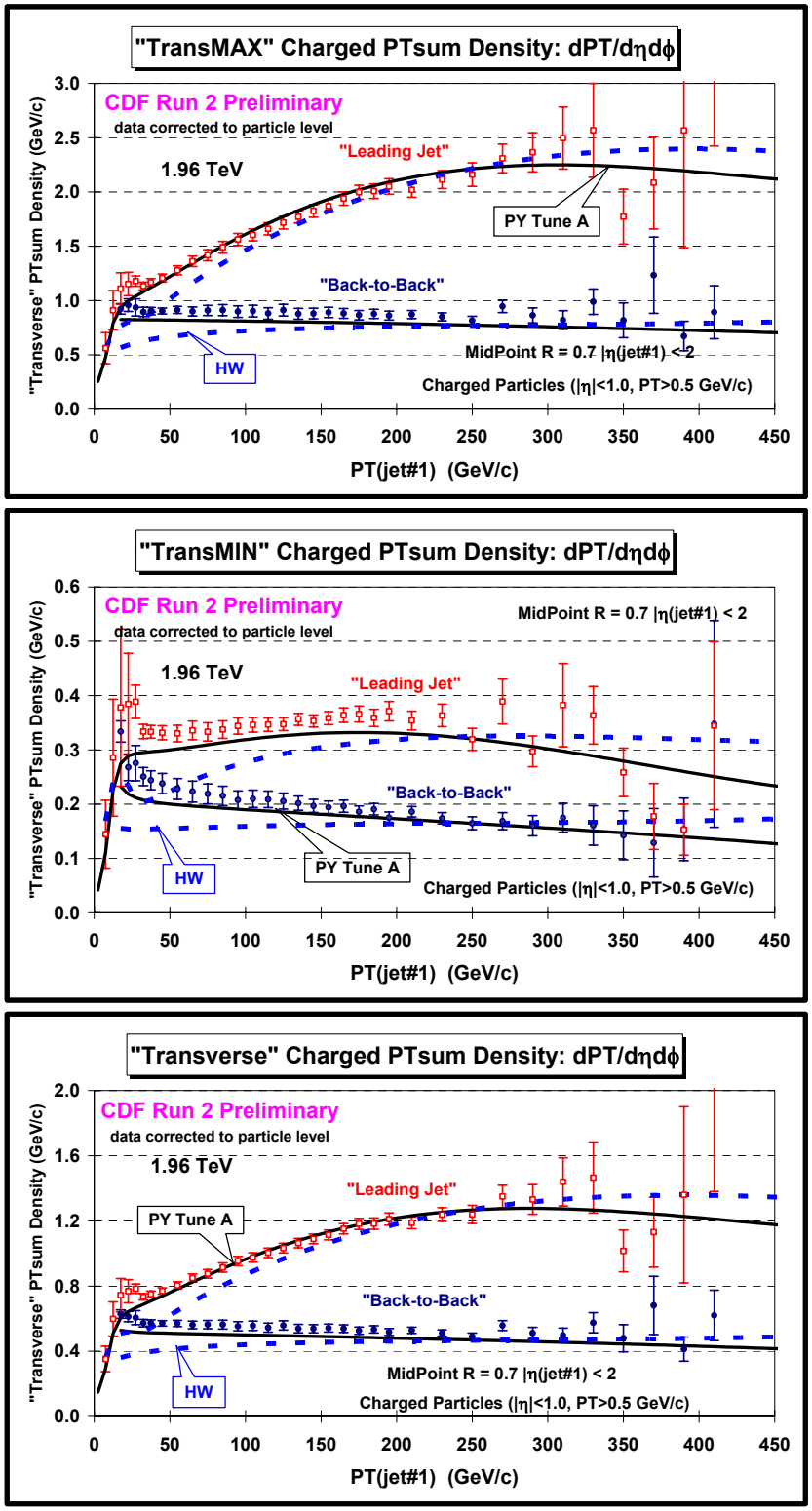

Fig. 52. Data at 1.96 TeV on charged PTsum density of charged particles, dPTsum/dηdϕ, with $p_T > 0.5$ GeV/c and $|\eta| < 1$ in the "transMAX" region (*top*), "transMIN" region (*middle*), and "transverse" region (average of "transMAX" and "transMIN") (*bottom*) for "leading jet" and "back-to-back" events defined in Fig. 5 as a function of the leading jet P_T compared with PYTHIA Tune A and HERWIG. The data are corrected to the particle level (with errors that include both the statistical error and the systematic uncertainty) and compared with the theory at the particle level (*i.e.* generator level).

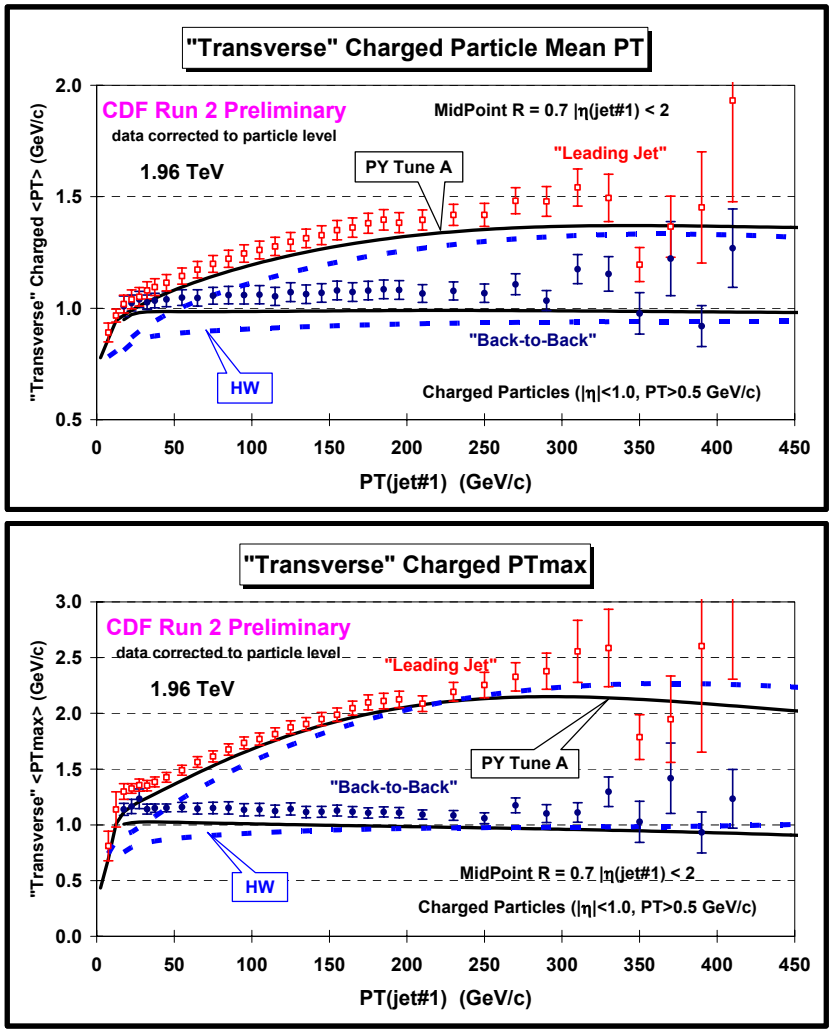

Fig. 53. Data at 1.96 TeV on the average $\langle p_T \rangle$ of charged particles (*top*) and the average maximum p_T, PTmax, for charged particles (*bottom*) with $p_T > 0.5$ GeV/c and $|\eta| < 1$ in the "transverse" region for "leading jet" and "back-to-back" events defined in Fig. 5 as a function of the leading jet P_T compared with PYTHIA Tune A and HERWIG. The data are corrected to the particle level (with errors that include both the statistical error and the systematic uncertainty) and compared with the theory at the particle level (*i.e.* generator level).

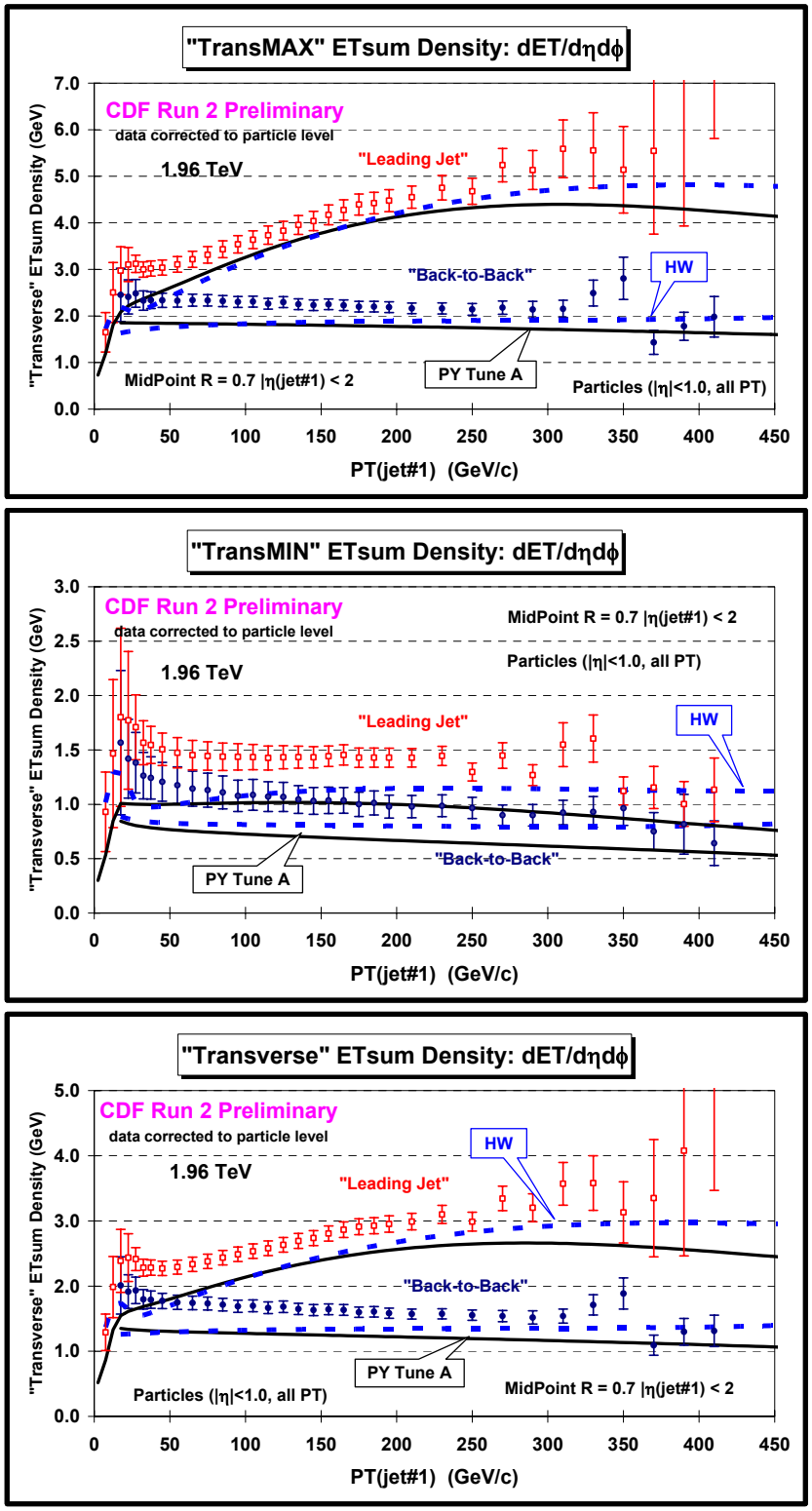

Fig. 54. Data at 1.96 TeV on the ETsum density, $dE_T/d\eta d\phi$, for particles with $|\eta| < 1$ in the "transMAX" region (*top*), "transMIN" region (*middle*), and "transverse" region (average of "transMAX" and "transMIN") (*bottom*) for "leading jet" and "back-to-back" events defined in Fig. 5 as a function of the leading jet P_T compared with PYTHIA Tune A and HERWIG. The data are corrected to the particle level (with errors that include both the statistical error and the systematic uncertainty) and compared with the theory at the particle level (*i.e.* generator level).

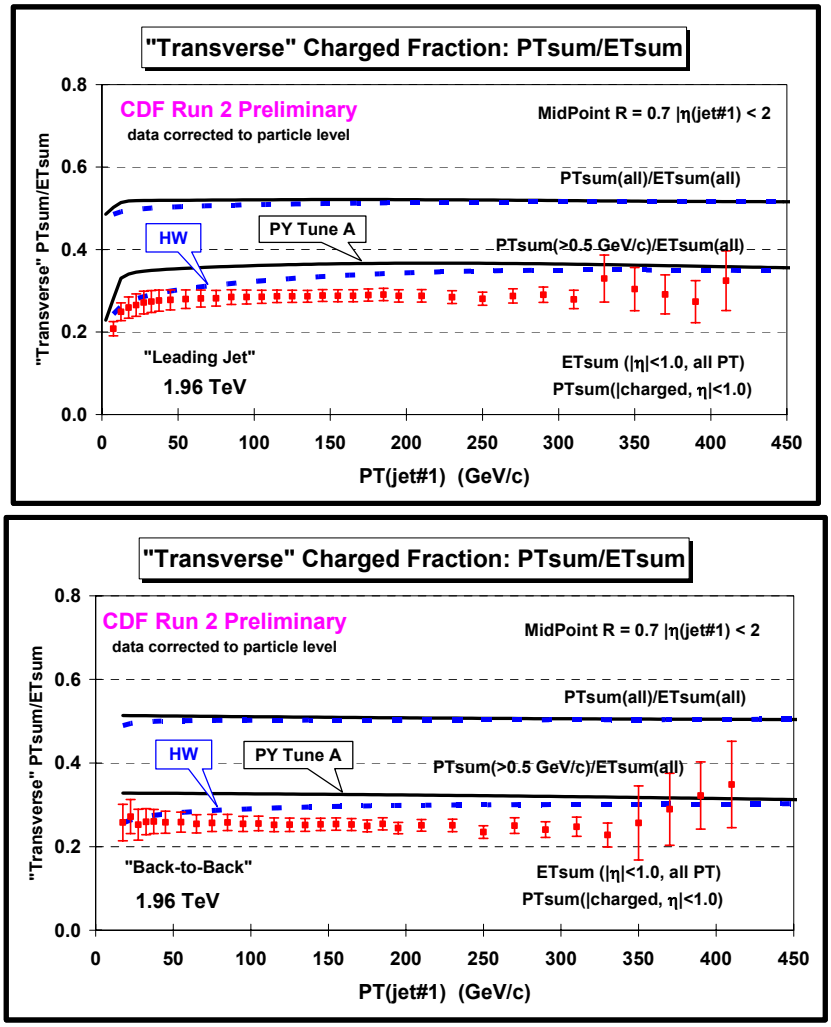

Fig. 55. Data at 1.96 TeV on the charged fraction, PTsum/ETsum, in the "transverse" region defined in Fig. 5 for "leading jet" events (*top*) and "back-to-back" events (*bottom*) as a function of the leading jet P_T, where PTsum includes charged particles with $p_T > 0.5$ GeV/c and $|\eta| < 1$ and the ETsum includes all particles with $|\eta| < 1$, compared with PYTHIA Tune A and HERWIG. The data are corrected to the particle level (with errors that include both the statistical error and the systematic uncertainty) and compared with the theory at the particle level (*i.e.* generator level).

The "transMIN" densities are more sensitive to the "beam-beam remnant" and multiple parton interaction component of the "underlying event". The "back-to-back" data show a decrease in the "transMIN" densities with increasing P_T(jet#1) which is described fairly well by PYTHIA Tune A (with multiple parton interactions) but not by HERWIG (without multiple parton interactions). The decrease of the "transMIN" densities with increasing P_T(jet#1) for the "back-to-back" events is very interesting and might be due to a "saturation" of the multiple parton interactions at small impact parameter. Such an effect is included in PYTHIA Tune A but not in HERWIG (without multiple parton interactions).

Fig. 53 compares the data on average $\langle p_T \rangle$ of charged particles and the average maximum charge particle p_T, PT_{max}, in the "transverse" region corrected to the particle level for "leading jet" and "back-to-back" events with PYTHIA Tune A and HERWIG at the particle level. Again the "leading jet" and "back-to-back" events behave quite differently.

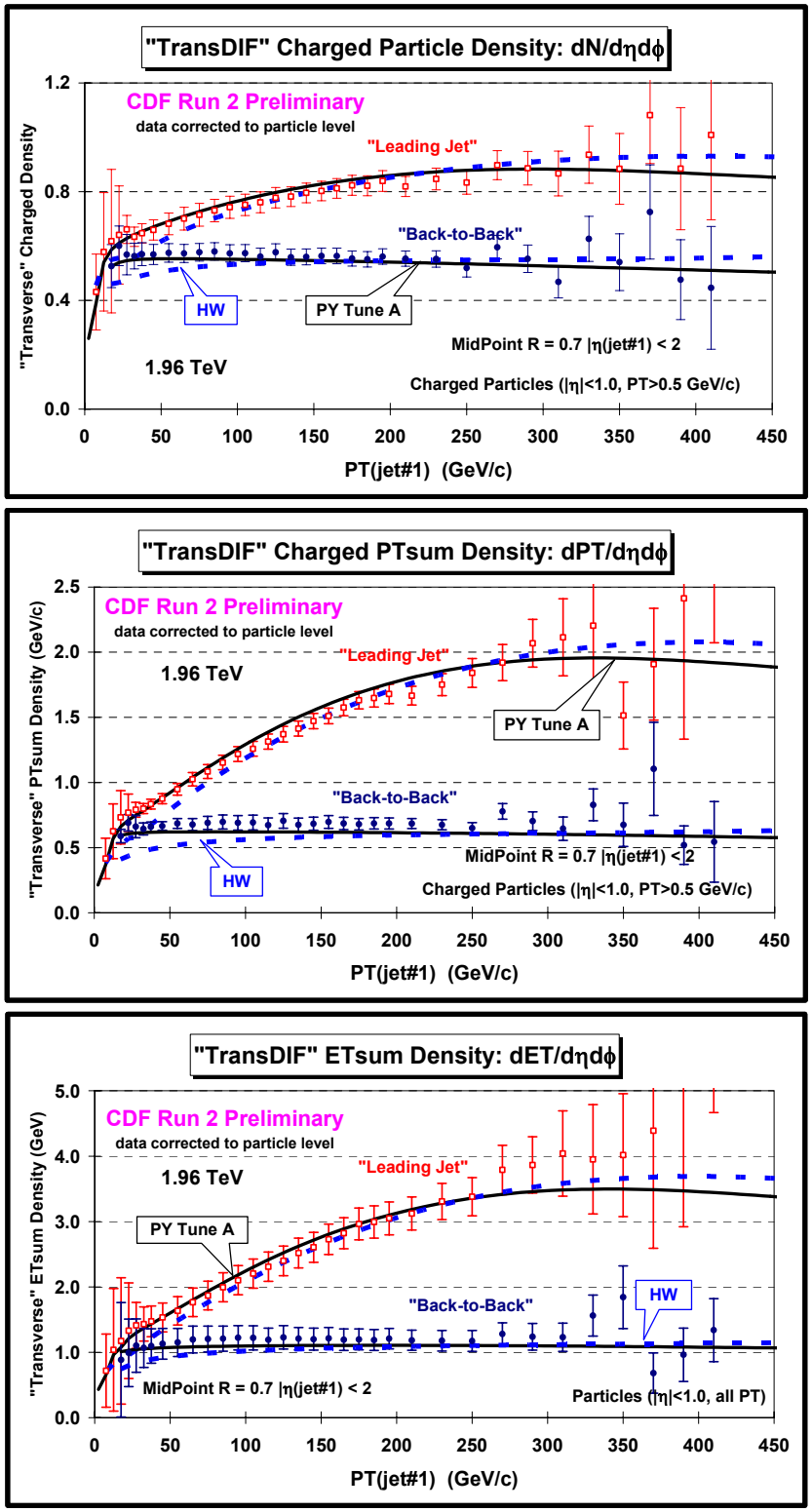

Fig. 56. Data at 1.96 TeV on the difference of the "transMAX" and "transMIN" region ("transDIF" = "transMAX" minus "transMIN") for "leading jet" and "back-to-back" events defined in Fig. 5 as a function of the leading jet P_T compared with PYTHIA Tune A and HERWIG. The data are corrected to the particle level (with errors that include both the statistical error and the systematic uncertainty) and compared with the theory at the particle level (*i.e.* generator level).

Fig. 54 shows the data corrected to the particle level on the ET_{sum} density, $dE_T/d\eta d\phi$, in the "transverse" region for "leading jet" and "back-to-back" events compared with PYTHIA Tune A and HERWIG at the particle level. Neither PYTHIA Tune A or HERWIG produce enough energy in the "transverse" region. HERWIG has more "soft" particles than PYTHIA Tune A does slightly better in describing the energy density in the "transMAX" and "transMIN" region.

Fig. 55 shows the data corrected on the charged fraction, PT_{sum}/ET_{sum}, in the "transverse" region for "leading jet" and "back-to-back" events compared with PYTHIA Tune A and HERWIG at the particle level. Neither PYTHIA Tune A or HERWIG produce enough energy in the "transverse" region and therefore predict too large of a charged fraction. Note that both PYTHIA Tune A and HERWIG predict a charged fraction of about 0.5 if one includes all particles in both PT_{sum} and ET_{sum}.

Fig. 56 shows the difference of the "transMAX" and "transMIN" region ("transDIF" = "transMAX" minus "transMIN") for "leading jet" and "back-to-back" events compared with PYTHIA Tune A and HERWIG. "TransDIF" is more sensitive to the hard scattering component of the "underlying event" (*i.e.* initial and final state radiation). Both PYTHIA Tune A and HERWIG underestimate the energy density in the "transMAX" and "transMIN" regions (see Fig. 54). However, they both fit the "transDIF" energy density. This indicates that the excess energy density seen in the data probably arises from the "soft" component of the "underlying event" (*i.e.* beam-beam remnants and/or multiple parton interactions).

(5) Tuned Version of JIMMY

JIMMY [11] is a model of multiple parton interaction which can be combined with HERWIG to enhance the "underlying event" thereby improving the agreement with data. Fig. 57 shows the energy density, the charged PT_{sum} density, and the density of charged particles in the "transMAX" and "transMIN" regions for "leading jet" events compared with PYTHIA Tune A and a tuned version of JIMMY. JIMMY was tuned to fit the "transverse" energy density in "leading jet" events (PTJIM = 3.25 GeV/c). The default JIMMY (PTJIM = 2.5 GeV/c) produces too much energy and charged PT_{sum} in the "transverse" region. Figs. 58-62 compare PYTHIA Tune A and tuned JIMMY with the data. Tuned JIMMY does a good job of fitting the energy and charged PT_{sum} density in the "transverse" region (although it produces slightly too much charged PT_{sum} at large P_T(jet#1)). However, the tuned JIMMY produces too many charged particles with $p_T > 0.5$ GeV/c. The particles produced by tuned JIMMY are too soft. This can be seen clearly in Fig. 62 which shows the average charge particle p_T in the "transverse" region.

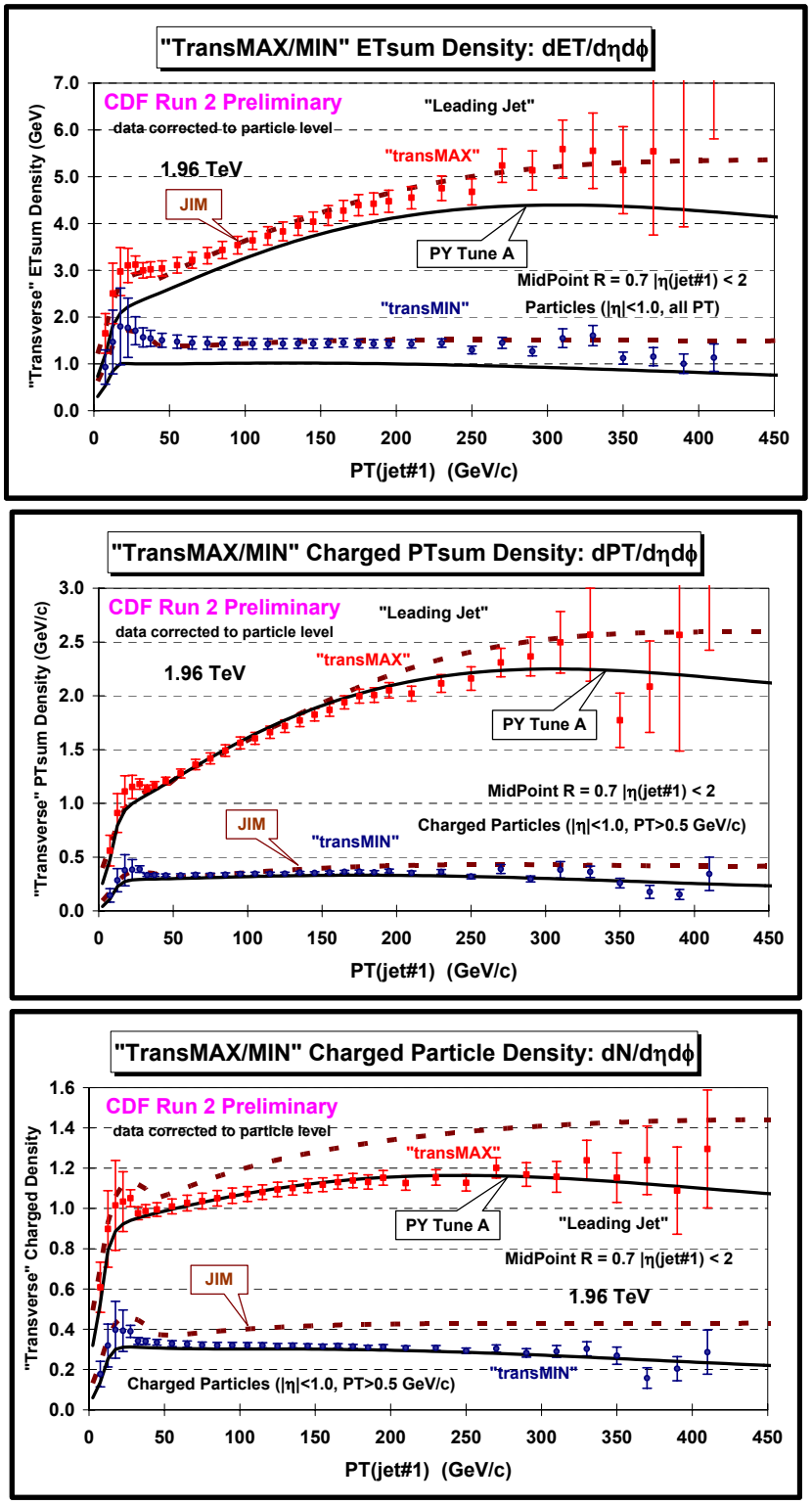

Fig. 57. Data at 1.96 TeV on the energy density (*top*), charged PTsum density (*middle*), and the density of charged particles (*bottom*) in the "transMAX" region and the "transMIN" region for "leading jet" events as a function of the leading jet P_T compared with PYTHIA Tune A and tuned JIMMY. JIMMY was tuned to fit the "transverse" energy density in "leading jet" events (PTJIM = 3.25 GeV/c). The data are corrected to the particle level (with errors that include both the statistical error and the systematic uncertainty) and compared with the theory at the particle level (*i.e.* generator level).

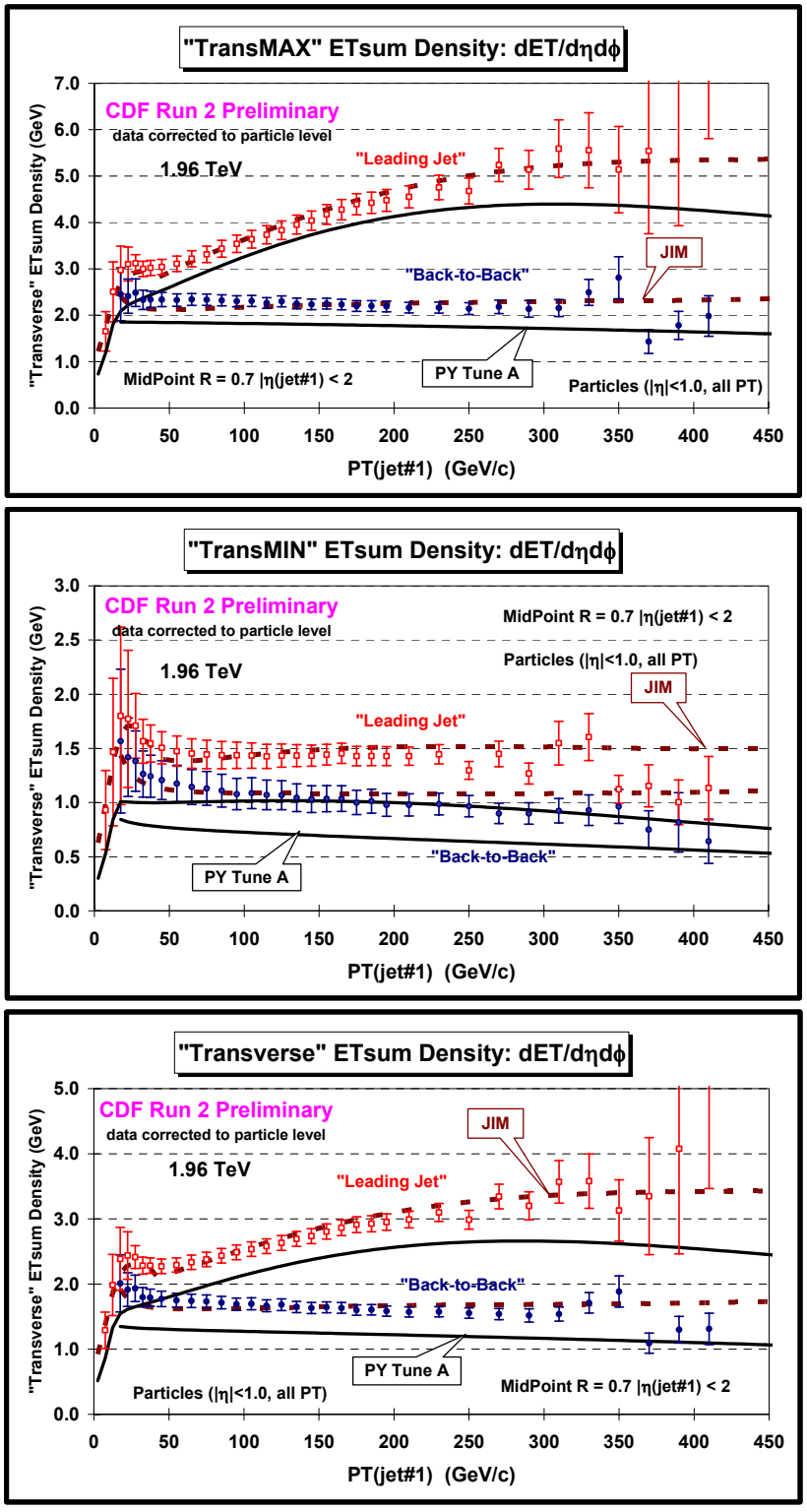

Fig. 58. Data at 1.96 TeV on the ETsum density, $dE_T/d\eta d\phi$, for particles with $|\eta| < 1$ in the "transMAX" region (*top*), "transMIN" region (*middle*), and "transverse" region (average of "transMAX" and "transMIN") (*bottom*) for "leading jet" and "back-to-back" events defined in Fig. 5 as a function of the leading jet P_T compared with PYTHIA Tune A and tuned JIMMY. JIMMY was tuned to fit the "transverse" energy density in "leading jet" events (PTJIM = 3.25 GeV/c). The data are corrected to the particle level (with errors that include both the statistical error and the systematic uncertainty) and compared with the theory at the particle level (*i.e.* generator level).

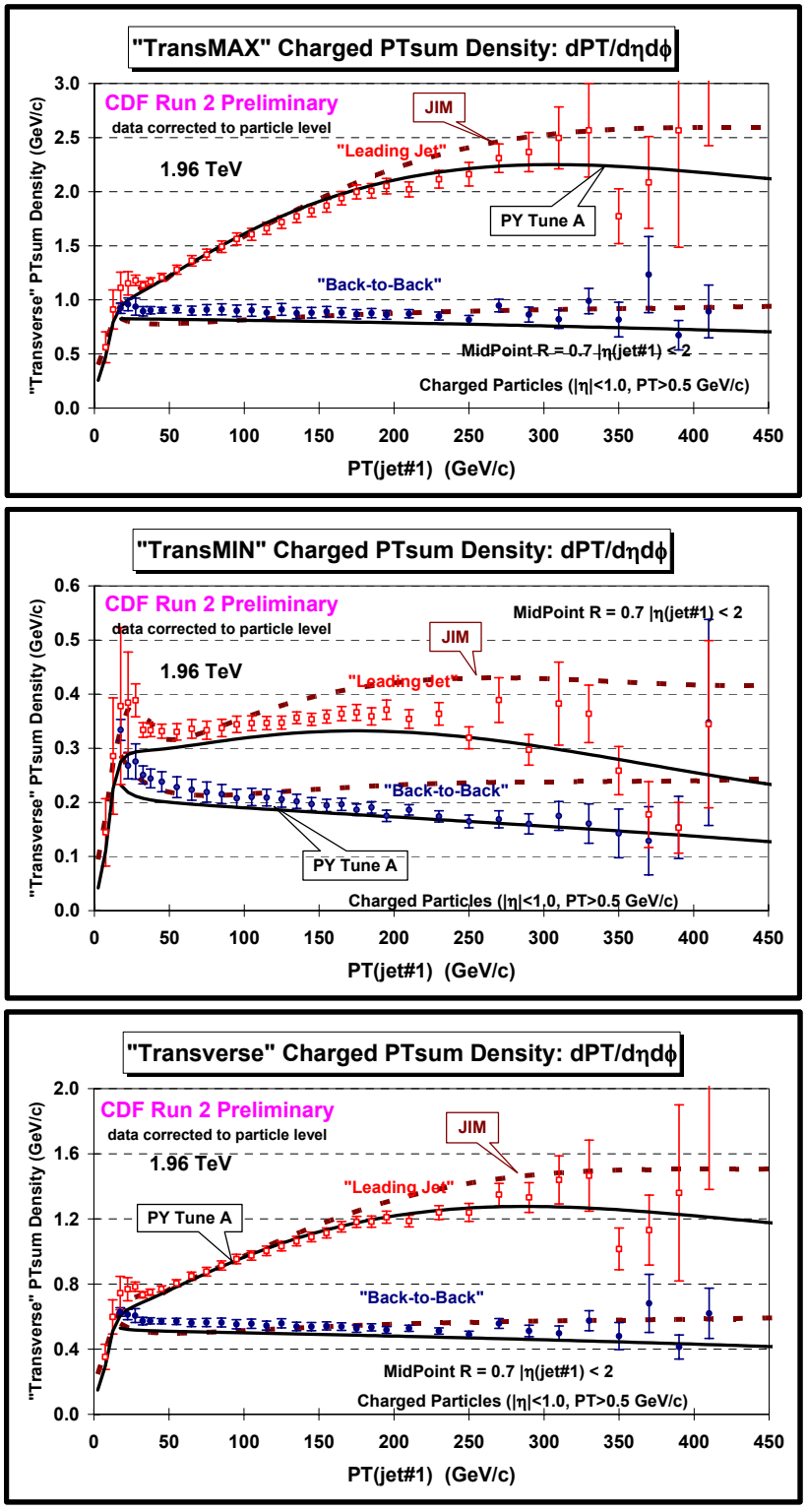

Fig. 59. Data at 1.96 TeV on charged PTsum density of charged particles, $dPT_{sum}/d\eta d\phi$, with $p_T > 0.5$ GeV/c and $|\eta| < 1$ in the "transMAX" region (*top*), "transMIN" region (*middle*), and "transverse" region (average of "transMAX" and "transMIN") (*bottom*) for "leading jet" and "back-to-back" events defined in Fig. 5 as a function of the leading jet P_T compared with PYTHIA Tune A and tuned JIMMY. JIMMY was tuned to fit the "transverse" energy density in "leading jet" events (PTJIM = 3.25 GeV/c). The data are corrected to the particle level (with errors that include both the statistical error and the systematic uncertainty) and compared with the theory at the particle level (*i.e.* generator level).

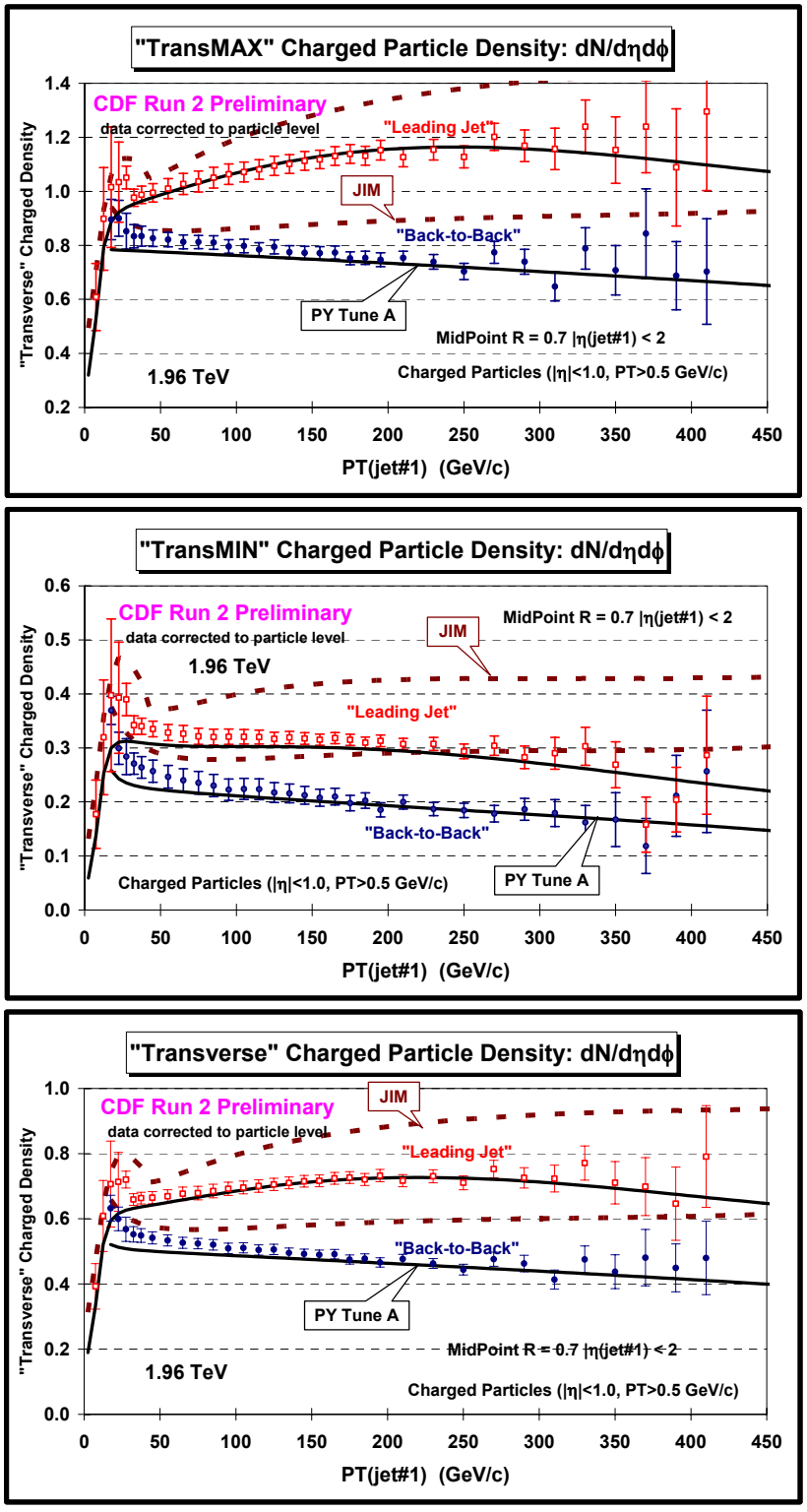

Fig. 60. Data at 1.96 TeV on the density of charged particles, $dN_{chg}/d\eta d\phi$, with $p_T > 0.5$ GeV/c and $|\eta| < 1$ in the "transMAX" region (*top*), "transMIN" region (*middle*), and "transverse" region (average of "transMAX" and "transMIN") (*bottom*) for "leading jet" and "back-to-back" events defined in Fig. 5 as a function of the leading jet P_T compared with PYTHIA Tune A and tuned JIMMY. JIMMY was tuned to fit the "transverse" energy density in "leading jet" events (PTJIM = 3.25 GeV/c). The data are corrected to the particle level (with errors that include both the statistical error and the systematic uncertainty) and compared with the theory at the particle level (*i.e.* generator level).

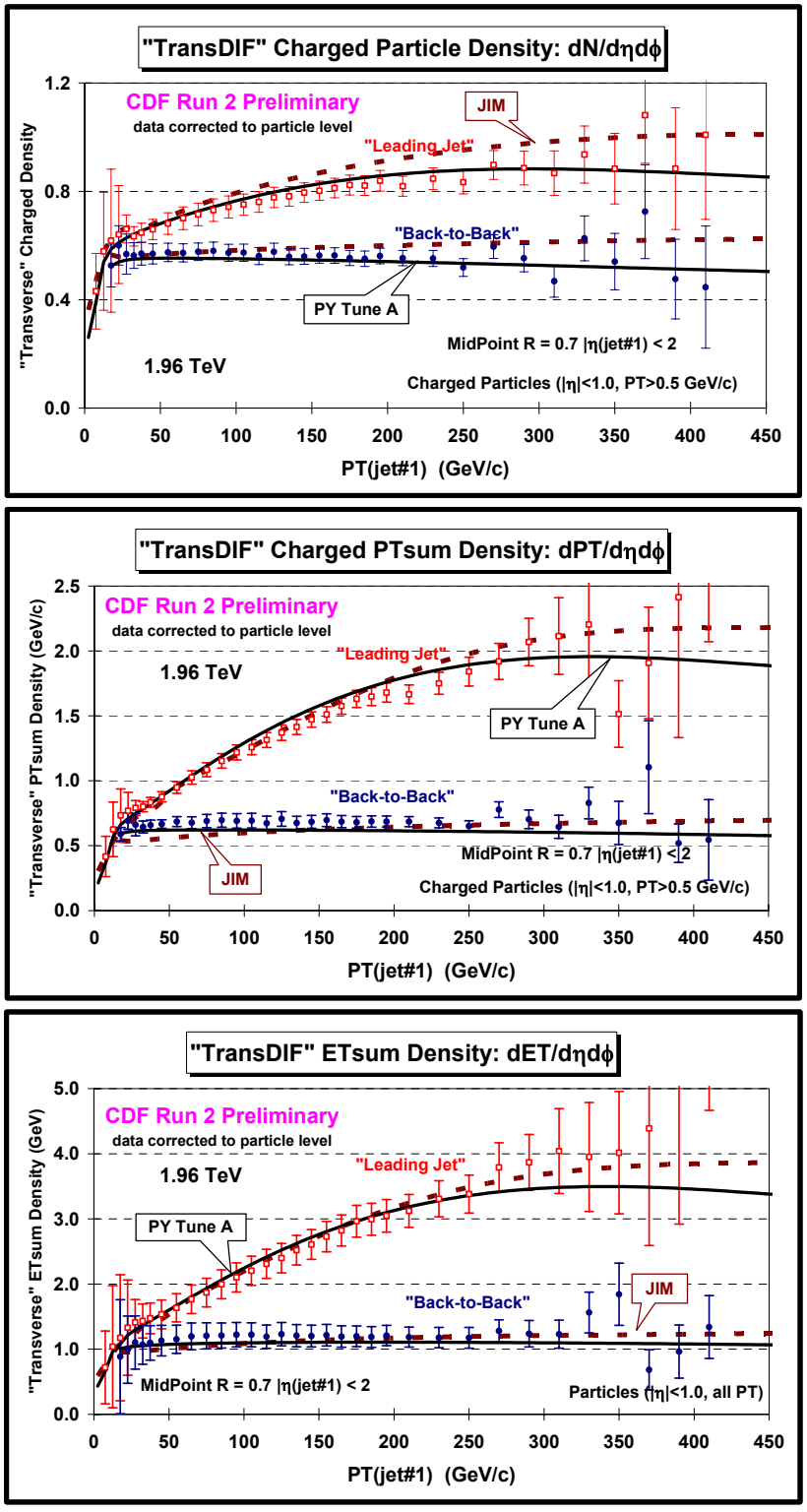

Fig. 61. Data at 1.96 TeV on the difference of the "transMAX" and "transMIN" region ("transDIF" = "transMAX" minus "transMIN") for "leading jet" and "back-to-back" events defined in Fig. 5 as a function of the leading jet P_T compared with PYTHIA Tune A and tuned JIMMY. JIMMY was tuned to fit the "transverse" energy density in "leading jet" events (PTJIM = 3.25 GeV/c). The data are corrected to the particle level (with errors that include both the statistical error and the systematic uncertainty) and compared with the theory at the particle level (*i.e.* generator level).

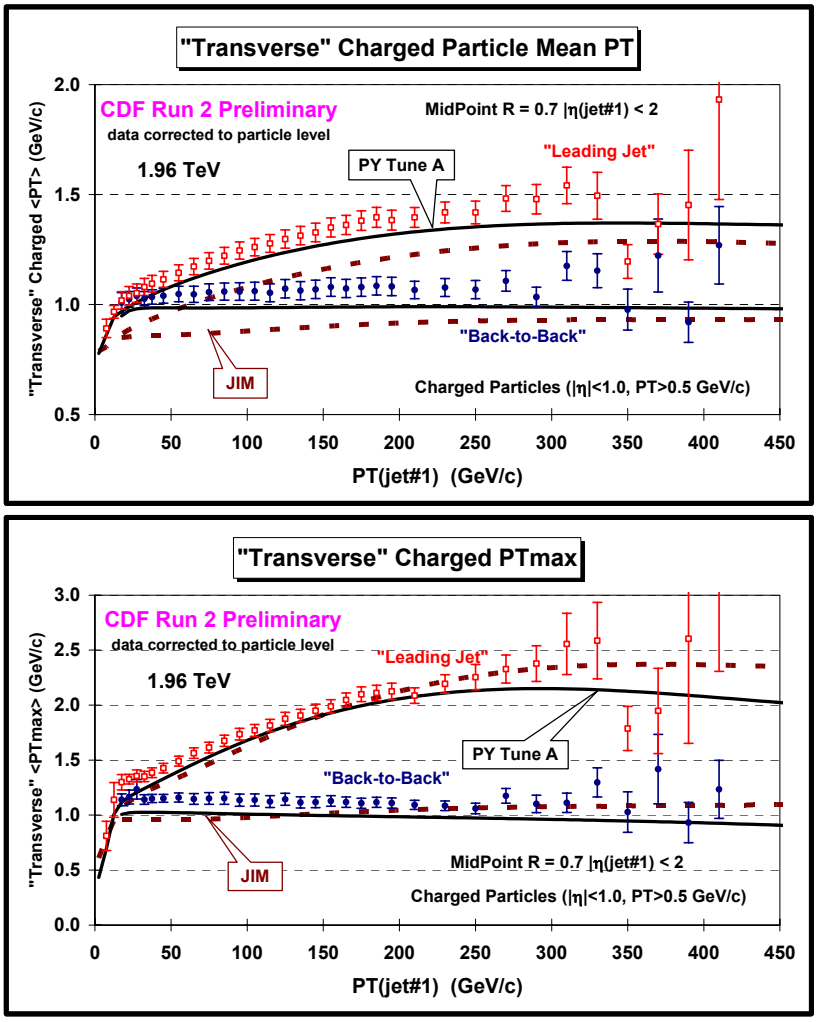

Fig. 62. Data at 1.96 TeV on the average $\langle p_T \rangle$ of charged particles (*top*) and the average maximum p_T, PTmax, for charged particles (*bottom*) with $p_T > 0.5$ GeV/c and $|\eta| < 1$ in the "transverse" region for "leading jet" and "back-to-back" events defined in Fig. 5 as a function of the leading jet P_T compared with PYTHIA Tune A and tuned JIMMY. JIMMY was tuned to fit the "transverse" energy density in "leading jet" events (PTJIM = 3.25 GeV/c). The data are corrected to the particle level (with errors that include both the statistical error and the systematic uncertainty) and compared with the theory at the particle level (*i.e.* generator level).

V. Summary

The goal of this analysis is to produce data on the "underlying event" that is corrected to the particle level so that it can be used to tune the QCD Monte-Carlo models without requiring CDF detector simulation (*i.e.* CDFSIM). Unlike our previous Run 2 "underlying event" analysis [5] which used JetClu to define "jets" and compared uncorrected data with PYTHIA Tune A and HERWIG after detector simulation (CDFSIM), in this analysis we use the MidPoint algorithm ($R = 0.7$, $f_{merge} = 0.75$) and correct the observables to the particle level. The corrected observables are then compared with PYTHIA Tune A and HERWIG at the particle level (*i.e.* generator level).

In this analysis we look at both the charged particle and the energy components of the "underlying event". We use the direction of the leading calorimeter jet in each event to define

two "transverse" regions of η-ϕ space that are very sensitive to the "underlying event". In addition, by selecting events with at least two jets that are nearly back-to-back ($\Delta\phi_{12} > 150^o$) with P_T(jet#3) < 15 GeV/c we are able to look closer at the "beam-beam remnant" and multiple parton interaction components of the "underlying event".

Comparing the corrected observables with PYTHIA Tune A and HERWIG at the particle level (*i.e.* generator level) leads to the same conclusions as we found when comparing the uncorrected data with the Monte-Carlo models after detector simulation (*i.e.* CDFSIM) [5]. PYTHIA Tune A (with multiple parton interactions) does a better job in describing the "underlying event" (*i.e.* "transverse" regions) for both "leading jet" and "back-to-back" events than does HERWIG (without multiple parton interactions). Herwig does not have enough activity in the "underlying event" for P_T(jet#1) less than about 150 GeV, which was also observed in our published Run 1 analysis [2].

This analysis gives our first look at the energy in the "underlying event" (*i.e.* the "transverse" region). Neither PYTHIA Tune A or HERWIG produce enough energy in the "transverse" region. However, they both fit the "transDIF" energy density ("transMAX" minus "transMIN"). This indicates that the excess energy density seen in the data probably arises from the "soft" component of the "underlying event" (*i.e.* beam-beam remnants and/or multiple parton interactions). HERWIG has more "soft" particles than PYTHIA Tune A and does slightly better in describing the energy density in the "transMAX" and "transMIN" regions. Tuned JIMMY does a good job of fitting the energy and charged PT_{sum} density in the "transverse" region (although it produces slightly too much charged PT_{sum} at large P_T(jet#1)). However, the tuned JIMMY produces too many charged particles with $p_T > 0.5$ GeV/c indicating that the particles produced by tuned JIMMY are too soft. Nevertheless it is quite interesting to compare tuned JIMMY with PYTHIA Tune A.

.

Acknowledgements

We would like to think Jay Dittmann and Nils Krumnack for supplying us with computing power (nbay02) in the CDF trailers.

References and Footnotes

1. T. Sjostrand, Phys. Lett. **157B**, 321 (1985); M. Bengtsson, T. Sjostrand, and M. van Zijl, Z. Phys. **C32**, 67 (1986); T. Sjostrand and M. van Zijl, Phys. Rev. **D36**, 2019 (1987).
2. *Charged Jet Evolution and the Underlying Event in Proton-Antiproton Collisions at 1.8 TeV*, The CDF Collaboration (T. Affolder et al.), Phys. Rev. **D65**, 092002, (2002).
3. *The Underlying Event in Large Transverse Momentum Charged Jet and Z-boson Production at 1.8 TeV*, talk presented by Rick Field at DPF2000, Columbus, OH, August 11, 2000.
4. *A Comparison of the Underlying Event in Jet and Min-Bias Events*, talk presented by Joey Huston at DPF2000, Columbus, OH, August 11, 2000. *The Underlying Event in Jet and Minimum Bias Events at the Tevatron*, talk presented by Valeria Tano at ISMD2001, Datong, China, September 1-7, 2001.

5. *The Underlying Event in Run 2*, Rick Field, CDF/ANAL/CDF/CDFR/6403 (2003). *Using MAX/MIN Transverse Regions and Associated Densities to Study the Underlying Event*, A. Cruz and R. Field, CDF/ANAL/CDF/CDFR/6759, November 2003. *Jet Topologies in Min-Bias and Hard Collisions in Run 2 at the Tevatron*, A. Cruz and R. Field, CDF/ANAL/CDF/CDFR/6819, December 2003. *Using Correlations in the Transverse Region to Study the Underlying Event in Run 2 at the Tevatron*, A. Cruz and R. Field, CDF/PUB/JET/PUBLIC/6821, December 2003.

6. *Min-Bias and the Underlying Event at the Tevatron and the LHC*, talk presented by R. Field at the Fermilab ME/MC Tuning Workshop, Fermilab, October 4, 2002. *Toward an Understanding of Hadron Collisions: From Feynman-Field until Now*, talk presented by R. Field at the Fermilab Joint Theoretical Experimental "Wine & Cheese" Seminar, Fermilab, October 4, 2002.

7. G. Marchesini and B. R. Webber, Nucl. Phys **B310**, 461 (1988); I. G. Knowles, Nucl. Phys. B310, 571 (1988); S. Catani, G. Marchesini, and B. R. Webber, Nucl. Phys. **B349**, 635 (1991).

8. *Hard Underlying Event Corrections to Inclusive Jet Cross-Sections*, Jon Pumplin, Phys. Rev. **D57**, 5787 (1998).

9. *Comparison of Soft Momentum Distribution in CDF data and Herwig+QFL at 1800 and 630 GeV*, Anwar Bhatti, Eve Kovacs, Joey Huston, and Valeria Tano, CDF/ANAL/JET/CDFR/5600. *Comparison of Underlying Event Energy in Herwig and CDF Data*, Anwar Bhatti, Joey Huston, Eve Kovacs, and Valeria Tano, CDF/ANAL/JET/CDFR/5214.

10. *Soft and Hard Interactions in Proton-AntiProton Collisions at 1800 and 630 GeV*, The CDF Collaboration (D. Acosta et al.), Phys. Rev. **D65**, 07200, (2002).

11. *Multiparton Interactions in Photoproduction at HERA*, J.M. Butterworth, J.R. Forshaw, and M.H. Seymour, Z. Phys. **C7**, 637-646 (1996).